

1           **Transverse energy analysis of**  
2           **relativistic heavy ion collisions**  
3   **through the use of identified particles**  
4           **spectra**

5                   A Thesis Presented for the  
6                   Master of Science  
7                   Degree  
8           The University of Tennessee, Knoxville

9                   Biswas Sharma  
10                  May 2018

11

© by Biswas Sharma, 2018

12

All Rights Reserved.

# 13 Table of Contents

14	<b>1 Introduction</b>	<b>1</b>
15	<b>2 Theoretical Background</b>	<b>3</b>
16	2.1 Quantum Chromodynamics . . . . .	3
17	2.2 Phase Transitions . . . . .	4
18	2.3 Quark-Gluon Plasma . . . . .	5
19	<b>3 Relativistic Heavy Ion Collisions</b>	<b>7</b>
20	3.1 RHIC and LHC . . . . .	7
21	3.2 Collision Energy and Geometry . . . . .	9
22	3.3 Kinematic Variables . . . . .	10
23	3.4 QGP Evolution . . . . .	13
24	3.5 Detection of Collision Products . . . . .	14
25	3.6 Detection of QGP Signatures . . . . .	15
26	3.6.1 Bjorken Energy Density . . . . .	15
27	3.6.2 Elliptic Flow . . . . .	15
28	3.6.3 Direct and Thermal Photons . . . . .	17
29	3.6.4 Strangeness Enhancement . . . . .	18
30	3.6.5 Jet Quenching . . . . .	19
31	3.7 The Beam Energy Scan Program . . . . .	20
32	<b>4 Measurement of Transverse Energy</b>	<b>21</b>
33	4.1 Definition of Transverse Energy . . . . .	21

34	4.2	$E_T$ Measurement with Calorimeters . . . . .	22
35	4.2.1	Calorimeter . . . . .	22
36	4.2.2	$E_T$ from PHENIX . . . . .	22
37	4.3	$E_T$ Measurement with Tracking Detectors . . . . .	23
38	4.3.1	Tracking and Particle Identification . . . . .	23
39	4.3.2	Calculation of $\frac{dE_T}{d\eta}$ from $p_T$ spectra . . . . .	24
40	4.3.3	Tracking Detectors in STAR . . . . .	25
41	<b>5</b>	<b>Data Analysis</b>	<b>27</b>
42	5.0.1	STAR $p_T$ spectra . . . . .	27
43	5.1	Extrapolation of Spectra . . . . .	28
44	5.1.1	Boltzmann-Gibbs Blast Wave . . . . .	29
45	5.1.2	Fitting Spectra to BGBW . . . . .	29
46	5.2	Calculations from the Spectral Fits . . . . .	30
47	5.2.1	Calculation of $\frac{dE_T}{dy}$ , $\frac{dE_T}{d\eta}$ , $\frac{dN_{ch}}{dy}$ , and $\frac{dN_{ch}}{d\eta}$ . . . . .	30
48	5.2.2	Corrections for Unidentified Particles and Estimation of Total $E_T$ . .	30
49	5.2.3	Lambdas Centralitiy Adjustments and $E_T$ Interpolations . . . . .	31
50	5.3	Uncertainties . . . . .	31
51	<b>6</b>	<b>Results</b>	<b>32</b>
52	<b>7</b>	<b>Conclusion</b>	<b>38</b>
53	<b>8</b>	<b>Future Work</b>	<b>39</b>
54	8.1	Goodness of Fit . . . . .	39
55	8.2	Bjorken Energy Density Estimate . . . . .	39
56	8.3	Asymmetric beams . . . . .	40
57		<b>Bibliography</b>	<b>41</b>
58		<b>Appendices</b>	<b>74</b>

# 59 List of Tables

<small>60</small>	3.1 Colliding species and associated collision energies at RHIC [24]. . . . .	10
<small>61</small>	5.1 Isospin states of different identified particles. . . . .	30

# List of Figures

63	2.1	Schematic of the QCD phase diagram [9]. . . . .	6
64	3.1	Initial layout of the RHIC.[26]. . . . .	8
65	3.2	An illustration of a mid-central collision of two nuclei traveling in the z	
66		direction. The X-axis is parallel to the line joining the centers of the two	
67		nuclei at the time of collision [14]. . . . .	11
68	3.3	An illustration of a collision consisting of participants (solid red) and	
69		spectators (open blue) within the colliding nuclei labeled A and B. $t_c$ denotes	
70		the time of maximum overlap of the two nuclei. The apparent narrowing of	
71		the volumes of the nuclei in the z-direction is due to Lorentz contraction [37].	12
72	3.4	Evolution of the QGP represented in a lightcone diagram. $\tau_0$ denotes the	
73		formation time of the QGP. $T_c$ is the critical temperature of the transition	
74		from the QGP to the hadron gas phase. $T_{ch}$ and $T_{fo}$ stand for the temperatures	
75		at, respectively, chemical freeze-out and thermal freeze-out [14]. . . . .	13
76	3.5	Minimum-bias Au+Au ( $\sqrt{s_{NN}} = 200GeV$ ) elliptic flow spectra for identified	
77		particles: (a) $v_2$ vs $p_T$ and (b) $v_2$ vs $KE_T$ . [4] . . . . .	16
78	3.6	Minimum-bias Au+Au ( $\sqrt{s_{NN}} = 200GeV$ ) elliptic flow spectra for identified	
79		particles: (a) $\frac{v_2}{n_q}$ vs $\frac{p_T}{n_q}$ and (b) $\frac{v_2}{n_q}$ vs $\frac{KE_T}{n_q}$ . [4] . . . . .	17
80	3.7	Feynman diagram representing the production of photons from quarks and	
81		gluons. (a) and (b) represent annihilation processes, whereas (c) and (d)	
82		represent Compton processes.[39] . . . . .	18

83	3.8	Illustration of jet quenching. Two jets are produced from each of the hard	
84		scatterings occuring at the locations of the solid dots. Jets originating closer	
85		to the initial surface are more probable to propagate outside the medium, as	
86		shown. Jets opposite to them interact with the medium, losing their energy	
87		and resulting in bow front shock waves.[36] . . . . .	19
88	4.1	Energy loss distribution in the STAR TPC for primary and secondary	
89		particles. [19]. . . . .	26
90	5.1	Transverse momentum spectra for $\pi^+$ , $\pi^-$ , $K^+$ , $K^-$ , $p$ , and $\bar{p}$ at midrapidity	
91		( $ y  < 0.1$ ) from 39 GeV Au+Au collisions at RHIC. The fitting curves	
92		on the 0-5% central collision spectra for pions, kaons, and protons/anti-	
93		protons represent, respectively, the Bose-Einstein, $m_T$ -exponential, and	
94		double-exponential functions. [2]. . . . .	28
95	5.2	Red curve shows the Boltzmann-Gibbs blast wave functional fit on the PRE-	
96		LIMINARY transverse momentum spectrum for lambda particles identified	
97		by the STAR detector for 19.6 GeV Au+Au collisions (10-15% central).	
98		Parameters extracted from the chi-square goodness-of-fit test, as well as other	
99		statistics, are shown in the box on the top right. . . . .	30
100	6.1	Parallel coordinates plot for 270 different spectra relating 6 different identified	
101		particles (color-coded) to their respective collision centrality classes, good-fit	
102		parameters, and the transverse energy calculated using said parameters. . . .	32
103	6.2	$(dE_T/d\eta)/0.5N_{part}$ at midrapidity as a function of $\sqrt{s_{NN}}$ for different central-	
104		ities. . . . .	33
105	6.3	$(dE_T/d\eta)/(dN_{ch}/d\eta)$ at midrapidity as a function of $\sqrt{s_{NN}}$ for different	
106		centralities. . . . .	33
107	6.4	$(dE_T/d\eta)/0.5N_{part}$ at midrapidity as a function of $N_{part}$ for different centralities.	34
108	6.5	$(dE_T/d\eta)/(dN_{ch}/d\eta)$ at midrapidity as a function of $N_{part}$ for different	
109		centralities. . . . .	34
110	6.6	$(dE_T/dy)/0.5N_{part}$ at midrapidity as a function of $\sqrt{s_{NN}}$ for different centralities.	35

111	6.7	$(dE_T/dy)/(dN_{ch}/dy)$ at midrapidity as a function of $\sqrt{s_{NN}}$ for different	
112		centralities. . . . .	35
113	6.8	$(dE_T/dy)/0.5N_{part}$ at midrapidity as a function of $N_{part}$ for different centralities.	36
114	6.9	$(dE_T/dy)/(dN_{ch}/dy)$ at midrapidity as a function of $N_{part}$ for different	
115		centralities. . . . .	36
116	6.10	$\frac{dE_T}{d\eta}/0.5N_{part}$ for 0-5% central collisions at midrapidity as a function of $\sqrt{s_{NN}}$ .	
117		The PHENIX data are from [3]. The error bars represent the total statistical	
118		and systematic uncertainties. . . . .	37



# Chapter 1

## Introduction

The Big Bang model is based on observational evidence, such as the cosmic microwave background radiation and the cosmological expansion, and suggests that at the beginning the universe must have been at a state of really high density and temperature. As the universe expanded, it went through several stages of cooling characterized by the formation of matters with different compositions. The matter we mostly observe today exists at temperatures and densities much lower compared to those in the early universe.

The Large Hadron Collider (LHC) at CERN and the Relativistic Heavy Ion Collider (RHIC) at the Brookhaven National Laboratory have the ability to collide heavy nuclei, such as those of gold and uranium, at nearly the speed of light, reaching temperatures of trillions of degrees Celcius. These laboratories have provided evidence of the formation of an exotic state of matter, called the quark-gluon plasma (QGP). It only exists for a brief amount of time after such collisions and instantly freezes out into a plethora of new particles, which carry the signatures we can use to deduct QGP properties. Its properties suggest that it should be similar to the matter that existed within microseconds of the genesis of the universe. It behaves like an almost perfect fluid with a viscosity near 0 [? ].

One of the methods to probe the properties of this matter is by analyzing the conversion of the beam-direction energy at the time of collision into transverse energy after the collision. These measurements can be used to estimate the energy density of the QGP. This analysis is generally done by using data from the calorimeters placed around the collision site. In this

thesis, I use the data collected by tracking detectors, instead of the conventional calorimeters, to calculate the transverse energy.

This thesis is structured as follows. chapter 2 touches on the theoretial background associated with the concept of the quark-gluon plasma. In chapter 3, I summarize the experimental concepts pertaining to relativistic heavy-ion collisions and the production and detection of QGP. chapter 4 consists of the formalism of the measurement of transverse energy using calorimeters as well as tracking detectors. It also describes what has been done using calorimeters. chapter 5 describes the data used to perform the analysis in this thesis and notes the relevant details of the analysis. In chapter 6, I present the results and compare them to the ones in literature obtained using a different method. Chapter ??ch:conclusion) concludes the thesis and discusses its implications. Finally, in chapter 8, I present arguments on what can be done in the future using the results of and the software developed for this analysis.

# Chapter 2

## Theoretical Background

### 2.1 Quantum Chromodynamics

The strong force is one of the four fundamental interactions in physics. At large scales, it is also known as the residual strong force, and it is responsible for binding the nucleons together to give the nucleus its structure. At smaller scales, it is called the fundamental nuclear force, and it binds the fundamental units of subnuclear matter, the quarks, together to form the nucleons. The force carriers of the interaction are the mesons at the former scale and the gluons at the latter. The electrodynamic interaction between charged particles such as protons and electrons is described by quantum electrodynamics (QED) as mediated by photons; the strong interaction, albeit more complicated, is explained under the framework of quantum chromodynamics (QCD) [22, 32]. The quarks and gluons of QCD are collectively known as partons. Gluons are the gauge bosons of the Yang-Mills theory.

The Yang-Mills theory is a non-Abelian gauge theory. It has a Lagrangian with several degrees of freedom, some of which are redundant and need to be gauged. This is done by a mathematical treatment as prescribed under a gauge theory. [7] The gauge theory associated with the Yang-Mills theory is based on the  $SU(N)$  group. It is non-Abelian as represented by the non-commutative transformations. QCD is a gauge theory that describes the application of the  $SU(3)$  symmetry transformations on the triplet (what does the tripleness imply?????????) of color charges, namely red, blue, and green. The electroweak interaction,

173 on the other hand, can be formalized under the gauge group  $SU(2) \times U(1)$ . Together, they  
 174 form the  $SU(3) \times SU(2) \times (U(1))$  gauge theory called the standard model.

175 One of the ways QCD is different from QED is the confinement of partons. In QED, the  
 176 fundamental particles are bound together by the Coulomb potential, which diminishes with  
 177 distance between the charge-carrying particles, as demonstrated by the relation 2.1:

$$V_C \propto \frac{1}{r} \quad (2.1)$$

178 where  $V_C$  is the Coulomb potential, and  $r$  is the spatial separation between the particles.  
 179 This means that bound QED particles can be isolated by increasing their spatial separation.  
 180 The QCD potential, on the other hand, has an extra linear term in it:

$$V_{QCD} = -\frac{4}{3} \frac{\alpha_S}{r} + kr \quad (2.2)$$

181 where  $\alpha_S$  is the QCD fine-structure constant and  $k$  is the strength of the color interaction  
 182 ( $\sim 1 \text{ GeV/fm}$ ) [? ]. This means that the potential increases linearly with distance at large  
 183 distances, and so an infinite amount of energy is required to separate quarks. Hence, we  
 184 never observe isolated quarks and they are said to be confined, not just bound, to form  
 185 composite structures called hadrons [29]. A quark and an anti-quark forms a meson and  
 186 that of three quarks forms a baryon. In addition to having a color charge, a quark also  
 187 carries a flavor. There are six different quarks based on the flavors they carry: up, down,  
 188 top, bottom, beauty, and strange.

## 189 2.2 Phase Transitions

190 In everyday life, we observe matter existing in four distinct phases: solid, liquid, gas, and  
 191 plasma. Changes in physical conditions can lead to a transition from one of these phases  
 192 to another, exemplified by the commonly observed conversion of ice to water. Distinctions  
 193 among the various phases can be represented in a chart called the phase diagram.

194 The phase diagram consists of thermodynamic observables such as temperature and  
 195 density on its axes. Curves in the phase diagram represent boundaries of physical conditions

at which two or more phases of matter can coexist in equilibrium. Crossing a boundary represents an abrupt transition from one phase to another; this abruptness is mathematically characterized by the discontinuity in the change of the derivative of the free energy – a thermodynamic variable – with respect to the physical quantities in the axes. There can also be regions in the diagram representing the ranges of physical conditions in which a smooth phase transition can take place. .... Christine believes this is only for a first order phase transition.....

One of the main focuses of current experimental and theoretical nuclear physics research is the study of the phase diagram of strongly interacting matter at a range of temperatures and baryon chemical potentials. In experiments involving the collisions of heavy ions at high and low energies, different regions of the phase diagram can be probed by varying the collision energy [3]. For instance, the high-baryon chemical potential regime corresponds to lower beam energies and higher temperatures correspond to higher beam energies. The results of these experiments and model calculations can be used to study the nature of transitions in the QCD phase diagram.

A schematic representing the QCD phase diagram as a function of the temperature ( $T$ ) and quark chemical potential ( $\mu$ ) is shown in Figure 2.1 [9]. A second-order transition is predicted at low baryon chemical potentials (close to baryon-antibaryon symmetry) and high temperatures reminiscent of the early universe. Methods to study this region of the phase space will be explored in this thesis. At low temperatures and high chemical potentials, loose predictions have been made regarding the existence of exotic phases of high density matter, and programs, such as the Compressed Baryonic Matter experiment at the Facility for Antiproton and Ion Research in Germany, are being designed to study this region of the phase diagram [? ].

## 2.3 Quark-Gluon Plasma

The confinement of quarks into the hadronic phase of QCD matter, as described in section 2.1, has its limitations. At very high densities, when the wave function of a single hadron overlaps with the spatial regions covered by multiple such hadrons, it is impossible to classify

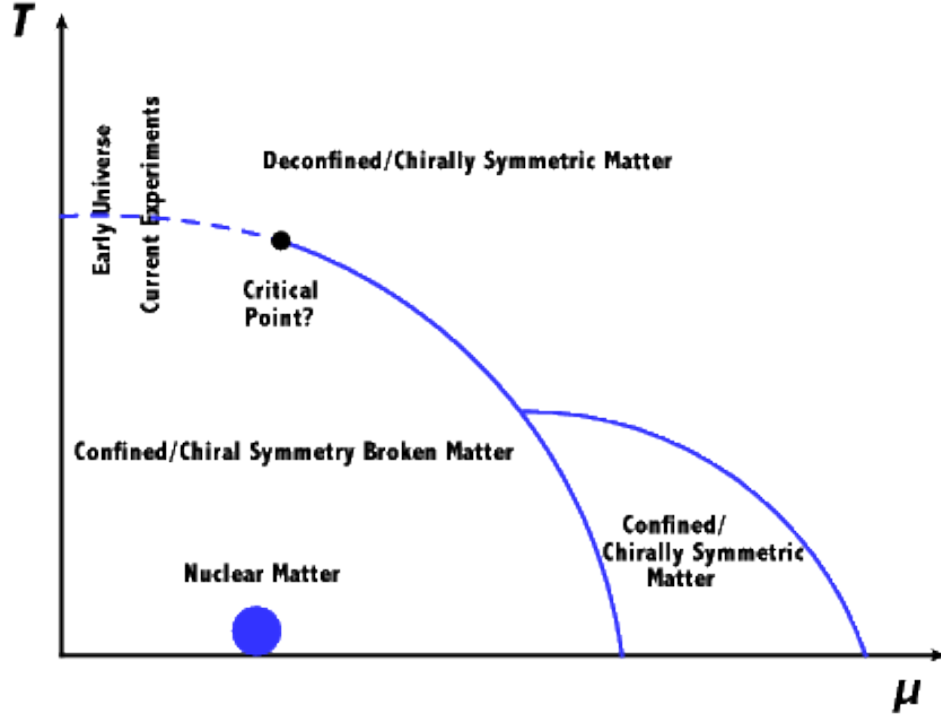


**Figure 2.1:** Schematic of the QCD phase diagram [9].

224 which pair or triplet of quarks belongs to which meson or baryon. As long as a particular  
 225 quark is close enough to the other quarks in the volume, it is deconfined in such a way that it  
 226 can freely move anywhere in the volume [29]. QCD predicts such phase transition, at energy  
 227 densities above  $0.2\text{-}1 \text{ GeV}/\text{fm}^3$  [1] and around a critical temperature of about  $160 \text{ MeV}$  [?  
 228 ], of strongly interacting matter to a phase with quarks and gluons in thermal and chemical  
 229 equilibrium representing the relevant degrees of freedom and behaving like an almost perfect  
 230 fluid [12]. This deconfined state of quarks and gluons is termed the quark-gluon plasma  
 231 (QGP) in analogy to the quantum electrodynamical plasma phase of matter.

## Chapter 3

# Relativistic Heavy Ion Collisions

The experimental evidence for the QGP come from the collisions of heavy nuclei. The signatures of such evidence are described in section 3.6. Physicists proposed the existence of such matter since as far back as 1984, when nuclei were accelerated and collided with stationary targets [18]. They were able to agree on a conclusive discovery of this matter during the 2000s, after colliding accelerated nuclei with other such nuclei or smaller species (protons, deuterons) at unprecedented energies and with improved detection schemes [34]. With further increases in collision energies and enhancements in detector technology, modern accelerator facilities provided additional evidence and estimates of some of the properties as well as the dynamics of the evolution of the QGP. The following sections describe two such facilities, the physics of the collisions and what happens after the collisions.

### 3.1 RHIC and LHC

The Relativistic Heavy Ion Collider (RHIC) is located in Upton, New York in the premises of the Brookhaven National Laboratory (BNL). Its construction started in 1991 and was completed in 1999. Figure 3.1 shows the layout, at the time of construction, of the collider along with the Alternating Gradient Synchrotron (AGS) complex and the locations of the original four detectors: Solenoidal Tracker At RHIC (STAR), Pioneering High Energy Nuclear Interaction eXperiment (PHENIX), Phobos and BRAHMS (Broad RAnge Hadron Magnetic Spectrometers). Phobos, BRAHMS, and PHENIX were decommissioned after the

252 completion of their science objectives, but STAR is still functional. The AGS was part of  
 253 BNL before the construction of the RHIC, and its capabilities were augmented with the  
 construction of the AGS Booster in 1991.

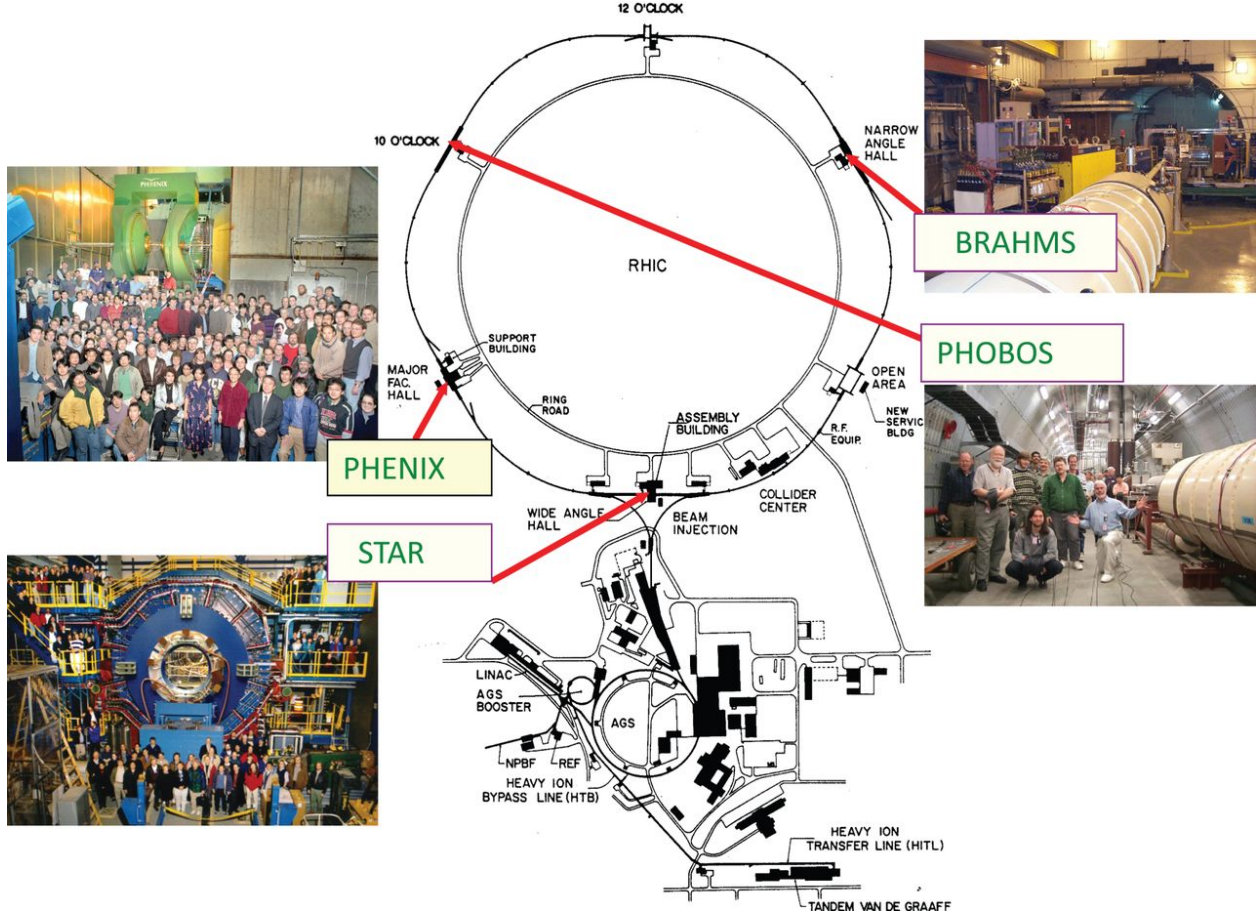


Figure 3.1: Initial layout of the RHIC.[26].

254

255 Heavy ion beams in RHIC are created in a series of steps before collision. In case of gold  
 256 ions, a pulsed sputter source produces negatively charged ions, which are stripped of some of  
 257 their electrons with a foil on the positive end of the high-voltage Tandem Van de Graaff. The  
 258 ions are now positively charged and are accelerated to 1MeV/u toward the negative terminal  
 259 of the Tandem. Upon exiting it, some more stripping takes place. The bending magnets then  
 260 selectively deliver +32 charge states of the ions to the Booster Synchrotron, which accelerates  
 261 them to 95MeV/u and strips them to a +77 charge state before injecting them to the AGS.  
 262 The AGS accelerates them to 10.8 GeV/u and strips them of the remaining two electrons at  
 263 the exit. The gold ions are then injected through the AGS-to-RHIC Beam Transfer Line to



the two RHIC rings. These rings carry beams moving in opposite directions and intersect at six symmetric locations in the 3.8 km circumference. The original four detectors are located in four of these six locations where the beams undergo head-on collisions.

The Large Hadron Collider (LHC) is located underground (between 45m and 170m) beneath the France-Switzerland border near the city of Geneva. The two rings of the collider were constructed between 1998 and 2008 by the European Organization for Nuclear Research (CERN) in the 26.7 km circular tunnel originally housing CERN's Large Electron-Positron collider. Analogous to the RHIC, the LHC gets its beams prepared by a series of machines in the CERN accelerator complex. The collisions occur at the locations of the four big LHC experiments: Compact Muon Solenoid (CMS), A Toroidal LHC ApparatuS (ATLAS), Large Hadron Collider beauty (LHCb) experiment, and A Large Ion Collider Experiment (ALICE). ALICE is dedicated to the study of heavy-ion collisions [16].

## 3.2 Collision Energy and Geometry

What happens in the aftermath of a collision depends on how much energy is available at the time of the collision as well as the geometry of the collision. The collision energy is determined by the collider configuration. The geometry of the collision is deduced from the constraints imposed by the static (eg. rest mass) and dynamic (eg. trajectory) properties of the detected products.

In collision experiments, it is convenient to use a reference frame in which the net momentum of the pair of colliding species is zero. This frame is called the center-of-mass frame. In this frame, the total energy of the species in the two beams is a function of the number of nucleons and the center-of-mass energy per nucleon. The collision energy is reported as the center-of-mass energy per nucleon pair,  $\sqrt{s_{NN}}$ .

RHIC has the unique capability of colliding species at a range of energies spanning almost two orders of magnitude. Table 3.1 lists the collision energies produced so far at RHIC for various collision systems. The LHC boasts the highest amount of collision energy for any collider on earth. It collided species (p+p, p+A, Pb+Pb) at a center of mass energy upto

291 2.76 TeV per nucleon pair at the end of 2010. At the end of 2015, 5.02 TeV Pb+Pb (13 TeV  
292 p+p) collisions were successfully completed [17].

Collision system	$\sqrt{s_{NN}}(GeV)$
p+p	200, 500
d+Au	200
Cu+Cu	62, 200
Au+Au	9, 20, 62, 130, 200

**Table 3.1:** Colliding species and associated collision energies at RHIC [24].

293 In general, any collision between two nuclei is not perfectly head-on. Some collisions are  
294 close to being head-on and are called central collisions. Some are glancing and are called  
295 peripheral collisions. By convention, 0% is the centrality of a perfectly head-on collision  
296 and 100% is that of the least head-on, i.e., the most peripheral collision. In practice, each  
297 collision event is deducted to belong to a specific centrality bin, for instance, 0-5%. Figure  
298 3.2 illustrates the aftermath of a mid-central collision, i.e, a collision in which about half of  
299 the volume of each of the nuclei intersects the other..... add brief discussion of Glauber  
300 model and STAR centrality determination.....

301 The collision of two nuclei can be modeled as collisions of the constituents that make  
302 up the nuclei. The nucleons that take part in the collisions and are called participants.  
303 The rest of the nucleons are known as spectators. Figure 3.3 illustrates the distribution of  
304 participants and spectators in two colliding nuclei. Expectedly, the number of participants  
305 is more in more central collisions.

### 306 3.3 Kinematic Variables

307 The description of the collision physics and the interpretation of its results are aided by the  
308 construction of variables that undergo simple transformations under a change of reference  
309 frame. Two such variables, rapidity and pseudorapidity, are described in this section.

310 The rapidity,  $y$ , of a particle is defined as:

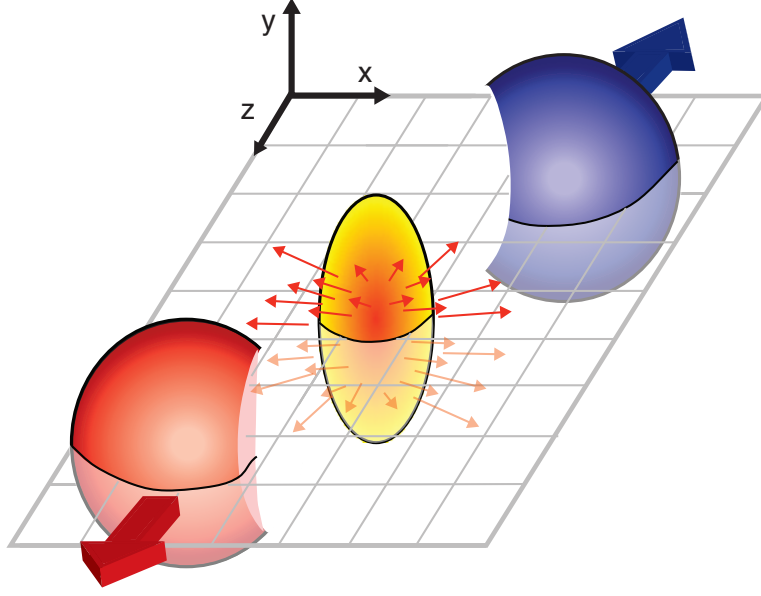


**Figure 3.2:** An illustration of a mid-central collision of two nuclei traveling in the  $z$  direction. The  $X$ -axis is parallel to the line joining the centers of the two nuclei at the time of collision [14].

$$y \equiv \frac{1}{2} \ln \frac{p_0 + p_z}{p_0 - p_z} \quad (3.1)$$

$$= \frac{1}{2} \ln \frac{E + p_z}{E - p_z}, \quad (3.2)$$

where  $p_0$  and  $p_z$  are the components of its contravariant four-momentum  $p = (p_0, p_x, p_y, p_z)$  with  $p_0 = \frac{E}{c}$ ,  $E$  being the relativistic energy of the particle and  $c$ , the speed of light, being equal to 1 in natural units.

The rapidity of a particle is used as a relativistic description of its velocity. Unlike the canonical velocity of a particle, its rapidity transforms simply additively under a Lorentz boost of the frame of reference. For example, suppose a particle has a rapidity  $y$  in the laboratory frame. Let  $y'$  denote its rapidity as measured in a frame that is Lorentz boosted with a velocity  $\beta$  in the  $z$ -direction with respect to the laboratory frame. Then the

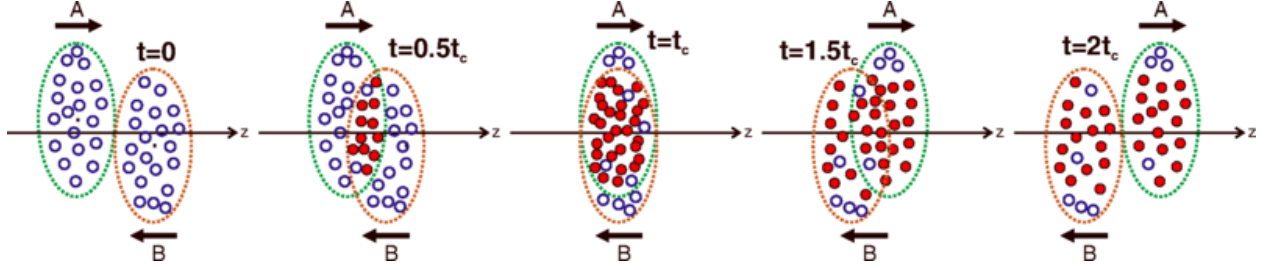


**Figure 3.3:** An illustration of a collision consisting of participants (solid red) and spectators (open blue) within the colliding nuclei labeled A and B.  $t_c$  denotes the time of maximum overlap of the two nuclei. The apparent narrowing of the volumes of the nuclei in the  $z$ -direction is due to Lorentz contraction [37].

relationship between the rapidities in the two different frames is simply

$$y' = y - y_\beta \quad (3.3)$$

Here,

$$y_\beta = \frac{1}{2} \ln \frac{1 + \beta}{1 - \beta} \quad (3.4)$$

is the rapidity the particle would have in the laboratory frame if it were moving with a velocity  $\beta$  in the  $z$ -direction with respect to the laboratory frame, as can be verified from equation 3.1 with  $p_0 = \gamma m$  and  $p_z = \gamma \beta m$ ,  $\gamma$  being the Lorentz factor  $\frac{1}{\sqrt{1-\beta^2}}$ . [39]

The convenience provided by this construct comes with a cost. As evident from equation 3.1, the calculation of the rapidity of a particle requires the measurement of two different observables associated with it, such as the energy and the  $z$ -direction momentum. However, experimental constraints may sometimes only facilitate the measurement of the direction of the detected particle with respect to the beam axis. What's more convenient in such a case is the use of another variable construct called pseudorapidity,  $\eta$ , defined as:

$$\eta \equiv -\ln \tan \frac{\theta}{2}, \quad (3.5)$$

where  $\theta$  is the angle the particle's momentum vector,  $\mathbf{p}$ , makes with the  $z$ -direction. The above equation can also be written in terms of the momentum as:

$$\eta = \frac{1}{2} \ln \frac{|\mathbf{p}| + p_z}{|\mathbf{p}| - p_z} \quad (3.6)$$

From equations 3.1 and 3.6, it is evident that  $\eta \approx y$  when  $|\mathbf{p}| \approx p_0$ , i.e., when the momentum is large. The transformation of the particle distribution from the  $y$ -space to the  $\eta$ -space is discussed in section 4.3.2.

### 3.4 QGP Evolution

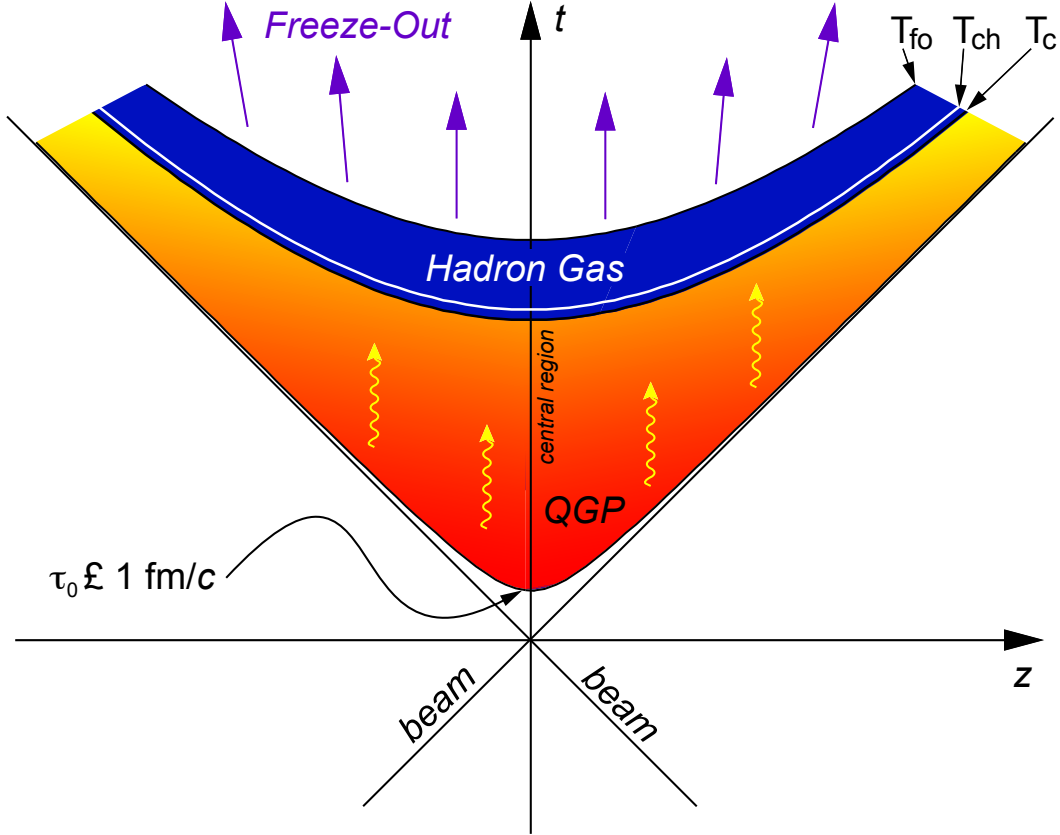


**Figure 3.4:** Evolution of the QGP represented in a lightcone diagram.  $\tau_0$  denotes the formation time of the QGP.  $T_c$  is the critical temperature of the transition from the QGP to the hadron gas phase.  $T_{ch}$  and  $T_{fo}$  stand for the temperatures at, respectively, chemical freeze-out and thermal freeze-out [14].

336 The evolution of the QGP is shown in a lightcone diagram in figure 3.4 [14]. The initial  
 337 state of the colliding nuclei is not well known and is the topic of research for upcoming  
 338 experiments. During the collision, the participants scatter off of each other while the  
 339 spectators keep traveling almost unperturbed in their original direction. The immediate  
 340 aftermath of a central collision of heavy ions at RHIC and LHC energies is the formation  
 341 of a hot fireball. This fireball evolves in time to form a liquid-like medium of quarks and  
 342 gluons. This medium attains a local equilibrium and remains in such a state, depending  
 343 on the collision energy, for about 1-10 fm/c. This equilibrium is broken as the liquid  
 344 QGP evolves by expanding and cooling to attain a density and temperature at which the  
 345 deconfinement of quarks and gluons is lost and they undergo a chemical freeze-out to form a  
 346 hadron gas. Collisions between the constituents of this gas become scant as it evolves with  
 347 further expansion and cooling, and the hadrons undergo a thermal freeze-out to attain their  
 348 final energies and momenta [14].

## 349 **3.5 Detection of Collision Products**

350 Detectors are placed around the collision site to perform measurements on the final state  
 351 particles emitting from the thermal freeze-out of the medium. These measurements typically  
 352 include the estimation of the location and time of production of the final states, the type of  
 353 particle, and the momentum and energy it carries.

354 Generally, a tracking detector surrounds the collision site, and there are particle identifiers  
 355 followed by calorimeters around it. A magnetic field is applied parallel to the beam direction  
 356 around the collision site. Due to this orientation of the magnetic field, the spectators  
 357 traveling parallel to it move undeflected and the final state charged particles with components  
 358 of velocity transverse to the beam axis get deflected around the beam axis with angular  
 359 frequency given by

$$\omega = \frac{qB}{m}, \quad (3.7)$$

360 where  $q$  is the electric charge of the particle,  $m$  is its mass and  $B$  is the applied magnetic field.  
 361 Two kinds of detectors most relevant to this thesis, tracking detectors and calorimeters, are  
 362 described in chapter 4.

## 3.6 Detection of QGP Signatures

The existence and properties of the QGP in the aftermath of high-energy heavy-ion collisions can be probed using different techniques relevant to several theoretical characteristics of the medium. No signature can alone be used to claim the production of the QGP, and some of the probes, which should be interpreted together, are described below.

### 3.6.1 Bjorken Energy Density

In 1983, J.D. Bjorken[11] prescribed a formula to use the final state particles to estimate the initial energy density,  $\epsilon_0$ , in a nucleus-nucleus collision. With slight changes in the original formula, the energy density is given by:

$$\epsilon_0 = \frac{1}{\tau_0 A_T} \langle \frac{dE_T}{dy} \rangle, \quad (3.8)$$

where  $\tau_0$  is the formation time of QGP equilibration,  $A_T$  is the transverse area of the intersection of the two nuclei, and  $\langle \frac{dE_T}{dy} \rangle$  is the mean transverse energy per unit rapidity.  $\tau_0$  is model-dependent and is normally estimated to be  $1 fm/c$ .  $A_T$  depends on the centrality of the collision and can be estimated using the Glauber models discussed earlier.  $\langle \frac{dE_T}{dy} \rangle$  is found from the measurement of the transverse energy carried by the final state particles from the collision and is the central theme of this thesis. Details about it are in the following chapters. The estimate of the initial energy density from Bjorken formula can be compared with the QCD prediction of the critical energy density[1] to check if the results from a collision imply the achievement of the critical physical condition required for the phase transition [21].

### 3.6.2 Elliptic Flow

The evolution of the medium produced after relativistic heavy ion collisions can be well described under the framework of relativistic hydrodynamics [30, 35]. This description indicates the presence of a collective flow, and hence a liquid-like and thermalized nature, of the constituents that make up the system. The momentum distribution of the final state particles emitted out of the collectively flowing system can be decomposed into its azimuthal

387 Fourier components. The second harmonic coefficient,  $\nu_2(y, p_T)$ , of this decomposition  
 388 characterizes what is known as the elliptic flow [20]. The magnitude of the elliptic flow  
 389 from a non-central collision represents the anisotropy in azimuthal momentum space of the  
 390 thermalized post-collision system [33]. The elliptic flow of the medium, as a function of  
 391 the momentum or the kinetic energy in the transverse direction, points towards quarks,  
 392 rather than hadrons, being the relevant degrees of freedom in the QGP. Figure 3.5 shows  $v_2$   
 393 as a function of the transverse momentum and the transverse kinetic energy for identified  
 394 particles. The spectra scale consistently at lower values of both  $p_T$  and  $KE_T$ . However,  
 395 they branch out at higher values:  $p_T \gtrsim 2\text{GeV}/c$  and  $KE_T \gtrsim 1\text{GeV}$ . Figure 3.6, on the other  
 396 hand, is similar to figure 3.5, with the exception that both the axes have quantities that are  
 397 normalized by the number of quarks,  $n_q$ . In this case, the  $KE_T$  spectra strongly exhibits a  
 398 scaling which is more comprehensively consistent with the number of quarks than in case of  
 399 figure 3.5. This universal quark-number scaling can be interpreted as the degrees of freedom  
 of the system being quark-like.[4]

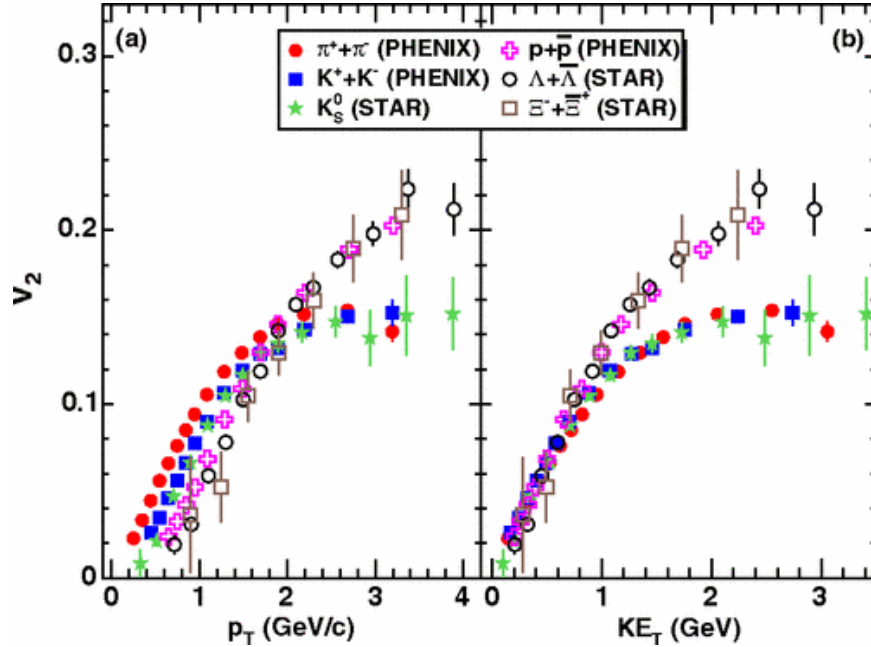


**Figure 3.5:** Minimum-bias Au+Au ( $\sqrt{s_{NN}} = 200\text{GeV}$ ) elliptic flow spectra for identified particles: (a)  $v_2$  vs  $p_T$  and (b)  $v_2$  vs  $KE_T$ . [4]



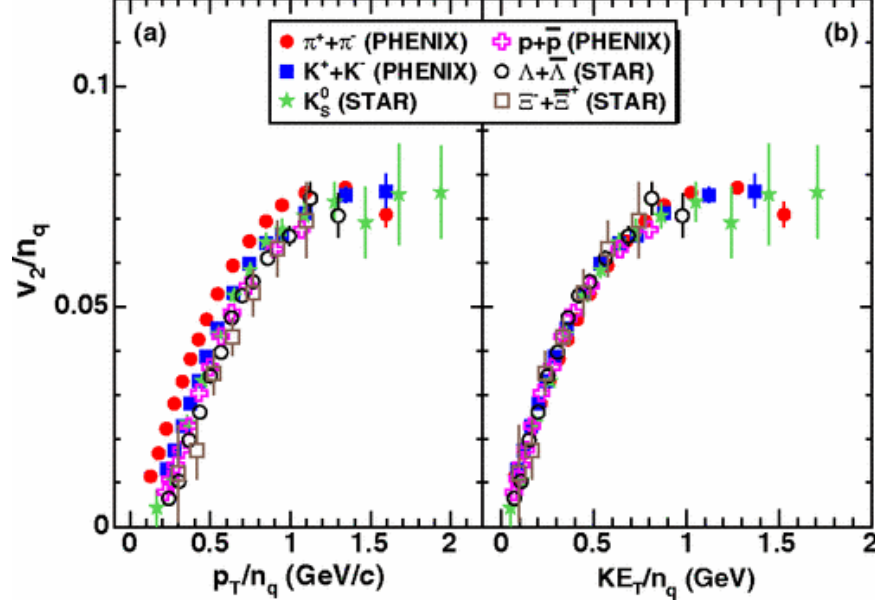


**Figure 3.6:** Minimum-bias Au+Au ( $\sqrt{s_{NN}} = 200\text{GeV}$ ) elliptic flow spectra for identified particles: (a)  $\frac{v_2}{n_q}$  vs  $\frac{p_T}{n_q}$  and (b)  $\frac{v_2}{n_q}$  vs  $\frac{KE_T}{n_q}$ . [4]

### 3.6.3 Direct and Thermal Photons

In the QGP, a quark and an antiquark can annihilate to produce a photon and a gluon. It is also possible for the pair to annihilate and produce two photons, but the probability of this process is smaller than the former by about two orders of magnitude. Furthermore, a quark (or an antiquark) can interact with a gluon to produce an antiquark (or a quark) and a photon, a process analogous to Compton scattering in QED. Just like the leptons described in the previous section, the photons produced in the QGP can only interact with the medium electromagnetically. Therefore, they undergo minimal scattering before being detected, and hence can be used to probe the thermodynamical state of the medium at the time of their creation.[39] Photons can also be produced after hadronization as a result of the scattering of the hadrons within the evolved medium. However, the nature of the  $p_T$  distribution is different in this case, and this difference helps distinguish these photons from the direct photons produced by partonic interactions.[38]

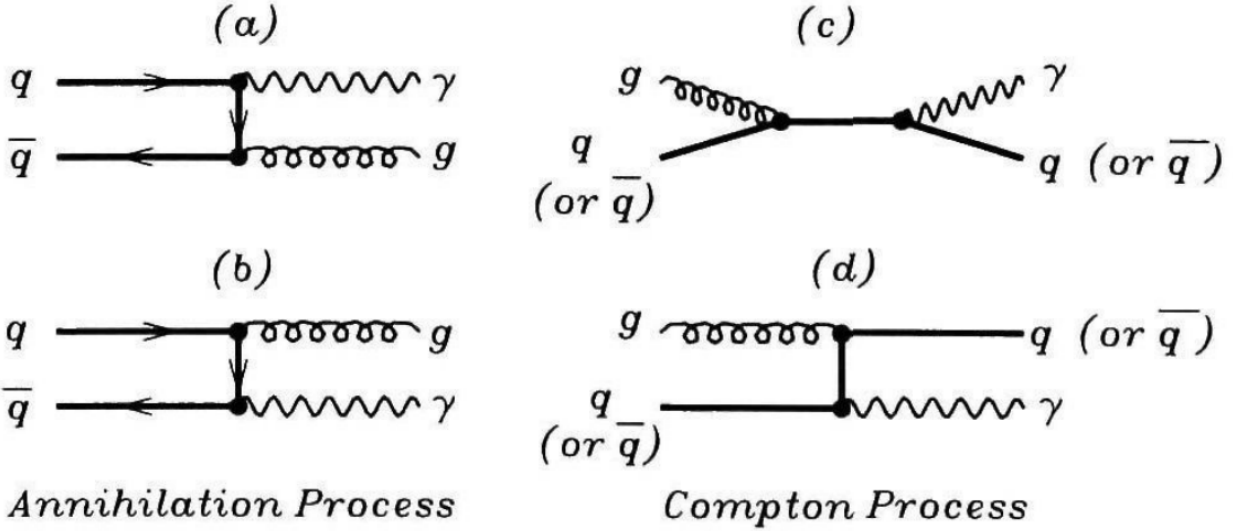


**Figure 3.7:** Feynman diagram representing the production of photons from quarks and gluons. (a) and (b) represent annihilation processes, whereas (c) and (d) represent Compton processes.[39]

### 3.6.4 Strangeness Enhancement

The interacting nuclei carry no net strangeness before colliding, and so a post-collision observation of strange and multi-strange particles can be a signal for an antecedent existence of deconfined quarks and gluons [15]. Strangeness can also be produced in hadron-hadron collisions. However, it is enhanced in nucleus-nucleus collisions in which a large number of hadrons are produced and are in chemical equilibrium at very high temperatures. The enhancement is exemplified by the ratio of the production of the strange kaons to that of the non-strange pions, which are the most abundant hadrons produced from nucleus-nucleus collisions. Kaon yield increases more rapidly than does pion yield as the temperature increases. This can be shown mathematically by treating the system as a hadron gas in thermal and chemical equilibrium that follows the Bose-Einstein distribution, but it is beyond the scope of this thesis [39]. ..... connect to big picture... why is strangeness enhancement interesting? .... phase space suppression? ..... chiral symmetry restoration.....?

### 3.6.5 Jet Quenching

A scattering event in which the participants transfer a large amount of their original momenta is called hard scattering. The products of the scattering are called jets. In heavy-ion collisions, most hard scatterings are the results of two partons from the opposite nuclei scattering off of each other. These partons can lose their momenta by strongly interacting with a medium made of deconfined quarks and gluons. Therefore, the properties of the jets, as carried by the final state hadrons, should be different for collisions that produce the QGP as compared to those that don't, and hence they can be used as signatures and probes of QGP. Figure 3.8 illustrates the quenching of jets that have to travel long distances in the medium. Formalisms developed to study jet quenching due to radiative and collisional energy losses are detailed in [28].

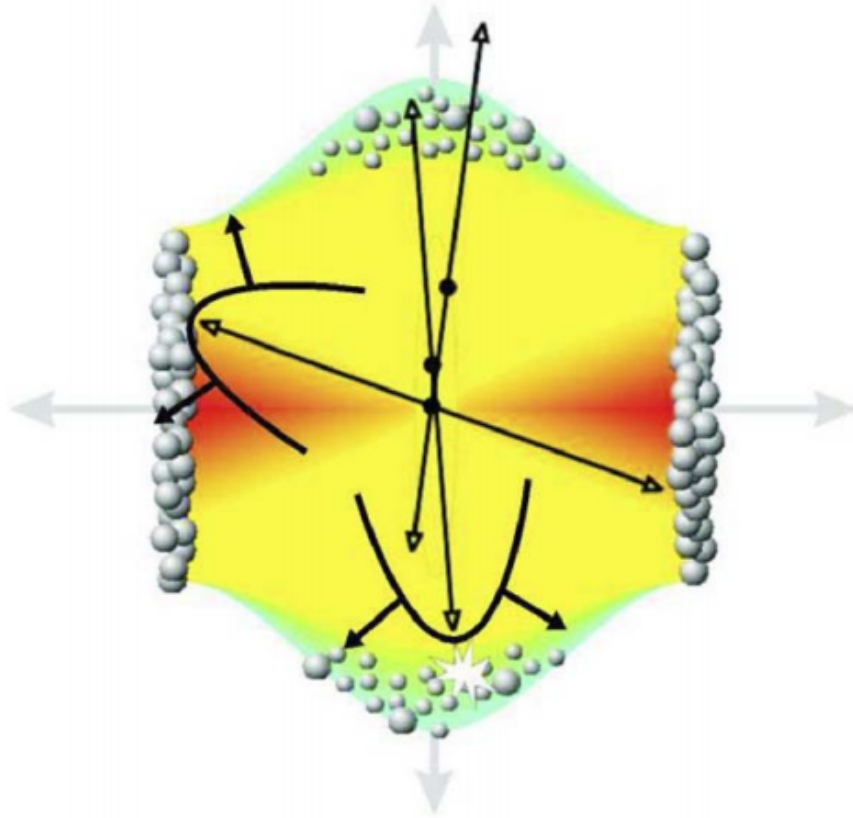


**Figure 3.8:** Illustration of jet quenching. Two jets are produced from each of the hard scatterings occurring at the locations of the solid dots. Jets originating closer to the initial surface are more probable to propagate outside the medium, as shown. Jets opposite to them interact with the medium, losing their energy and resulting in bow front shock waves.[36]

## 3.7 The Beam Energy Scan Program

The RHIC, in 2010, started a multi-phase Beam Energy Scan (BES) program to study the QCD phase diagram. The collider has two different detectors that are currently operational, STAR and PHENIX, which facilitate the cross-checking of results. Between 2010 and 2011, under the exploratory phase I of the BES program, 7.7, 11.5 (not completed in PHENIX), 19.6, 27, and 39 GeV collisions were completed using pairs of Au nuclei. Together with the data formerly collected by the RHIC at higher collision energies, BES phase I data can scan the interval from 450 MeV to 20 MeV in  $\mu_B$  space [25, 23]. One of the things that can be studied with the data associated with this region of the phase space is statedly the possibility of a “turn-off of new phenomena already established at higher RHIC energies” (<https://drupal.star.bnl.gov/STAR/starnotes/public/sn0493>). Results corresponding to the high- $\mu_B$  region might provide evidence of a first order phase transition, and possibly the critical point [23].

The manifestation of such phenomena would be in terms of the fluctuations in the properties of the post-collision system. One can, for instance, study the scaling of the transverse energy after the collision with the longitudinal energy at the time of the collision,  $\sqrt{s_{NN}}$ . This can be done in multiple ways for a detector like STAR or PHENIX that is made up of sub-systems such as the TOF detectors, TPCs/Time Expansion Chambers, as well as calorimeters. The next chapter gives an example of the measurement of transverse energy using BES data from PHENIX calorimeters. Also, the next chapter and the ones after it contain the procedures and the results of the analysis of the BES data from STAR using the identified particles spectra.

# Chapter 4

## Measurement of Transverse Energy

This chapter introduces the definitions of transverse energy, ways to measure it using different detectors, and particular examples for the detectors at the RHIC.

### 4.1 Definition of Transverse Energy

In theory,  $E_T$  from a collision can be defined as the sum of the transverse masses,  $m_T$ , of all the particles produced in the collision, i.e.,

$$E_T \equiv \sum_i m_{T,i} \quad (4.1)$$

with

$$m_T \equiv \sqrt{p_T^2 + m^2} \quad (4.2)$$

where  $m$  is the rest mass of the particle and  $p_T$  is its transverse momentum. Using this definition to calculate the  $E_T$  requires perfect identification of all the particles. It has not been possible to do so in experiments, and so a more feasible, operational definition of  $E_T$  is fabricated. A commonly accepted definition in case of the feasibility of calorimetric measurements is [5, 12]:

$$E_T = \sum_i E_i \sin \theta_i, \quad (4.3)$$

473

$$\frac{dE_T}{d\eta} = \sin\theta \frac{dE}{d\eta}, \quad (4.4)$$

474 where the index  $i$  runs over all the particles going into a fixed solid angle for each event,  
 475  $\theta$  is the polar angle, i.e, the angle with respect to the beam axis,  $\eta$  is the pseudorapidity  
 476 defined as

$$\eta \equiv -\ln \tan \frac{\theta}{2}, \quad (4.5)$$

477 and  $E_i$  is the energy deposited in the calorimeter by the  $i^{th}$  particle.  $E_i$  is considered to be,  
 478 by convention [6], the following

$$E_i = \begin{cases} E_i^{tot} - m_0 & \text{for baryons} \\ E_i^{tot} + m_0 & \text{for anti-baryons} \\ E_i^{tot} & \text{otherwise} \end{cases} \quad (4.6)$$

479 where  $E_i^{tot}$  is the total energy of the  $i^{th}$  particle defined canonically as

$$E^{tot} \equiv \sqrt{p^2 + m_0^2} \quad (4.7)$$

480 and  $m_0$  is the particle's rest mass. In order to account for the portion of the emitted  
 481 transverse energy not detected or overestimated by the calorimeters, corrections are made  
 482 based on GEANT simulations.

## 483 **4.2 $E_T$ Measurement with Calorimeters**

### 484 **4.2.1 Calorimeter**

### 485 **4.2.2 $E_T$ from PHENIX**

486 Adare et al. [3] use calorimetry in PHENIX to analyze the transverse energy corresponding  
 487 to several different pairs of species colliding at a range of energies. They use the raw  
 488 transverse energy measured by the EMCal,  $E_{TEMC}$ , to obtain the total hadronic  $E_T$  by

489 making corrections in three different steps. They first scale the data by a constant factor  
 490 calculated to account for the fiducial acceptance in azimuth and pseudorapidity. The second  
 491 factor is calculated to adjust for the effects of the calorimeter towers that are disabled. The  
 492 third factor,  $k$ , is computed as follows

$$k = k_{response} \times k_{inflow} \times k_{losses} \quad (4.8)$$

493 where  $k_{response}$  corresponds to hadronic particles only depositing a fraction of their total  
 494 energy while passing through the EMCal,  $k_{inflow}$  is attributable to the energy deposited  
 495 by particles coming from outside the EMCal's fiducial aperture, and  $k_{losses}$  accounts for  
 496 the energy not registered in the EMCal due to energy thresholds, edge effects, and more  
 497 importantly due to the particles that make it into the fiducial aperture but decay into  
 498 products outside the aperture.

## 499 4.3 $E_T$ Measurement with Tracking Detectors

500 Transverse energy analysis can be done using tracking detectors as well if they are able  
 501 to produce measurements of other physical quantities that implicitly contain information  
 502 about the transverse energy. Specifically, the charged particle multiplicity distributions with  
 503 respect to the transverse momenta can be used to calculate the particle's transverse energy  
 504 pseudorapidity density. In fact, since the corrections related to the tracking detectors are  
 505 very different from those related to the calorimeters, results from the two different methods  
 506 can be used to test the assumptions involved in each.

### 507 4.3.1 Tracking and Particle Identification

508 The tracking detectors in experiments such as the STAR (Solenoidal Tracker At RHIC)  
 509 experiment and ALICE (A Large Ion Collider Experiment) at CERN include Time Projection  
 510 Chambers (TPCs) and Time-of-Flight (TOF) detectors that can give us the  $p_T$  spectra, yields  
 511 and particle ratios of the identified charged hadrons [27, 2]. The TPCs provide measurements  
 512 of particle trajectories – that can be used to determine the momenta for low-momentum

513 particles – and of their specific energy loss,

$$\frac{dE}{dx}, \quad (4.9)$$

514 which can be used with the trajectories to make particle identifications (PID) using the  
 515 Bethe-Bloch formula [10]. TOF detectors, on the other hand, cover the high-momentum part  
 516 of the measurements. In ALICE, the combination of the measurements of the TPC with those  
 517 of the Inner Tracking System (ITS) effectively adds the tracking length, thereby improving  
 518 the resolution of the measured  $p_T$  spectrum. Details about the PID and momentum  
 519 determination capabilities of the detectors in ALICE can be found in [13].

520 The  $p_T$  spectra, available as the counts  $\frac{d^2N}{dydp_T}$  with respect to  $p_T$ , can be used to calculate  
 521  $\frac{dE_T}{d\eta}$  as formulated in the following section.

### 522 4.3.2 Calculation of $\frac{dE_T}{d\eta}$ from $p_T$ spectra

523 In relativistic heavy ion collisions, rapidity ( $y$ ) is defined as follows:

$$y \equiv \frac{1}{2} \ln \frac{E + p_z}{E - p_z}, \quad (4.10)$$

where  $E$  is given by equation 4.7 and  $p_z$  is the component of the momentum parallel to the beam axis. Pseudorapidity,  $\eta$ , is just  $y$  with  $m_0 = 0$ :

$$\begin{aligned} \eta &= \frac{1}{2} \ln \frac{p + p_z}{p - p_z} \\ &= \frac{1}{2} \ln \frac{1 + \cos \theta}{1 - \cos \theta} \\ &= \frac{1}{2} \ln \frac{2 \cos^2 \frac{\theta}{2}}{2 \sin^2 \frac{\theta}{2}} \end{aligned}$$

$$\therefore \eta = - \ln \left| \tan \frac{\theta}{2} \right| \quad (4.11)$$



524 Note that the absolute value is not necessary for  $0 \leq \theta \leq \pi$ . Then, taking the exponential  
 525 of both sides of the above equation and using Euler's formula, we get:

$$\sin \theta = \frac{1}{\cosh \eta}. \quad (4.12)$$

Hence,

$$\begin{aligned} p &= \frac{p_T}{\sin \theta} \\ &= p_T \cosh \eta, \end{aligned}$$

526 and so we have

$$E_T = E \sin \theta = \frac{\sqrt{p_T^2 \cosh^2 \eta + m_0^2}}{\cosh \eta} \quad (4.13)$$

527 The Jacobian for the transformation from  $y$ -space to  $\eta$ -space is derived, by differentiating  
 528  $y$  with respect to  $\eta$  (obtained from equations 4.10 and 4.11), to be:

$$\frac{\partial y}{\partial \eta} = \frac{p_T \cosh \eta}{\sqrt{m_0^2 + p_T^2 \cosh^2 \eta}} \quad (4.14)$$

529 From equations 4.13 and 4.14, we can see that the product of  $E_T$  with the Jacobian is  
 530 equal to  $p_T$ . That leads to a formulation of  $\frac{dE_T}{d\eta}$  as a function of only  $\eta$  and  $p_T$ :

$$\frac{dE_T}{d\eta} = \frac{1}{2a} \int_0^{10 \text{ GeV}/c} \int_{-a}^a p_T \frac{d^2 N}{dy dp_T} d\eta dp_T \quad (4.15)$$

531 where  $a$  and  $-a$  are the bounds for  $\eta$ .

### 532 4.3.3 Tracking Detectors in STAR

533 In the STAR experiment, the TPC is the primary tracking detector. It is 4.2 m long and it  
 534 cylindrically enshrouds the accelerator beam pipe from its outside, with an inner diameter  
 535 of 1 m and an outer diameter of 4 m [24]. It covers a pseudorapidity range of  $|y| < 1.8$   
 536 in all of azimuth in terms of acceptance of charged particles. It can identify particles with

537 momenta over 100 MeV/c up to about 1 GeV/c as well as measure their momenta from  
 538 100 MeV/c to 30 GeV/c [8]. Figure 4.1 shows the PID capability of the STAR TPC for  
 539 very high-multiplicity events [19]. Separation of pions from protons is demonstrated up to a  
 540 little more than 1 GeV/c. At higher momenta, separating particles is more difficult because  
 541 their energy loss has lower dependence on the rest mass [8]. The TOF system in STAR,  
 542 with a time resolution of  $\lesssim 100$  ps, aids PID at higher momenta. However, at intermediate  
 543  $p_T$ , between  $\approx 2.0$  and 4.0 GeV/c, the TPC by itself cannot distinguish between pions and  
 544 protons and the TOF by itself cannot separate pions from kaons. This problem is resolved  
 545 by utilizing the fact that the dependence of the particle velocity on  $p_T$  – in case of the TPC  
 546 – is different from that of the energy loss on  $p_T$  in case of the TPC; combining the results  
 from the two, hence, makes PID feasible in this  $p_T$  range. [31]

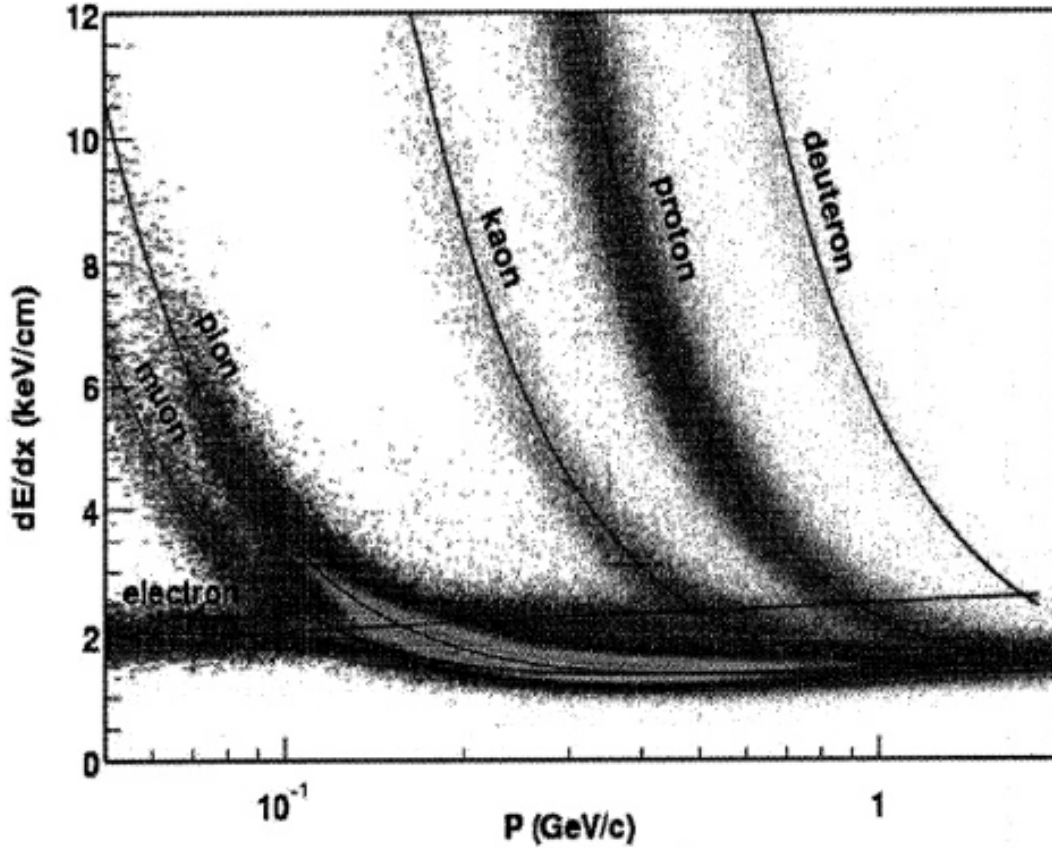


**Figure 4.1:** Energy loss distribution in the STAR TPC for primary and secondary particles.  
 [19].

547

# Chapter 5

## Data Analysis

The analysis of the data involved extrapolating the available spectra and using the results from the fits to calculate the transverse energy for all the available spectra and the particle multiplicity corresponding to charged particles. Details follow.

### 5.0.1 STAR $p_T$ spectra

This thesis details the method of transverse energy analysis through the use of  $p_T$  spectra from the STAR BES data. As described in section 4.3.3, the TPCs and TOF detectors in STAR can identify particles as well as their trajectories and ultimately their multiplicity distributions with respect to the momenta. Adamczyk et al. [2] report the results for the  $p_T$  spectra for six different identified hadrons,  $\pi^+$ ,  $\pi^-$ ,  $K^+$ ,  $K^-$ ,  $p$ , and  $\bar{p}$ , from the STAR experiment. The spectra come from Au+Au collisions – at  $\sqrt{s_{NN}} = 7.7$ , 11.5, and 39 GeV in the year 2010 and at  $\sqrt{s_{NN}} = 19.6$  and 27 GeV in 2011 – under the BES Program. Figure 5.1 [2] shows the spectra corresponding to 39 GeV collisions categorized into seven different collision centralitiy classes. These spectra, and their counterparts for the rest of the energies, were used to calculate an estimate of the total transverse energy per event per particle species. This result was then used to estimate the total transverse energy due to all the collision products.

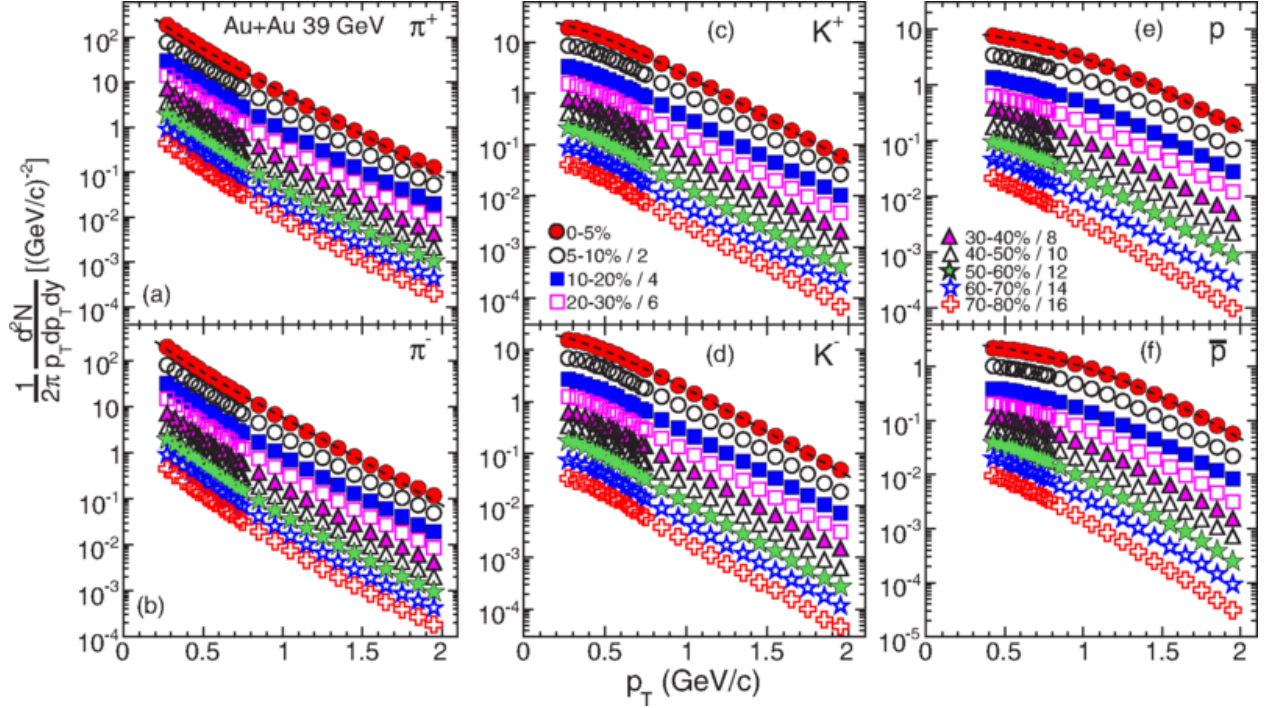


**Figure 5.1:** Transverse momentum spectra for  $\pi^+$ ,  $\pi^-$ ,  $K^+$ ,  $K^-$ ,  $p$ , and  $\bar{p}$  at midrapidity ( $|y| < 0.1$ ) from 39 GeV Au+Au collisions at RHIC. The fitting curves on the 0-5% central collision spectra for pions, kaons, and protons/anti-protons represent, respectively, the Bose-Einstein,  $m_T$ -exponential, and double-exponential functions. [2].

The corrections applied by Adamczyk et al. [2] to the raw data to obtain the spectra and the reported systematic uncertainties in their results are discussed below (under construction)

.....

## 5.1 Extrapolation of Spectra

The available spectra were limited to a range of transverse momenta ranging from around 0.25 GeV/c to around 2 GeV/c (for pions). To account for the transverse energy corresponding to the momenta for which there was no available data, an extrapolation had to be used. The model used for the extrapolation and the associated statistics are discussed below.

### 5.1.1 Boltzmann-Gibbs Blast Wave

The blast wave is a common model used in the analysis of the particle spectra.[????] The specific model used in this thesis is the Boltzmann-Gibbs blast wave (BGBW) as represented in equation ?? . It has the parameters mass, temperature, beta, v, and n. I assume that any anomalies in the magnitude of the normalization parameter do not affect the results significantly insomuch as they don't lead to:

- (a) unreasonable relative errors in the extrapolated values of the transverse energy,
- (b) any of the spectral fits having the extrapolated transverse energy more than that calculated from just the available spectra, and
- (c) for the 200 GeV collision samples, at least, the extrapolation at higher  $p_T$  being more than that at lower  $p_T$ .

$$BGBW \tag{5.1}$$

### 5.1.2 Fitting Spectra to BGBW

Figure 5.2 presents an example of a Boltzmann-Gibbs Blast Wave (BGBW) fit on one of the individual particle spectra with the goodness-of-fit as well as other statistics and the associated errors. A parallel-coordinates plot is presented in the next chapter in fig. 6.1, which shows the measured centralities, two of the good-fit parameters, and the calculated transverse energies for 270 different particles (lambdas not included).

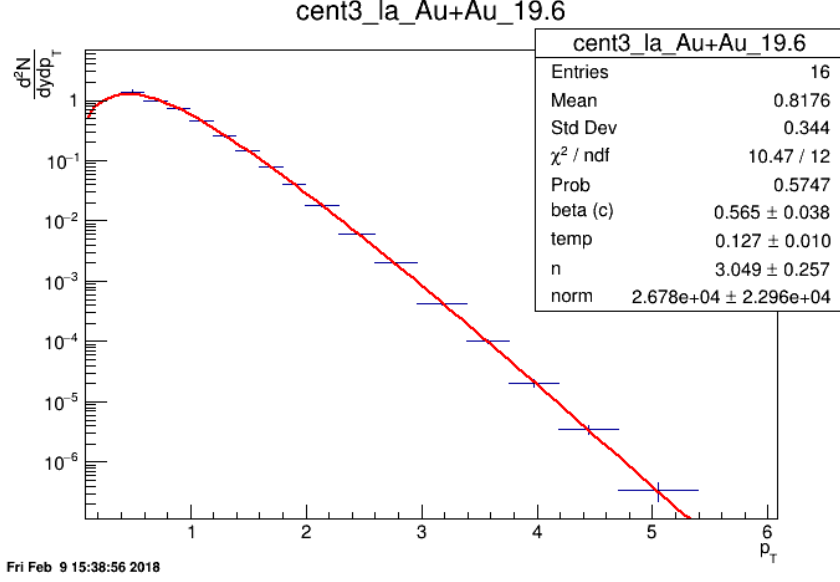


**Figure 5.2:** Red curve shows the Boltzmann-Gibbs blast wave functional fit on the PRELIMINARY transverse momentum spectrum for lambda particles identified by the STAR detector for 19.6 GeV Au+Au collisions (10-15% central). Parameters extracted from the chi-square goodness-of-fit test, as well as other statistics, are shown in the box on the top right.

## 5.2 Calculations from the Spectral Fits

### 5.2.1 Calculation of $\frac{dE_T}{dy}$ , $\frac{dE_T}{d\eta}$ , $\frac{dN_{ch}}{dy}$ , and $\frac{dN_{ch}}{d\eta}$

### 5.2.2 Corrections for Unidentified Particles and Estimation of Total $E_T$

It is reasonable to assume that, at high energies, there should be roughly the same multiplicity of all the isospin states of a final state particle. Table 5.1 lists the isospin states associated with the pion, the kaon, the proton, and the lambda particles.

Particle	Isospin multiplets
pion	$\pi^+, \pi^0, \pi^-$
kaon	$K^+, K^0, K^-, \bar{K}^0$
proton	$p, n$
lambda	$\Lambda$

**Table 5.1:** Isospin states of different identified particles.

598 .....text content.....

$$E_T = 3E_T^\pi + 4E_T^K + 4E_T^p + 2E_T^\Lambda \quad (5.2)$$

599 .....text content.....

### 600 **5.2.3 Lambdas Centralitiy Adjustments and $E_T$ Interpolations**

601 The centrality bins corresponding to the lambdas spectra were slightly different from those  
602 corresponding to the rest of the particles.....

## 603 **5.3 Uncertainties**

604 ..... 100% correlated point-to-point and uncorrelated between particles..... ?

# Chapter 6

## Results

Present results and comparisons to Adare et al.....

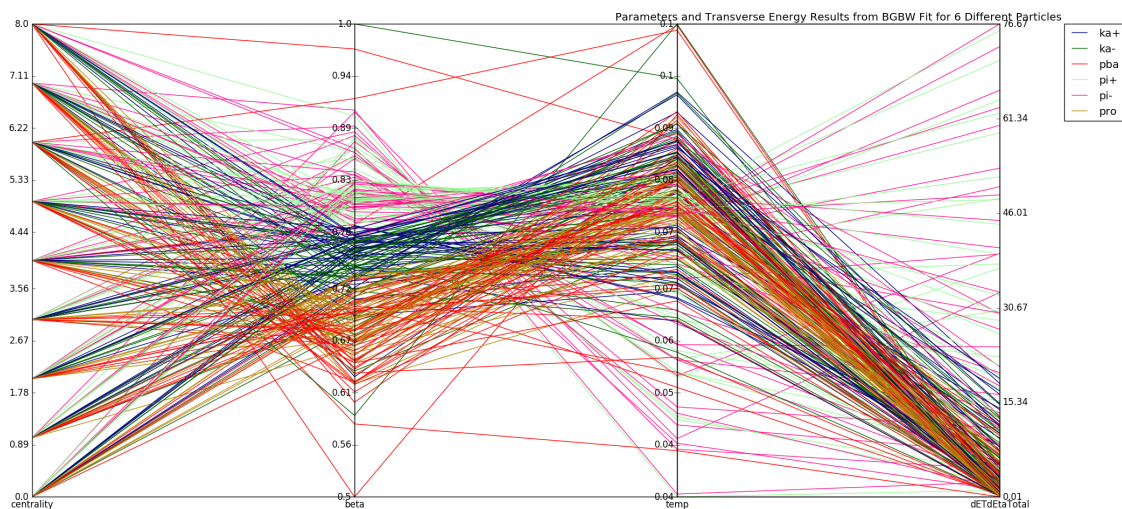


**Figure 6.1:** Parallel coordinates plot for 270 different spectra relating 6 different identified particles (color-coded) to their respective collision centrality classes, good-fit parameters, and the transverse energy calculated using said parameters.



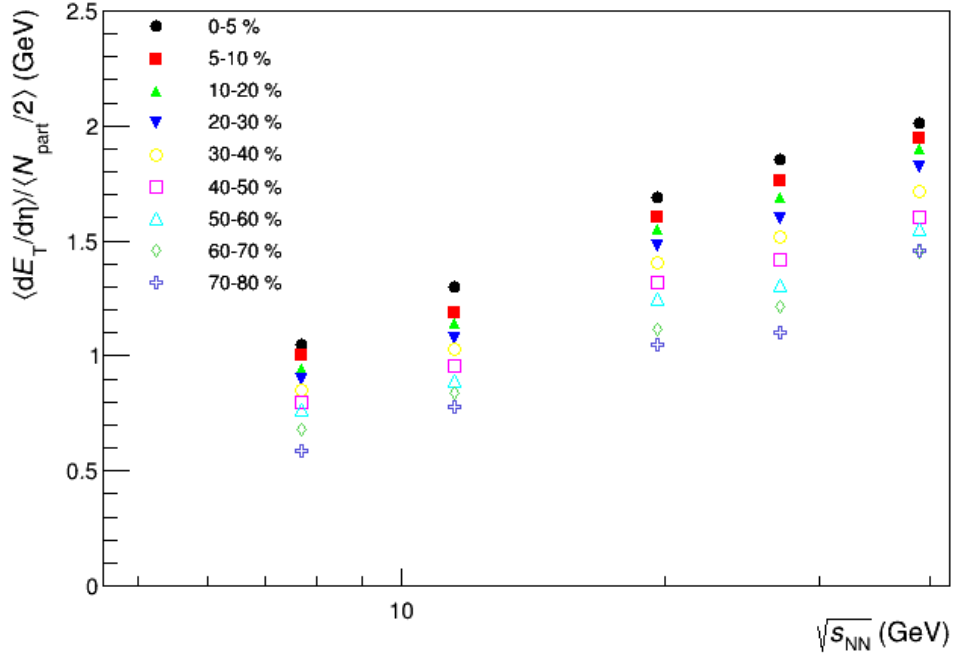


**Figure 6.2:**  $(dE_T/d\eta)/0.5N_{part}$  at midrapidity as a function of  $\sqrt{s_{NN}}$  for different centralities.

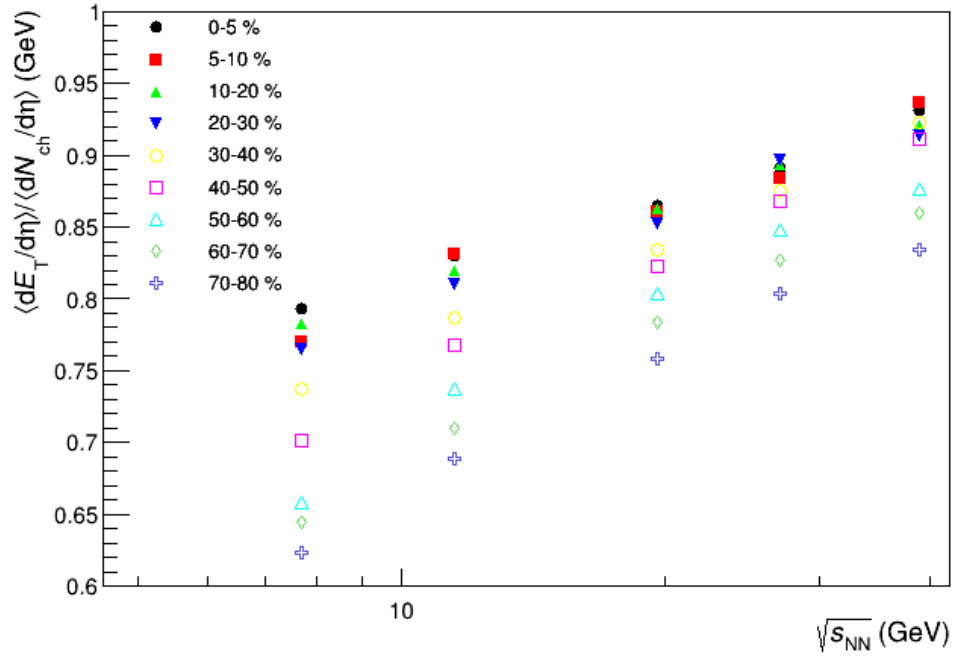


**Figure 6.3:**  $(dE_T/d\eta)/(dN_{ch}/d\eta)$  at midrapidity as a function of  $\sqrt{s_{NN}}$  for different centralities.

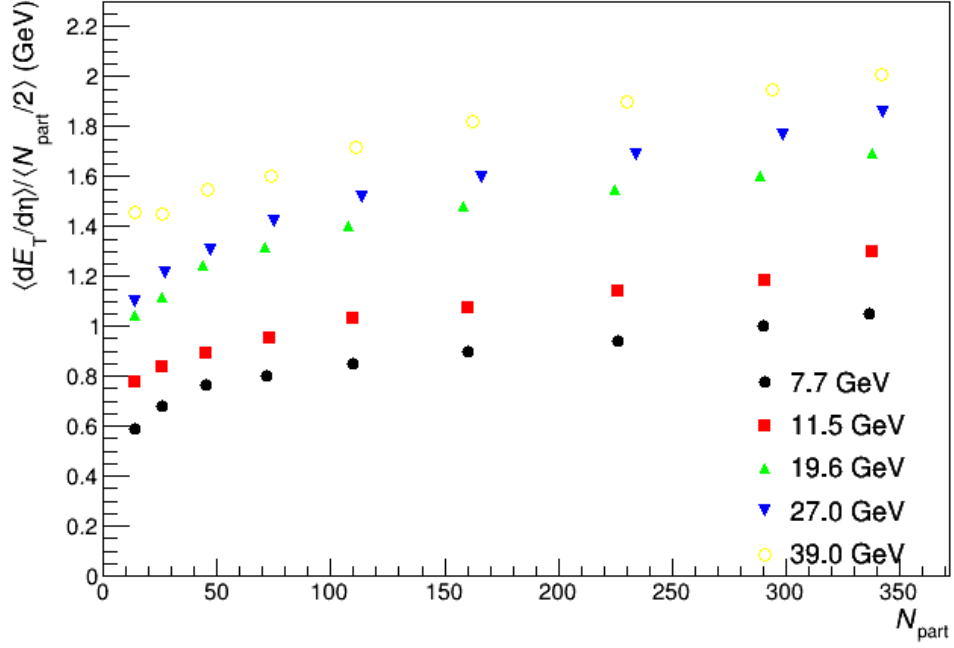


**Figure 6.4:**  $\langle dE_T/d\eta \rangle / 0.5N_{part}$  at midrapidity as a function of  $N_{part}$  for different centralities.

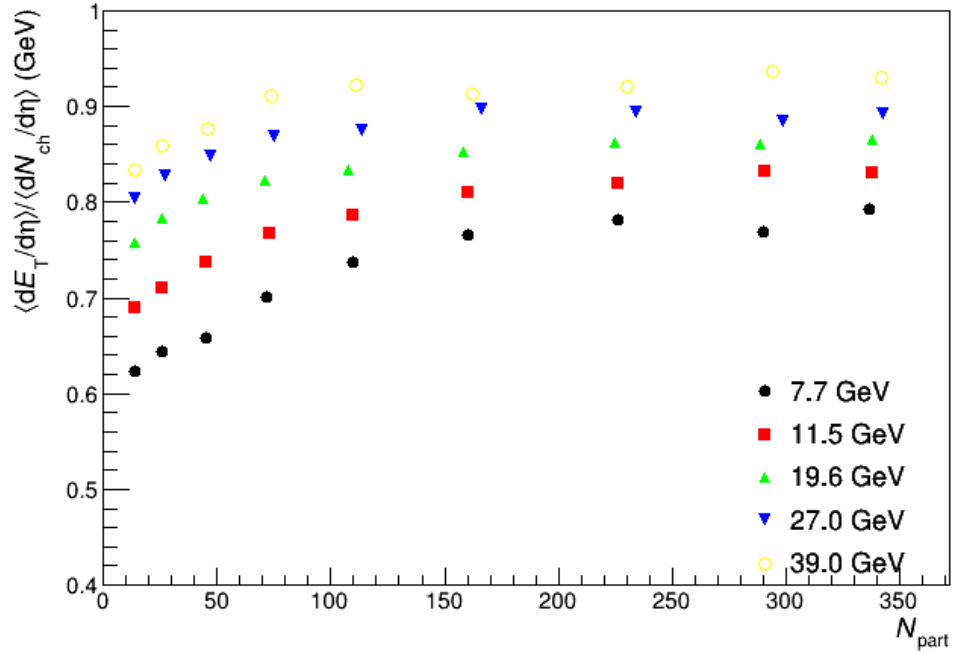


**Figure 6.5:**  $\langle dE_T/d\eta \rangle / \langle dN_{ch}/d\eta \rangle$  at midrapidity as a function of  $N_{part}$  for different centralities.

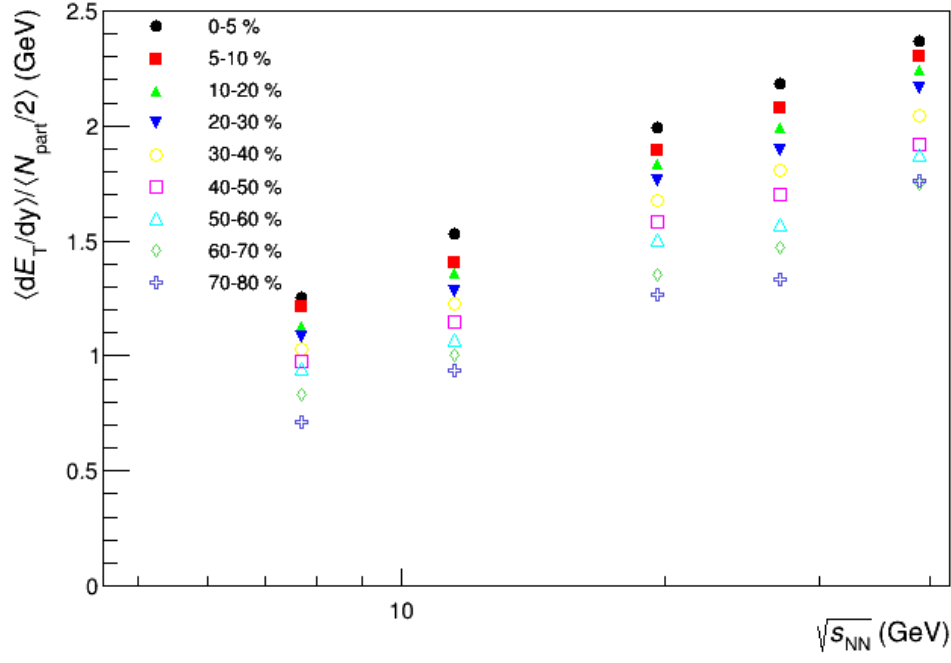


**Figure 6.6:**  $\langle dE_T/dy \rangle / 0.5N_{part}$  at midrapidity as a function of  $\sqrt{s_{NN}}$  for different centralities.

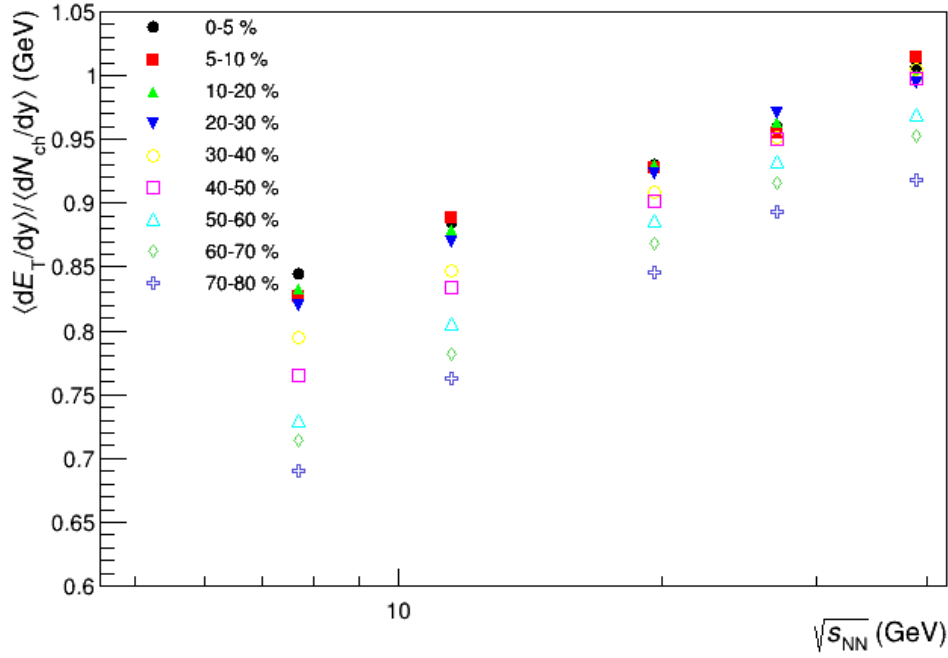


**Figure 6.7:**  $\langle dE_T/dy \rangle / \langle dN_{ch}/dy \rangle$  at midrapidity as a function of  $\sqrt{s_{NN}}$  for different centralities.

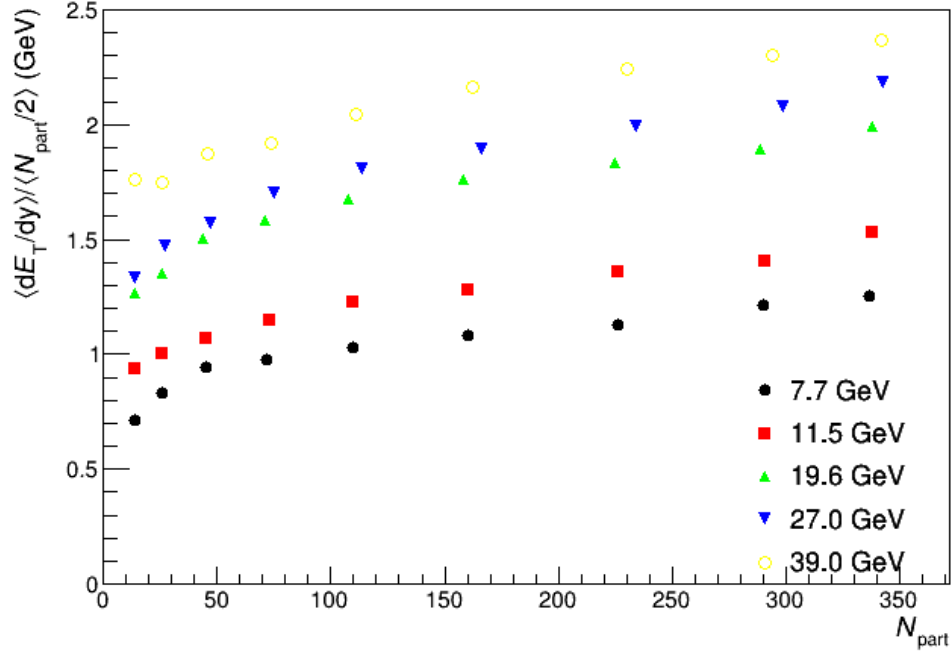


**Figure 6.8:**  $\langle dE_T/dy \rangle / 0.5N_{part}$  at midrapidity as a function of  $N_{part}$  for different centralities.

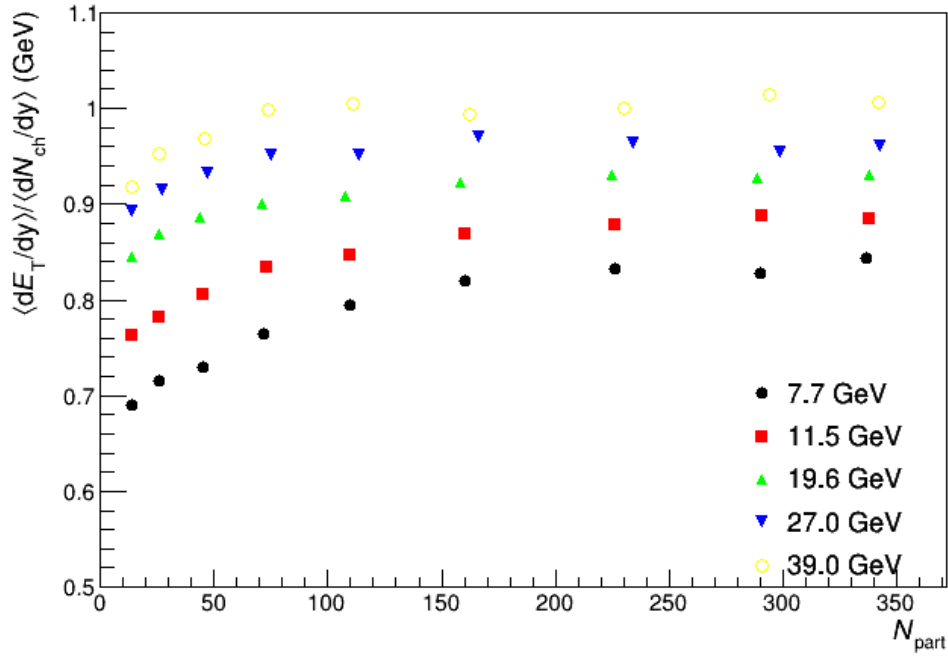


**Figure 6.9:**  $\langle dE_T/dy \rangle / \langle dN_{ch}/dy \rangle$  at midrapidity as a function of  $N_{part}$  for different centralities.

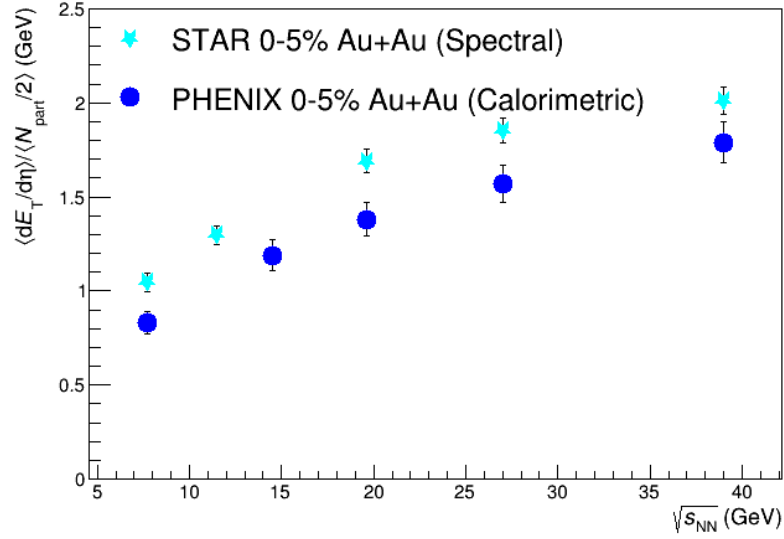


**Figure 6.10:**  $\frac{dE_T}{d\eta} / 0.5N_{part}$  for 0-5% central collisions at midrapidity as a function of  $\sqrt{s_{NN}}$ . The PHENIX data are from [3]. The error bars represent the total statistical and systematic uncertainties.

## 608 **Chapter 7**

## 609 **Conclusion**

610 Summary and implications

# Chapter 8

## Future Work

### 8.1 Goodness of Fit

A maximum likelihood? fit method can be adopted to compare the results with those using the chi-squared fits.

### 8.2 Bjorken Energy Density Estimate

Apart from the transverse energy, the calculation of the initial energy density,  $\epsilon$ , as given by the Bjorken formula in eq. 3.8, requires the estimate of other physical quantities. Adare et al.[3] use the Glauber model to determine  $A_T$ , the area of the intersection of the two nuclei in the transverse plane. Since the results in this thesis are cross-checked with those in [3], it would be reasonable to use the same model in the future work pertaining to this thesis.  $\tau_0$ , the proper time at the moment of QGP equilibration, also depends on the model of the collision. However, the product of  $\epsilon$  and  $\tau_0$  is often used instead of just  $\epsilon$  to study how the energy density scales with the collision energy and the number of participants.

## 625 **8.3 Asymmetric beams**

626 The codes in the repository can be used to analyze more data. In fact, since there is more  
627 data available on collisions of asymmetric systems such as d+Au?, we can expect it to be a  
628 test to tell if the assumptions? used in this analysis scale to such domains?



# Bibliography

630 [1] Adam, J., Adamova, D., Aggarwal, M. M., Aglieri Rinella, G., Agnello, M., Agrawal,  
 631 N., Ahammed, Z., Ahmad, S., Ahn, S. U., Aiola, S., Akindinov, A., Alam, S. N., Silva  
 632 De Albuquerque, D., Aleksandrov, D., Alessandro, B., Alexandre, D., Alfaro Molina,  
 633 J. R., Alici, A., Alkin, A., Millan Almaraz, J. R., Alme, J., Alt, T., Altinpinar, S.,  
 634 Altsybeev, I., Alves Garcia Prado, C., Andrei, C., Andronic, A., Anguelov, V., Anticic,  
 635 T., Antinori, F., Antonioli, P., Aphecetche, L. B., Appelshaeuser, H., Arcelli, S., Arnaldi,  
 636 R., Arnold, O. W., Arsene, I. C., Arslanok, M., Audurier, B., Augustinus, A., Averbek,  
 637 R. P., Azmi, M. D., Badala, A., Baek, Y. W., Bagnasco, S., Bailhache, R. M., Bala,  
 638 R., Balasubramanian, S., Baldisseri, A., Baral, R. C., Barbano, A. M., Barbera, R.,  
 639 Barile, F., Barnafoldi, G. G., Barnby, L. S., Ramillien Barret, V., Bartalini, P., Barth,  
 640 K., Bartke, J. G., Bartsch, E., Basile, M., Bastid, N., Basu, S., Bathen, B., Batigne,  
 641 G., Batista Camejo, A., Batyunya, B., Batzing, P. C., Bearden, I. G., Beck, H., Bedda,  
 642 C., Behera, N. K., Belikov, I., Bellini, F., Bello Martinez, H., Bellwied, R., Belmont Iii,  
 643 R. J., Belmont Moreno, E., Belyaev, V., Bencedi, G., Beole, S., Berceanu, I., Bercuci, A.,  
 644 Berdnikov, Y., Berenyi, D., Bertens, R. A., Berzano, D., Betev, L., Bhasin, A., Bhat, I. R.,  
 645 Bhati, A. K., Bhattacharjee, B., Bhom, J., Bianchi, L., Bianchi, N., Bianchin, C., Bielcik,  
 646 J., Bielcikova, J., Bilandzic, A., Biro, G., Biswas, R., Biswas, S., Bjelogric, S., Blair, J. T.,  
 647 Blau, D., Blume, C., Bock, F., Bogdanov, A., Boggild, H., Boldizar, L., Bombara, M.,  
 648 Book, J. H., Borel, H., Borissov, A., Borri, M., Bossu, F., Botta, E., Bourjau, C., Braun-  
 649 Munzinger, P., Bregant, M., Breitner, T. G., Broker, T. A., Browning, T. A., Broz, M.,  
 650 Brucken, E. J., Bruna, E., Bruno, G. E., Budnikov, D., Buesching, H., Bufalino, S., Buncic,  
 651 P., Busch, O., Buthelezi, E. Z., Bashir Butt, J., Buxton, J. T., Cabala, J., Caffarri, D.,  
 652 Cai, X., Caines, H. L., Calero Diaz, L., Caliva, A., Calvo Villar, E., Camerini, P., Carena,  
 653 F., Carena, W., Carnesecchi, F., Castillo Castellanos, J. E., Castro, A. J., Casula, E.  
 654 A. R., Ceballos Sanchez, C., Cepila, J., Cerello, P., Cerkala, J., Chang, B., Chapeland,  
 655 S., Chartier, M., Charvet, J.-L. F., Chattopadhyay, S., Chattopadhyay, S., Chauvin, A.,  
 656 Chelnokov, V., Cherney, M. G., Cheshkov, C. V., Cheynis, B., Chibante Barroso, V. M.,  
 657 Dobrigkeit Chinellato, D., Cho, S., Chochula, P., Choi, K., Chojnacki, M., Choudhury, S.,  
 658 Christakoglou, P., Christensen, C. H., Christiansen, P., Chujo, T., Chung, S.-U., Cicalo,  
 659 C., Cifarelli, L., Cindolo, F., Cleymans, J. W. A., Colamaria, F. F., Colella, D., Collu, A.,

660 Colocci, M., Conesa Balbastre, G., Conesa Del Valle, Z., Connors, M. E., Contreras Nuno,  
 661 J. G., Cormier, T. M., Corrales Morales, Y., Cortes Maldonado, I., Cortese, P., Cosentino,  
 662 M. R., Costa, F., Crochet, P., Cruz Albino, R., Cuautle Flores, E., Cunqueiro Mendez,  
 663 L., Dahms, T., Dainese, A., Danisch, M. C., Danu, A., Das, D., Das, I., Das, S., Dash,  
 664 A. K., Dash, S., De, S., De Caro, A., De Cataldo, G., De Conti, C., De Cuveland, J.,  
 665 De Falco, A., De Gruttola, D., De Marco, N., De Pasquale, S., Deisting, A., Deloff,  
 666 A., Denes, E. S., Deplano, C., Dhankher, P., Di Bari, D., Di Mauro, A., Di Nezza,  
 667 P., Diaz Corchero, M. A., Dietel, T., Dillenseger, P., Divia, R., Djuvsland, O., Dobrin,  
 668 A. F., Domenicis Gimenez, D., Donigus, B., Dordic, O., Drozhzhova, T., Dubey, A. K.,  
 669 Dubla, A., Ducroux, L., Dupieux, P., Ehlers Iii, R. J., Elia, D., Endress, E., Engel, H.,  
 670 Epple, E., Erasmus, B. E., Erdemir, I., Erhardt, F., Espagnon, B., Estienne, M. D.,  
 671 Esumi, S., Eum, J., Evans, D., Evdokimov, S., Eyyubova, G., Fabbietti, L., Fabris, D.,  
 672 Faivre, J., Fantoni, A., Fasel, M., Feldkamp, L., Feliciello, A., Feofilov, G., Ferencei, J.,  
 673 Fernandez Tellez, A., Gonzalez Ferreiro, E., Ferretti, A., Festanti, A., Feuillard, V. J. G.,  
 674 Figiel, J., Araujo Silva Figueredo, M., Filchagin, S., Finogeev, D., Fionda, F., Fiore, E. M.,  
 675 Fleck, M. G., Floris, M., Foertsch, S. V., Foka, P., Fokin, S., Fragiacomio, E., Francescon,  
 676 A., Frankenfeld, U. M., Fronze, G. G., Fuchs, U., Furget, C., Furs, A., Fusco Girard, M.,  
 677 Gaardhoeje, J. J., Gagliardi, M., Gago Medina, A. M., Gallio, M., Gangadharan, D. R.,  
 678 Ganoti, P., Gao, C., Garabatos Cuadrado, J., Garcia-Solis, E. J., Gargiulo, C., Gasik, P. J.,  
 679 Gauger, E. F., Germain, M., Gheata, M., Ghosh, P., Ghosh, S. K., Gianotti, P., Giubellino,  
 680 P., Giubilato, P., Gladysz-Dziadus, E., Glassel, P., Gomez Coral, D. M., Gomez Ramirez,  
 681 A., Sanchez Gonzalez, A., Gonzalez, V., Gonzalez Zamora, P., Gorbunov, S., Gorlich,  
 682 L. M., Gotovac, S., Grabski, V., Grachov, O. A., Graczykowski, L. K., Graham, K. L.,  
 683 Grelli, A., Grigoras, A. G., Grigoras, C., Grigoryev, V., Grigoryan, A., Grigoryan, S.,  
 684 Grynyov, B., Grion, N., Gronefeld, J. M., Grosse-Oetringhaus, J. F., Grosso, R., Guber,  
 685 F., Guernane, R., Guerzoni, B., Gulbrandsen, K. H., Gunji, T., Gupta, A., Gupta, R.,  
 686 Haake, R., Haaland, O. S., Hadjidakis, C. M., Haiduc, M., Hamagaki, H., Hamar, G.,  
 687 Hamon, J. C., Harris, J. W., Harton, A. V., Hatzifotiadou, D., Hayashi, S., Heckel, S. T.,  
 688 Hellbar, E., Helstrup, H., Herghelegiu, A. I., Herrera Corral, G. A., Hess, B. A., Hetland,  
 689 K. F., Hillemanns, H., Hippolyte, B., Horak, D., Hosokawa, R., Hristov, P. Z., Humanic,

690 T., Hussain, N., Hussain, T., Hutter, D., Hwang, D. S., Ilkaev, R., Inaba, M., Incani,  
 691 E., Ippolitov, M., Irfan, M., Ivanov, M., Ivanov, V., Izucheev, V., Jacazio, N., Jacobs,  
 692 P. M., Jadhav, M. B., Jadlovská, S., Jadlovsky, J., Jahnke, C., Jakubowska, M. J., Jang,  
 693 H. J., Janik, M. A., Pahula Hewage, S., Jena, C., Jena, S., Jimenez Bustamante, R. T.,  
 694 Jones, P. G., Jusko, A., Kalinak, P., Kalweit, A. P., Kamin, J. A., Kang, J. H., Kaplin,  
 695 V., Kar, S., Karasu Uysal, A., Karavichev, O., Karavicheva, T., Karayan, L., Karpechev,  
 696 E., Kebschull, U. W., Keidel, R., Keijden, D. L., Keil, M., Khan, M. M., Khan, P.,  
 697 Khan, S. A., Khanzadeev, A., Kharlov, Y., Kileng, B., Kim, D. W., Kim, D. J., Kim,  
 698 D., Kim, H., Kim, J., Kim, M., Kim, S. Y., Kim, T., Kirsch, S., Kisel, I., Kiselev,  
 699 S., Kisiel, A. R., Kiss, G., Klay, J. L., Klein, C., Klein, J., Klein-Boesing, C., Klewin,  
 700 S., Kluge, A., Knichel, M. L., Knospe, A. G., Kobdaj, C., Kofarago, M., Kollegger, T.,  
 701 Kolozhvari, A., Kondratev, V., Kondratyeva, N., Kondratyuk, E., Konevskikh, A., Kopicik,  
 702 M., Kostarakis, P., Kour, M., Kouzinopoulos, C., Kovalenko, O., Kovalenko, V., Kowalski,  
 703 M., Koyithatta Meethalevedu, G., Kralik, I., Kravcukova, A., Krivda, M., Krizek, F.,  
 704 Kryshen, E., Krzewicki, M., Kubera, A. M., Kucera, V., Kuhn, C. C., Kuijer, P. G.,  
 705 Kumar, A., Kumar, J., Kumar, L., Kumar, S., Kurashvili, P., Kurepin, A., Kurepin, A.,  
 706 Kuryakin, A., Kweon, M. J., Kwon, Y., La Pointe, S. L., La Rocca, P., Ladron De Guevara,  
 707 P., Lagana Fernandes, C., Lakomov, I., Langoy, R., Lapidus, K., Lara Martinez, C. E.,  
 708 Lardeux, A. X., Lattuca, A., Laudi, E., Lea, R., Leardini, L., Lee, G. R., Lee, S., Lehas, F.,  
 709 Lemmon, R. C., Lenti, V., Leogrande, E., Leon Monzon, I., Leon Vargas, H., Leoncino, M.,  
 710 Levai, P., Li, S., Li, X., Lien, J. A., Lietava, R., Lindal, S., Lindenstruth, V., Lippmann,  
 711 C., Lisa, M. A., Ljunggren, H. M., Lodato, D. F., Lonne, P.-I., Loginov, V., Loizides, C.,  
 712 Lopez, X. B., Lopez Torres, E., Lowe, A. J., Luettig, P. J., Lunardon, M., Luparello,  
 713 G., Lutz, T. H., Maevskaya, A., Mager, M., Mahajan, S., Mahmood, S. M., Maire,  
 714 A., Majka, R. D., Malaev, M., Maldonado Cervantes, I. A., Malinina, L., Mal'Kevich,  
 715 D., Malzacher, P., Mamonov, A., Manko, V., Manso, F., Manzari, V., Marchisone, M.,  
 716 Mares, J., Margagliotti, G. V., Margotti, A., Margutti, J., Marin, A. M., Markert, C.,  
 717 Marquard, M., Martin, N. A., Martin Blanco, J., Martinengo, P., Martinez Hernandez,  
 718 M. I., Martinez-Garcia, G., Martinez Pedreira, M., Mas, A. J.-M., Masciocchi, S., Masera,  
 719 M., Masoni, A., Mastroserio, A., Matyja, A. T., Mayer, C., Mazer, J. A., Mazzoni,

720 A. M., Mcdonald, D., Meddi, F., Melikyan, Y., Menchaca-Rocha, A. A., Meninno, E.,  
 721 Mercado-Perez, J., Meres, M., Miake, Y., Mieskolainen, M. M., Mikhaylov, K., Milano,  
 722 L., Milosevic, J., Mischke, A., Mishra, A. N., Miskowiec, D. C., Mitra, J., Mitu, C. M.,  
 723 Mohammadi, N., Mohanty, B., Molnar, L., Montano Zetina, L. M., Montes Prado, E.,  
 724 Moreira De Godoy, D. A., Perez Moreno, L. A., Moretto, S., Morreale, A., Morsch, A.,  
 725 Muccifora, V., Mudnic, E., Muhlheim, D. M., Muhuri, S., Mukherjee, M., Mulligan, J. D.,  
 726 Gameiro Munhoz, M., Munzer, R. H., Murakami, H., Murray, S., Musa, L., Musinsky,  
 727 J., Naik, B., Nair, R., Nandi, B. K., Nania, R., Nappi, E., Naru, M. U., Ferreira Natal  
 728 Da Luz, P. H., Nattrass, C., Rosado Navarro, S., Nayak, K., Nayak, R., Nayak, T. K.,  
 729 Nazarenko, S., Nedosekin, A., Nellen, L., Ng, F., Nicassio, M., Niculescu, M., Niedziela,  
 730 J., Nielsen, B. S., Nikolaev, S., Nikulin, S., Nikulin, V., Noferini, F., Nomokonov, P.,  
 731 Nooren, G., Cabanillas Noris, J. C., Norman, J., Nyanin, A., Nystrand, J. I., Oeschler,  
 732 H. O., Oh, S., Oh, S. K., Ohlson, A. E., Okatan, A., Okubo, T., Olah, L., Oleniacz,  
 733 J., Oliveira Da Silva, A. C., Oliver, M. H., Onderwaater, J., Oppedisano, C., Orava, R.,  
 734 Oravec, M., Ortiz Velasquez, A., Oskarsson, A. N. E., Otwinowski, J. T., Oyama, K.,  
 735 Ozdemir, M., Pachmayer, Y. C., Pagano, D., Pagano, P., Paic, G., Pal, S. K., Pan, J.,  
 736 Pandey, A. K., Papikyan, V., Pappalardo, G., Pareek, P., Park, W., Parmar, S., Passfeld,  
 737 A., Paticchio, V., Patra, R. N., Paul, B., Pei, H., Peitzmann, T., Pereira Da Costa, H.  
 738 D. A., Peresunko, D. Y., Perez Lara, C. E., Perez Lezama, E., Peskov, V., Pestov, Y.,  
 739 Petracek, V., Petrov, V., Petrovici, M., Petta, C., Piano, S., Pikna, M., Pillot, P., Ozelin  
 740 De Lima Pimentel, L., Pinazza, O., Pinsky, L., Piyaathana, D., Ploskon, M. A., Planinic,  
 741 M., Pluta, J. M., Pochybova, S., Podesta Lerma, P. L. M., Poghosyan, M., Polishchuk,  
 742 B., Poljak, N., Poonsawat, W., Pop, A., Porteboeuf, S. J., Porter, R. J., Pospisil, J.,  
 743 Prasad, S. K., Preghenella, R., Prino, F., Pruneau, C. A., Pshenichnov, I., Puccio, M.,  
 744 Puddu, G., Pujahari, P. R., Punin, V., Putschke, J. H., Qvigstad, H., Rachevski, A., Raha,  
 745 S., Rajput, S., Rak, J., Rakotozafindrabe, A. M., Ramello, L., Rami, F., Raniwala, R.,  
 746 Raniwala, S., Rasanen, S. S., Rascanu, B. T., Rathee, D., Read, K. F., Redlich, K., Reed,  
 747 R. J., Rehman, A. U., Reichelt, P. S., Reidt, F., Ren, X., Renfordt, R. A. E., Reolon, A. R.,  
 748 Reshetin, A., Reygers, K. J., Riabov, V., Ricci, R. A., Richert, T. O. H., Richter, M. R.,  
 749 Riedler, P., Riegler, W., Riggi, F., Ristea, C.-L., Rocco, E., Rodriguez Cahuantzi, M.,

750 Rodriguez Manso, A., Roeed, K., Rogochaya, E., Rohr, D. M., Roehrich, D., Ronchetti,  
 751 F., Ronflette, L., Rosnet, P., Rossi, A., Roukoutakis, F., Roy, A., Roy, C. S., Roy, P. K.,  
 752 Rubio Montero, A. J., Rui, R., Russo, R., Di Ruzza, B., Ryabinkin, E., Ryabov, Y.,  
 753 Rybicki, A., Saarinen, S., Sadhu, S., Sadovskiy, S., Safarik, K., Sahlmuller, B., Sahoo, P.,  
 754 Sahoo, R., Sahoo, S., Sahu, P. K., Saini, J., Sakai, S., Saleh, M. A., Salzwedel, J. S. N.,  
 755 Sambyal, S. S., Samsonov, V., Sandor, L., Sandoval, A., Sano, M., Sarkar, D., Sarkar, N.,  
 756 Sarma, P., Scapparone, E., Scarlassara, F., Schiaua, C. C., Schicker, R. M., Schmidt, C. J.,  
 757 Schmidt, H. R., Schuchmann, S., Schukraft, J., Schulc, M., Schutz, Y. R., Schwarz, K. E.,  
 758 Schweda, K. O., Scioli, G., Scomparin, E., Scott, R. M., Sefcik, M., Seger, J. E., Sekiguchi,  
 759 Y., Sekihata, D., Selyuzhenkov, I., Senosi, K., Senyukov, S., Serradilla Rodriguez, E.,  
 760 Sevcenco, A., Shabanov, A., Shabetai, A., Shadura, O., Shahoyan, R., Shahzad, M. I.,  
 761 Shangaraev, A., Sharma, A., Sharma, M., Sharma, M., Sharma, N., Sheikh, A. I., Shigaki,  
 762 K., Shou, Q., Shtejer Diaz, K., Sibiryak, Y., Siddhanta, S., Sielewicz, K. M., Siemiarczuk,  
 763 T., Silvermyr, D. O. R., Silvestre, C. M., Simatovic, G., Simonetti, G., Singaraju, R. N.,  
 764 Singh, R., Singha, S., Singhal, V., Sinha, B., Sarkar Sinha, T., Sitar, B., Sitta, M., Skaali,  
 765 B., Slupecki, M., Smirnov, N., Snellings, R., Snellman, T. W., Song, J., Song, M., Song,  
 766 Z., Soramel, F., Sorensen, S. P., Derradi De Souza, R., Sozzi, F., Spacek, M., Spiriti, E.,  
 767 Sputowska, I. A., Spyropoulou-Stassinaki, M., Stachel, J., Stan, I., Stankus, P., Stenlund,  
 768 E. A., Steyn, G. F., Stiller, J. H., Stocco, D., Strmen, P., Alarcon Do Passo Suaide, A.,  
 769 Sugitate, T., Suire, C. P., Suleymanov, M. K. O., Suljic, M., Sultanov, R., Sumbera,  
 770 M., Sumowidagdo, S., Szabo, A., Szanto De Toledo, A., Szarka, I., Szczepankiewicz, A.,  
 771 Szymanski, M. P., Tabassam, U., Takahashi, J., Tambave, G. J., Tanaka, N., Tarhini,  
 772 M., Tariq, M., Tarzila, M.-G., Tauro, A., Tejeda Munoz, G., Telesca, A., Terasaki, K.,  
 773 Terrevoli, C., Teyssier, B., Thaeder, J. M., Thakur, D., Thomas, D., Tieulent, R. N.,  
 774 Tikhonov, A., Timmins, A. R., Toia, A., Trogolo, S., Trombetta, G., Trubnikov, V.,  
 775 Trzaska, W. H., Tsuji, T., Tumkin, A., Turrisi, R., Tveter, T. S., Ullaland, K., Uras, A.,  
 776 Usai, G., Utrobicic, A., Vala, M., Valencia Palomo, L., Vallero, S., Van Der Maarel, J.,  
 777 Van Hoorne, J. W., Van Leeuwen, M., Vanat, T., Vande Vyvre, P., Varga, D., Diozcora  
 778 Vargas Trevino, A., Vargyas, M., Varma, R., Vasileiou, M., Vasiliev, A., Vauthier, A.,  
 779 Vazquez Doce, O., Vechernin, V., Veen, A. M., Veldhoen, M., Velure, A., Vercellin, E.,

Vergara Limon, S., Vernet, R., Verweij, M., Vickovic, L., Viinikainen, J. S., Vilakazi, Z., Villalobos Baillie, O., Villatoro Tello, A., Vinogradov, A., Vinogradov, L., Vinogradov, Y., Virgili, T., Vislavicius, V., Viyogi, Y., Vodopyanov, A., Volkl, M. A., Voloshin, K., Voloshin, S., Volpe, G., Von Haller, B., Vorobyev, I., Vranic, D., Vrlakova, J., Vulpescu, B., Wagner, B., Wagner, J., Wang, H., Wang, M., Watanabe, D., Watanabe, Y., Weber, M., Weber, S. G., Weiser, D. F., Wessels, J. P., Westerhoff, U., Whitehead, A. M., Wiechula, J., Wikne, J., Wilk, G. A., Wilkinson, J. J., Williams, C., Windelband, B. S., Winn, M. A., Yang, P., Yano, S., Yasin, Z., Yin, Z., Yokoyama, H., Yoo, I.-K., Yoon, J. H., Yurchenko, V., Yushmanov, I., Zaborowska, A., Zaccolo, V., Zaman, A., Zampolli, C., Correia Zanolini, H. J., Zaporozhets, S., Zardoshti, N., Zarochentsev, A., Zavada, P., Zavyalov, N., Zbroszczyk, H. P., Zgura, S. I., Zhalov, M., Zhang, H., Zhang, X., Zhang, Y., Chunchui, Z., Zhang, Z., Zhao, C., Zhigareva, N., Zhou, D., Zhou, Y., Zhou, Z., Zhu, H., Zhu, J., Zichichi, A., Zimmermann, A., Zimmermann, M. B., Zinovjev, G., and Zyzak, M. (2016). Measurement of transverse energy at midrapidity in Pb-Pb collisions at  $\sqrt{s_{NN}} = 2.76$  TeV. *Phys. Rev. C*, 94(CERN-EP-2016-071. CERN-EP-2016-071):034903. 30 p. 30 pages, 14 captioned figures, 2 tables, authors from page 25, published version, figures at <http://aliceinfo.cern.ch/ArtSubmission/node/2400>. 6, 15

[2] Adamczyk, L., Adkins, J. K., Agakishiev, G., Aggarwal, M. M., Ahammed, Z., Ajitanand, N. N., Alekseev, I., Anderson, D. M., Aoyama, R., Aparin, A., Arkhipkin, D., Aschenauer, E. C., Ashraf, M. U., Attri, A., Averichev, G. S., Bai, X., Bairathi, V., Behera, A., Bellwied, R., Bhasin, A., Bhati, A. K., Bhattarai, P., Bielcik, J., Bielcikova, J., Bland, L. C., Bordyuzhin, I. G., Bouchet, J., Brandenburg, J. D., Brandin, A. V., Brown, D., Bunzarov, I., Butterworth, J., Caines, H., Calderón de la Barca Sánchez, M., Campbell, J. M., Cebra, D., Chakaberia, I., Chaloupka, P., Chang, Z., Chankova-Bunzarova, N., Chatterjee, A., Chattopadhyay, S., Chen, X., Chen, J. H., Chen, X., Cheng, J., Cherney, M., Christie, W., Contin, G., Crawford, H. J., Das, S., De Silva, L. C., Debbe, R. R., Dedovich, T. G., Deng, J., Derevschikov, A. A., Didenko, L., Dilks, C., Dong, X., Drachenberg, J. L., Draper, J. E., Dunkelberger, L. E., Dunlop, J. C., Efimov, L. G., Elsey, N., Engelage, J., Eppley, G., Esha, R., Esumi, S., Evdokimov, O., Ewigleben,

809 J., Eyser, O., Fatemi, R., Fazio, S., Federic, P., Federicova, P., Fedorisin, J., Feng, Z.,  
 810 Filip, P., Finch, E., Fisyak, Y., Flores, C. E., Fulek, L., Gagliardi, C. A., Garand, D.,  
 811 Geurts, F., Gibson, A., Girard, M., Grosnick, D., Gunarathne, D. S., Guo, Y., Gupta, A.,  
 812 Gupta, S., Guryn, W., Hamad, A. I., Hamed, A., Harlenderova, A., Harris, J. W., He, L.,  
 813 Heppelmann, S., Heppelmann, S., Hirsch, A., Hoffmann, G. W., Horvat, S., Huang, T.,  
 814 Huang, B., Huang, X., Huang, H. Z., Humanic, T. J., Huo, P., Igo, G., Jacobs, W. W.,  
 815 Jentsch, A., Jia, J., Jiang, K., Jowzaee, S., Judd, E. G., Kabana, S., Kalinkin, D., Kang,  
 816 K., Kauder, K., Ke, H. W., Keane, D., Kechechyan, A., Khan, Z., Kikoła, D. P., Kisel,  
 817 I., Kisiel, A., Kochenda, L., Kocmanek, M., Kollegger, T., Kosarzewski, L. K., Kraishan,  
 818 A. F., Kravtsov, P., Krueger, K., Kulathunga, N., Kumar, L., Kvapil, J., Kwasizur, J. H.,  
 819 Lacey, R., Landgraf, J. M., Landry, K. D., Lauret, J., Lebedev, A., Lednický, R., Lee,  
 820 J. H., Li, X., Li, C., Li, W., Li, Y., Lidrych, J., Lin, T., Lisa, M. A., Liu, H., Liu,  
 821 P., Liu, Y., Liu, F., Ljubicic, T., Llope, W. J., Lomnitz, M., Longacre, R. S., Luo, S.,  
 822 Luo, X., Ma, G. L., Ma, L., Ma, Y. G., Ma, R., Magdy, N., Majka, R., Mallick, D.,  
 823 Margetis, S., Markert, C., Matis, H. S., Meehan, K., Mei, J. C., Miller, Z. W., Minaev,  
 824 N. G., Mioduszewski, S., Mishra, D., Mizuno, S., Mohanty, B., Mondal, M. M., Morozov,  
 825 D. A., Mustafa, M. K., Nasim, M., Nayak, T. K., Nelson, J. M., Nie, M., Nigmatkulov,  
 826 G., Niida, T., Nogach, L. V., Nonaka, T., Nurushev, S. B., Odyniec, G., Ogawa, A.,  
 827 Oh, K., Okorokov, V. A., Olvitt, D., Page, B. S., Pak, R., Pandit, Y., Panebratsev, Y.,  
 828 Pawlik, B., Pei, H., Perkins, C., Pile, P., Pluta, J., Poniatowska, K., Porter, J., Posik,  
 829 M., Poskanzer, A. M., Pruthi, N. K., Przybycien, M., Putschke, J., Qiu, H., Quintero, A.,  
 830 Ramachandran, S., Ray, R. L., Reed, R., Rehbein, M. J., Ritter, H. G., Roberts, J. B.,  
 831 Rogachevskiy, O. V., Romero, J. L., Roth, J. D., Ruan, L., Rusnak, J., Rusnakova, O.,  
 832 Sahoo, N. R., Sahu, P. K., Salur, S., Sandweiss, J., Saur, M., Schambach, J., Schmäh,  
 833 A. M., Schmidke, W. B., Schmitz, N., Schweid, B. R., Seger, J., Sergeeva, M., Seyboth, P.,  
 834 Shah, N., Shahaliev, E., Shanmuganathan, P. V., Shao, M., Sharma, A., Sharma, M. K.,  
 835 Shen, W. Q., Shi, Z., Shi, S. S., Shou, Q. Y., Sichtermann, E. P., Sikora, R., Simko,  
 836 M., Singha, S., Skoby, M. J., Smirnov, N., Smirnov, D., Solyst, W., Song, L., Sorensen,  
 837 P., Spinka, H. M., Srivastava, B., Stanislaus, T. D. S., Strikhanov, M., Stringfellow, B.,  
 838 Sugiura, T., Sumbera, M., Summa, B., Sun, Y., Sun, X. M., Sun, X., Surrow, B., Svirida,



D. N., Tang, A. H., Tang, Z., Taranenko, A., Tarnowsky, T., Tawfik, A., Thäder, J., Thomas, J. H., Timmins, A. R., Tlusty, D., Todoroki, T., Tokarev, M., Trentalange, S., Tribble, R. E., Tribedy, P., Tripathy, S. K., Trzeciak, B. A., Tsai, O. D., Ullrich, T., Underwood, D. G., Upsal, I., Van Buren, G., van Nieuwenhuizen, G., Vasiliev, A. N., Videbæk, F., Vokal, S., Voloshin, S. A., Vossen, A., Wang, G., Wang, Y., Wang, F., Wang, Y., Webb, J. C., Webb, G., Wen, L., Westfall, G. D., Wieman, H., Wissink, S. W., Witt, R., Wu, Y., Xiao, Z. G., Xie, W., Xie, G., Xu, J., Xu, N., Xu, Q. H., Xu, Y. F., Xu, Z., Yang, Y., Yang, Q., Yang, C., Yang, S., Ye, Z., Ye, Z., Yi, L., Yip, K., Yoo, I.-K., Yu, N., Zbroszczyk, H., Zha, W., Zhang, Z., Zhang, X. P., Zhang, J. B., Zhang, S., Zhang, J., Zhang, Y., Zhang, J., Zhang, S., Zhao, J., Zhong, C., Zhou, L., Zhou, C., Zhu, X., Zhu, Z., and Zyzak, M. (2017). Bulk properties of the medium produced in relativistic heavy-ion collisions from the beam energy scan program. *Phys. Rev. C*, 96:044904. vii, 23, 27, 28

[3] Adare, A., Afanasiev, S., Aidala, C., Ajitanand, N. N., Akiba, Y., Akimoto, R., Al-Bataineh, H., Alexander, J., Alfred, M., Al-Jamel, A., Al-Ta'ani, H., Angerami, A., Aoki, K., Apadula, N., Aphecetche, L., Aramaki, Y., Armendariz, R., Aronson, S. H., Asai, J., Asano, H., Aschenauer, E. C., Atomssa, E. T., Auerbeck, R., Awes, T. C., Azmoun, B., Babintsev, V., Bai, M., Bai, X., Baksay, G., Baksay, L., Baldisseri, A., Bandara, N. S., Bannier, B., Barish, K. N., Barnes, P. D., Bassalleck, B., Basye, A. T., Bathe, S., Batsouli, S., Baublis, V., Bauer, F., Baumann, C., Baumgart, S., Bazilevsky, A., Beaumier, M., Beckman, S., Belikov, S., Belmont, R., Bennett, R., Berdnikov, A., Berdnikov, Y., Bhom, J. H., Bickley, A. A., Bjorndal, M. T., Black, D., Blau, D. S., Boissevain, J. G., Bok, J. S., Borel, H., Boyle, K., Brooks, M. L., Brown, D. S., Bryslawskyj, J., Bucher, D., Buesching, H., Bumazhnov, V., Bunce, G., Burward-Hoy, J. M., Butsyk, S., Campbell, S., Caringi, A., Castera, P., Chai, J.-S., Chang, B. S., Charvet, J.-L., Chen, C.-H., Chernichenko, S., Chi, C. Y., Chiba, J., Chiu, M., Choi, I. J., Choi, J. B., Choi, S., Choudhury, R. K., Christiansen, P., Chujo, T., Chung, P., Churn, A., Chvala, O., Cianciolo, V., Citron, Z., Cleven, C. R., Cobigo, Y., Cole, B. A., Comets, M. P., Conesa del Valle, Z., Connors, M., Constantin, P., Cronin, N., Crossette, N., Csanád, M., Csörgő, T., Dahms,

868 T., Dairaku, S., Danchev, I., Danley, T. W., Das, K., Datta, A., Daugherty, M. S.,  
 869 David, G., Dayananda, M. K., Deaton, M. B., DeBlasio, K., Dehmelt, K., Delagrange,  
 870 H., Denisov, A., d'Enterria, D., Deshpande, A., Desmond, E. J., Dharmawardane, K. V.,  
 871 Dietzsch, O., Ding, L., Dion, A., Diss, P. B., Do, J. H., Donadelli, M., D'Orazio, L.,  
 872 Drachenberg, J. L., Drapier, O., Drees, A., Drees, K. A., Dubey, A. K., Durham, J. M.,  
 873 Durum, A., Dutta, D., Dzhordzhadze, V., Edwards, S., Efremenko, Y. V., Egdemir, J.,  
 874 Ellinghaus, F., Emam, W. S., Engelmores, T., Enokizono, A., En'yo, H., Espagnon, B.,  
 875 Esumi, S., Eyser, K. O., Fadem, B., Feege, N., Fields, D. E., Finger, M., Finger, M.,  
 876 Fleuret, F., Fokin, S. L., Forestier, B., Fraenkel, Z., Frantz, J. E., Franz, A., Frawley,  
 877 A. D., Fujiwara, K., Fukao, Y., Fung, S.-Y., Fusayasu, T., Gadrat, S., Gainey, K., Gal,  
 878 C., Gallus, P., Garg, P., Garishvili, A., Garishvili, I., Gastineau, F., Ge, H., Germain, M.,  
 879 Giordano, F., Glenn, A., Gong, H., Gong, X., Gonin, M., Gosset, J., Goto, Y., Granier de  
 880 Cassagnac, R., Grau, N., Greene, S. V., Grim, G., Grosse Perdekamp, M., Gu, Y., Gunji,  
 881 T., Guo, L., Guragain, H., Gustafsson, H.-A., Hachiya, T., Hadj Henni, A., Haegemann,  
 882 C., Haggerty, J. S., Hagiwara, M. N., Hahn, K. I., Hamagaki, H., Hamblen, J., Hamilton,  
 883 H. F., Han, R., Han, S. Y., Hanks, J., Harada, H., Hartouni, E. P., Haruna, K., Harvey,  
 884 M., Hasegawa, S., Haseler, T. O. S., Hashimoto, K., Haslum, E., Hasuko, K., Hayano, R.,  
 885 Hayashi, S., He, X., Heffner, M., Hemmick, T. K., Hester, T., Heuser, J. M., Hiejima, H.,  
 886 Hill, J. C., Hobbs, R., Hohlmann, M., Hollis, R. S., Holmes, M., Holzmann, W., Homma,  
 887 K., Hong, B., Horaguchi, T., Hori, Y., Hornback, D., Hoshino, T., Hotvedt, N., Huang, J.,  
 888 Huang, S., Hur, M. G., Ichihara, T., Ichimiya, R., Inuma, H., Ikeda, Y., Imai, K., Imazu,  
 889 Y., Imrek, J., Inaba, M., Inoue, Y., Iordanova, A., Isenhowe, D., Isenhowe, L., Ishihara,  
 890 M., Isinhue, A., Isobe, T., Issah, M., Isupov, A., Ivanishchev, D., Iwanaga, Y., Jacak,  
 891 B. V., Javani, M., Jeon, S. J., Jezghani, M., Jia, J., Jiang, X., Jin, J., Jinnouchi, O.,  
 892 Johnson, B. M., Jones, T., Joo, K. S., Jouan, D., Jumper, D. S., Kajihara, F., Kametani,  
 893 S., Kamihara, N., Kamin, J., Kanda, S., Kaneta, M., Kaneti, S., Kang, B. H., Kang, J. H.,  
 894 Kang, J. S., Kanou, H., Kapustinsky, J., Karatsu, K., Kasai, M., Kawagishi, T., Kawall,  
 895 D., Kawashima, M., Kazantsev, A. V., Kelly, S., Kempel, T., Key, J. A., Khachatryan, V.,  
 896 Khandai, P. K., Khanzadeev, A., Kijima, K. M., Kikuchi, J., Kim, A., Kim, B. I., Kim, C.,  
 897 Kim, D. H., Kim, D. J., Kim, E., Kim, E.-J., Kim, G. W., Kim, H. J., Kim, K.-B., Kim,

898 M., Kim, Y.-J., Kim, Y. K., Kim, Y.-S., Kimelman, B., Kinney, E., Kiss, A., Kistenev, E.,  
 899 Kitamura, R., Kiyomichi, A., Klatsky, J., Klay, J., Klein-Boesing, C., Kleinjan, D., Kline,  
 900 P., Koblesky, T., Kochenda, L., Kochetkov, V., Kofarago, M., Komatsu, Y., Komkov,  
 901 B., Konno, M., Koster, J., Kotchetkov, D., Kotov, D., Kozlov, A., Král, A., Kravitz, A.,  
 902 Krizek, F., Kroon, P. J., Kubart, J., Kunde, G. J., Kurihara, N., Kurita, K., Kurosawa,  
 903 M., Kweon, M. J., Kwon, Y., Kyle, G. S., Lacey, R., Lai, Y. S., Lajoie, J. G., Lebedev,  
 904 A., Le Bornec, Y., Leckey, S., Lee, B., Lee, D. M., Lee, G. H., Lee, J., Lee, K. B.,  
 905 Lee, K. S., Lee, M. K., Lee, S., Lee, S. H., Lee, S. R., Lee, T., Leitch, M. J., Leite, M.  
 906 A. L., Leitgab, M., Lenzi, B., Lewis, B., Li, X., Li, X. H., Lichtenwalner, P., Liebing, P.,  
 907 Lim, H., Lim, S. H., Linden Levy, L. A., Liška, T., Litvinenko, A., Liu, H., Liu, M. X.,  
 908 Love, B., Lynch, D., Maguire, C. F., Makdisi, Y. I., Makek, M., Malakhov, A., Malik,  
 909 M. D., Manion, A., Manko, V. I., Mannel, E., Mao, Y., Maruyama, T., Mašek, L., Masui,  
 910 H., Masumoto, S., Matathias, F., McCain, M. C., McCumber, M., McGaughey, P. L.,  
 911 McGlinchey, D., McKinney, C., Means, N., Meles, A., Mendoza, M., Meredith, B., Miake,  
 912 Y., Mibe, T., Midori, J., Mignerey, A. C., Mikeš, P., Miki, K., Miller, T. E., Milov, A.,  
 913 Mioduszewski, S., Mishra, D. K., Mishra, G. C., Mishra, M., Mitchell, J. T., Mitrovski,  
 914 M., Miyachi, Y., Miyasaka, S., Mizuno, S., Mohanty, A. K., Mohapatra, S., Montuenga,  
 915 P., Moon, H. J., Moon, T., Morino, Y., Morreale, A., Morrison, D. P., Moskowitz, M.,  
 916 Moss, J. M., Motschwiller, S., Moukhanova, T. V., Mukhopadhyay, D., Murakami, T.,  
 917 Murata, J., Mwai, A., Nagae, T., Nagamiya, S., Nagashima, K., Nagata, Y., Nagle, J. L.,  
 918 Naglis, M., Nagy, M. I., Nakagawa, I., Nakagomi, H., Nakamiya, Y., Nakamura, K. R.,  
 919 Nakamura, T., Nakano, K., Nam, S., Natrass, C., Nederlof, A., Netrakanti, P. K., Newby,  
 920 J., Nguyen, M., Nihashi, M., Niida, T., Nishimura, S., Norman, B. E., Nouicer, R., Novák,  
 921 T., Novitzky, N., Nukariya, A., Nyanin, A. S., Nystrand, J., Oakley, C., Obayashi, H.,  
 922 O'Brien, E., Oda, S. X., Ogilvie, C. A., Ohnishi, H., Oide, H., Ojha, I. D., Oka, M.,  
 923 Okada, K., Omiwade, O. O., Onuki, Y., Orjuela Koop, J. D., Osborn, J. D., Oskarsson,  
 924 A., Otterlund, I., Ouchida, M., Ozawa, K., Pak, R., Pal, D., Palounek, A. P. T., Pantuev,  
 925 V., Papavassiliou, V., Park, B. H., Park, I. H., Park, J., Park, J. S., Park, S., Park, S. K.,  
 926 Park, W. J., Pate, S. F., Patel, L., Patel, M., Pei, H., Peng, J.-C., Pereira, H., Perepelitsa,  
 927 D. V., Perera, G. D. N., Peresedov, V., Peressounko, D., Perry, J., Petti, R., Pinkenburg,

928 C., Pinson, R., Pisani, R. P., Proissl, M., Purschke, M. L., Purwar, A. K., Qu, H., Rak,  
 929 J., Rakotozafindrabe, A., Ramson, B. J., Ravinovich, I., Read, K. F., Rembeczki, S.,  
 930 Reuter, M., Reygers, K., Reynolds, D., Riabov, V., Riabov, Y., Richardson, E., Rinn, T.,  
 931 Riveli, N., Roach, D., Roche, G., Rolnick, S. D., Romana, A., Rosati, M., Rosen, C. A.,  
 932 Rosendahl, S. S. E., Rosnet, P., Rowan, Z., Rubin, J. G., Rukoyatkin, P., Ružička, P.,  
 933 Rykov, V. L., Ryu, M. S., Ryu, S. S., Sahlmueller, B., Saito, N., Sakaguchi, T., Sakai, S.,  
 934 Sakashita, K., Sakata, H., Sako, H., Samsonov, V., Sano, M., Sano, S., Sarsour, M., Sato,  
 935 H. D., Sato, S., Sato, T., Sawada, S., Schaefer, B., Schmoll, B. K., Sedgwick, K., Seele,  
 936 J., Seidl, R., Sekiguchi, Y., Semenov, V., Sen, A., Seto, R., Sett, P., Sexton, A., Sharma,  
 937 D., Shaver, A., Shea, T. K., Shein, I., Shevel, A., Shibata, T.-A., Shigaki, K., Shimomura,  
 938 M., Shohjoh, T., Shoji, K., Shukla, P., Sickles, A., Silva, C. L., Silvermyr, D., Silvestre,  
 939 C., Sim, K. S., Singh, B. K., Singh, C. P., Singh, V., Skolnik, M., Skutnik, S., Slunečka,  
 940 M., Smith, W. C., Snowball, M., Solano, S., Soldatov, A., Soltz, R. A., Sondheim, W. E.,  
 941 Sorensen, S. P., Sourikova, I. V., Staley, F., Stankus, P. W., Steinberg, P., Stenlund, E.,  
 942 Stepanov, M., Ster, A., Stoll, S. P., Stone, M. R., Sugitate, T., Suire, C., Sukhanov, A.,  
 943 Sullivan, J. P., Sumita, T., Sun, J., Sziklai, J., Tabaru, T., Takagi, S., Takagui, E. M.,  
 944 Takahara, A., Taketani, A., Tanabe, R., Tanaka, K. H., Tanaka, Y., Taneja, S., Tanida, K.,  
 945 Tannenbaum, M. J., Tarafdar, S., Taranenko, A., Tarján, P., Tennant, E., Themann, H.,  
 946 Thomas, D., Thomas, T. L., Tieulent, R., Timilsina, A., Todoroki, T., Togawa, M., Toia,  
 947 A., Tojo, J., Tomášek, L., Tomášek, M., Torii, H., Towell, C. L., Towell, R., Towell, R. S.,  
 948 Tram, V.-N., Tserruya, I., Tsuchimoto, Y., Tsuji, T., Tuli, S. K., Tydesjö, H., Tyurin,  
 949 N., Vale, C., Valle, H., van Hecke, H. W., Vargyas, M., Vazquez-Zambrano, E., Veicht,  
 950 A., Velkovska, J., Vértési, R., Vinogradov, A. A., Virius, M., Voas, B., Vossen, A., Vrba,  
 951 V., Vznuzdaev, E., Wagner, M., Walker, D., Wang, X. R., Watanabe, D., Watanabe, K.,  
 952 Watanabe, Y., Watanabe, Y. S., Wei, F., Wei, R., Wessels, J., Whitaker, S., White, A. S.,  
 953 White, S. N., Willis, N., Winter, D., Wolin, S., Woody, C. L., Wright, R. M., Wysocki, M.,  
 954 Xia, B., Xie, W., Xue, L., Yalcin, S., Yamaguchi, Y. L., Yamaura, K., Yang, R., Yanovich,  
 955 A., Yasin, Z., Ying, J., Yokkaichi, S., Yoo, J. H., Yoon, I., You, Z., Young, G. R., Younus,  
 956 I., Yu, H., Yushmanov, I. E., Zajc, W. A., Zaudtke, O., Zelenski, A., Zhang, C., Zhou, S.,

Zimanyi, J., Zolin, L., and Zou, L. (2016). Transverse energy production and charged-particle multiplicity at midrapidity in various systems from  $\sqrt{s_{NN}} = 7.7$  to 200 gev. *Phys. Rev. C*, 93:024901. viii, 5, 22, 37, 39

[4] Adare, A., Afanasiev, S., Aidala, C., Ajitanand, N. N., Akiba, Y., Al-Bataineh, H., Alexander, J., Al-Jamel, A., Aoki, K., Aphecetche, L., and et al. (2007). Scaling Properties of Azimuthal Anisotropy in Au+Au and Cu+Cu Collisions at  $s_{NN}=200\text{GeV}$ . *Physical Review Letters*, 98(16):162301. vi, 16, 17

[5] Adler, S. S., Afanasiev, S., Aidala, C., Ajitanand, N. N., Akiba, Y., Al-Jamel, A., Alexander, J., Aoki, K., Aphecetche, L., Armendariz, R., Aronson, S. H., Auerbeck, R., Awes, T. C., Azmoun, B., Babintsev, V., Baldisseri, A., Barish, K. N., Barnes, P. D., Bassalleck, B., Bathe, S., Batsouli, S., Baublis, V., Bauer, F., Bazilevsky, A., Belikov, S., Bennett, R., Berdnikov, Y., Bjorndal, M. T., Boissevain, J. G., Borel, H., Boyle, K., Brooks, M. L., Brown, D. S., Bruner, N., Bucher, D., Buesching, H., Bumazhnov, V., Bunce, G., Burward-Hoy, J. M., Butsyk, S., Camard, X., Campbell, S., Chai, J.-S., Chand, P., Chang, W. C., Chernichenko, S., Chi, C. Y., Chiba, J., Chiu, M., Choi, I. J., Choudhury, R. K., Chujo, T., Cianciolo, V., Cleven, C. R., Cobigo, Y., Cole, B. A., Comets, M. P., Constantin, P., Csanád, M., Csörgő, T., Cussonneau, J. P., Dahms, T., Das, K., David, G., Deák, F., Delagrange, H., Denisov, A., d'Enterria, D., Deshpande, A., Desmond, E. J., Devismes, A., Dietzsch, O., Dion, A., Drachenberg, J. L., Drapier, O., Drees, A., Dubey, A. K., Durum, A., Dutta, D., Dzhordzhadze, V., Efremenko, Y. V., Egdemir, J., Enokizono, A., En'yo, H., Espagnon, B., Esumi, S., Fields, D. E., Finck, C., Fleuret, F., Fokin, S. L., Forestier, B., Fox, B. D., Fraenkel, Z., Frantz, J. E., Franz, A., Frawley, A. D., Fukao, Y., Fung, S.-Y., Gadrat, S., Gastineau, F., Germain, M., Glenn, A., Gonin, M., Gosset, J., Goto, Y., Granier de Cassagnac, R., Grau, N., Greene, S. V., Grosse Perdekamp, M., Gunji, T., Gustafsson, H.-A., Hachiya, T., Hadj Henni, A., Haggerty, J. S., Hagiwara, M. N., Hamagaki, H., Hansen, A. G., Harada, H., Hartouni, E. P., Haruna, K., Harvey, M., Haslum, E., Hasuko, K., Hayano, R., He, X., Heffner, M., Hemmick, T. K., Heuser, J. M., Hidas, P., Hiejima, H., Hill, J. C., Hobbs, R., Holmes, M., Holzmann, W., Homma, K., Hong, B., Hoover, A., Horaguchi, T., Hur, M. G., Ichihara, T.,

986 Iinuma, H., Ikonnikov, V. V., Imai, K., Inaba, M., Inuzuka, M., Isenhowe, D., Isenhowe,  
 987 L., Ishihara, M., Isobe, T., Issah, M., Isupov, A., Jacak, B. V., Jia, J., Jin, J., Jinnouchi,  
 988 O., Johnson, B. M., Johnson, S. C., Joo, K. S., Jouan, D., Kajihara, F., Kametani,  
 989 S., Kamihara, N., Kaneta, M., Kang, J. H., Katou, K., Kawabata, T., Kawagishi, T.,  
 990 Kazantsev, A. V., Kelly, S., Khachaturov, B., Khanzadeev, A., Kikuchi, J., Kim, D. J.,  
 991 Kim, E., Kim, E. J., Kim, G.-B., Kim, H. J., Kim, Y.-S., Kinney, E., Kiss, A., Kistenev, E.,  
 992 Kiyomichi, A., Klein-Boesing, C., Kobayashi, H., Kochenda, L., Kochetkov, V., Kohara,  
 993 R., Komkov, B., Konno, M., Kotchetkov, D., Kozlov, A., Kroon, P. J., Kuberg, C. H.,  
 994 Kunde, G. J., Kurihara, N., Kurita, K., Kweon, M. J., Kwon, Y., Kyle, G. S., Lacey, R.,  
 995 Lajoie, J. G., Lebedev, A., Le Bornec, Y., Leckey, S., Lee, D. M., Lee, M. K., Leitch,  
 996 M. J., Leite, M. A. L., Li, X. H., Lim, H., Litvinenko, A., Liu, M. X., Maguire, C. F.,  
 997 Makdisi, Y. I., Malakhov, A., Malik, M. D., Manko, V. I., Mao, Y., Martinez, G., Masui,  
 998 H., Matathias, F., Matsumoto, T., McCain, M. C., McGaughey, P. L., Miake, Y., Miller,  
 999 T. E., Milov, A., Mioduszewski, S., Mishra, G. C., Mitchell, J. T., Mohanty, A. K.,  
 1000 Morrison, D. P., Moss, J. M., Moukhanova, T. V., Mukhopadhyay, D., Muniruzzaman,  
 1001 M., Murata, J., Nagamiya, S., Nagata, Y., Nagle, J. L., Naglis, M., Nakamura, T., Newby,  
 1002 J., Nguyen, M., Norman, B. E., Nyanin, A. S., Nystrand, J., O'Brien, E., Ogilvie, C. A.,  
 1003 Ohnishi, H., Ojha, I. D., Okada, K., Omiwade, O. O., Oskarsson, A., Otterlund, I., Oyama,  
 1004 K., Ozawa, K., Pal, D., Palounek, A. P. T., Pantuev, V., Papavassiliou, V., Park, J., Park,  
 1005 W. J., Pate, S. F., Pei, H., Penev, V., Peng, J.-C., Pereira, H., Peresedov, V., Peressounko,  
 1006 D., Pierson, A., Pinkenburg, C., Pisani, R. P., Purschke, M. L., Purwar, A. K., Qu, H.,  
 1007 Qualls, J. M., Rak, J., Ravinovich, I., Read, K. F., Reuter, M., Reygers, K., Riabov,  
 1008 V., Riabov, Y., Roche, G., Romana, A., Rosati, M., Rosendahl, S. S. E., Rosnet, P.,  
 1009 Rukoyatkin, P., Rykov, V. L., Ryu, S. S., Sahlmuehler, B., Saito, N., Sakaguchi, T., Sakai,  
 1010 S., Samsonov, V., Sanfratello, L., Santo, R., Sarsour, M., Sato, H. D., Sato, S., Sawada,  
 1011 S., Schutz, Y., Semenov, V., Seto, R., Sharma, D., Shea, T. K., Shein, I., Shibata, T.-A.,  
 1012 Shigaki, K., Shimomura, M., Shohjoh, T., Shoji, K., Sickles, A., Silva, C. L., Silvermyr, D.,  
 1013 Sim, K. S., Singh, C. P., Singh, V., Skutnik, S., Smith, W. C., Soldatov, A., Soltz, R. A.,  
 1014 Sondheim, W. E., Sorensen, S. P., Sourikova, I. V., Staley, F., Stankus, P. W., Stenlund,  
 1015 E., Stepanov, M., Ster, A., Stoll, S. P., Sugitate, T., Suire, C., Sullivan, J. P., Sziklai, J.,

Tabaru, T., Takagi, S., Takagui, E. M., Taketani, A., Tanaka, K. H., Tanaka, Y., Tanida, K., Tannenbaum, M. J., Taranenko, A., Tarján, P., Thomas, T. L., Togawa, M., Tojo, J., Torii, H., Towell, R. S., Tram, V.-N., Tserruya, I., Tsuchimoto, Y., Tuli, S. K., Tydesjö, H., Tyurin, N., Uam, T. J., Vale, C., Valle, H., van Hecke, H. W., Velkovska, J., Velkovsky, M., Vértesi, R., Veszprémi, V., Vinogradov, A. A., Volkov, M. A., Vznuzdaev, E., Wagner, M., Wang, X. R., Watanabe, Y., Wessels, J., White, S. N., Willis, N., Winter, D., Wohn, F. K., Woody, C. L., Wysocki, M., Xie, W., Yanovich, A., Yokkaichi, S., Young, G. R., Younus, I., Yushmanov, I. E., Zajc, W. A., Zaudtke, O., Zhang, C., Zhou, S., Zimányi, J., Zolin, L., and Zong, X. (2014). Transverse-energy distributions at midrapidity in  $p + p$ ,  $d + \text{Au}$ , and  $\text{Au} + \text{Au}$  collisions at  $\sqrt{s_{\text{NN}}} = 62.4 \sim 200$  gev and implications for particle-production models. *Phys. Rev. C*, 89:044905. 21

[6] Adler, S. S., Afanasiev, S., Aidala, C., Ajitanand, N. N., Akiba, Y., Alexander, J., Amirikas, R., Aphecetche, L., Aronson, S. H., Auerbeck, R., Awes, T. C., Azmoun, R., Babintsev, V., Baldissieri, A., Barish, K. N., Barnes, P. D., Bassalleck, B., Bathe, S., Batsouli, S., Baublis, V., Bazilevsky, A., Belikov, S., Berdnikov, Y., Bhagavatula, S., Boissevain, J. G., Borel, H., Borenstein, S., Brooks, M. L., Brown, D. S., Bruner, N., Bucher, D., Buesching, H., Bumazhnov, V., Bunce, G., Burward-Hoy, J. M., Butsyk, S., Camard, X., Chai, J.-S., Chand, P., Chang, W. C., Chernichenko, S., Chi, C. Y., Chiba, J., Chiu, M., Choi, I. J., Choi, J., Choudhury, R. K., Chujo, T., Cianciolo, V., Cobigo, Y., Cole, B. A., Constantin, P., d’Enterria, D. G., David, G., Delagrange, H., Denisov, A., Deshpande, A., Desmond, E. J., Dietzsch, O., Drapier, O., Drees, A., Rietz, R. d., Durum, A., Dutta, D., Efremenko, Y. V., Chenawi, K. E., Enokizono, A., En’yo, H., Esumi, S., Ewell, L., Fields, D. E., Fleuret, F., Fokin, S. L., Fox, B. D., Fraenkel, Z., Frantz, J. E., Franz, A., Frawley, A. D., Fung, S.-Y., Garpman, S., Ghosh, T. K., Glenn, A., Gogiberidze, G., Gonin, M., Gosset, J., Goto, Y., Cassagnac, R. G. d., Grau, N., Greene, S. V., Perdekamp, M. G., Guryn, W., Gustafsson, H.-A., Hachiya, T., Haggerty, J. S., Hamagaki, H., Hansen, A. G., Hartouni, E. P., Harvey, M., Hayano, R., He, X., Heffner, M., Hemmick, T. K., Heuser, J. M., Hibino, M., Hill, J. C., Holzmann, W., Homma, K., Hong, B., Hoover, A., Ichihara, T., Ikonnikov, V. V., Imai, K., Isenhower, D., Ishihara,

1045 M., Issah, M., Isupov, A., Jacak, B. V., Jang, W. Y., Jeong, Y., Jia, J., Jinnouchi, O.,  
 1046 Johnson, B. M., Johnson, S. C., Joo, K. S., Jouan, D., Kametani, S., Kamihara, N.,  
 1047 Kang, J. H., Kapoor, S. S., Katou, K., Kelly, S., Khachaturov, B., Khanzadeev, A.,  
 1048 Kikuchi, J., Kim, D. H., Kim, D. J., Kim, D. W., Kim, E., Kim, G.-B., Kim, H. J.,  
 1049 Kistenev, E., Kiyomichi, A., Kiyoyama, K., Klein-Boesing, C., Kobayashi, H., Kochenda,  
 1050 L., Kochetkov, V., Koehler, D., Kohama, T., Kopytine, M., Kotchetkov, D., Kozlov, A.,  
 1051 Kroon, P. J., Kuberg, C. H., Kurita, K., Kuroki, Y., Kweon, M. J., Kwon, Y., Kyle,  
 1052 G. S., Lacey, R., Ladygin, V., Lajoie, J. G., Lebedev, A., Leckey, S., Lee, D. M., Lee, S.,  
 1053 Leitch, M. J., Li, X. H., Lim, H., Litvinenko, A., Liu, M. X., Liu, Y., Maguire, C. F.,  
 1054 Makdisi, Y. I., Malakhov, A., Manko, V. I., Mao, Y., Martinez, G., Marx, M. D., Masui,  
 1055 H., Matathias, F., Matsumoto, T., McGaughey, P. L., Melnikov, E., Mendenhall, M.,  
 1056 Messer, F., Miake, Y., Milan, J., Miller, T. E., Milov, A., Mioduszewski, S., Mischke,  
 1057 R. E., Mishra, G. C., Mitchell, J. T., Mohanty, A. K., Morrison, D. P., Moss, J. M.,  
 1058 Mühlbacher, F., Mukhopadhyay, D., Muniruzzaman, M., Murata, J., Nagamiya, S., Nagle,  
 1059 J. L., Nakamura, T., Nandi, B. K., Nara, M., Newby, J., Nilsson, P., Nyanin, A. S.,  
 1060 Nystrand, J., O'Brien, E., Ogilvie, C. A., Ohnishi, H., Ojha, I. D., Okada, K., Ono, M.,  
 1061 Onuchin, V., Oskarsson, A., Otterlund, I., Oyama, K., Ozawa, K., Pal, D., Palounek, A.  
 1062 P. T., Pantuev, V. S., Papavassiliou, V., Park, J., Parmar, A., Pate, S. F., Peitzmann,  
 1063 T., Peng, J.-C., Peresedov, V., Pinkenburg, C., Pisani, R. P., Plasil, F., Purschke, M. L.,  
 1064 Purwar, A. K., Rak, J., Ravinovich, I., Read, K. F., Reuter, M., Reygers, K., Riabov, V.,  
 1065 Riabov, Y., Roche, G., Romana, A., Rosati, M., Rosnet, P., Ryu, S. S., Sadler, M. E.,  
 1066 Saito, N., Sakaguchi, T., Sakai, M., Sakai, S., Samsonov, V., Sanfratello, L., Santo, R.,  
 1067 Sato, H. D., Sato, S., Sawada, S., Schutz, Y., Semenov, V., Seto, R., Shaw, M. R., Shea,  
 1068 T. K., Shibata, T.-A., Shigaki, K., Shiina, T., Silva, C. L., Silvermyr, D., Sim, K. S., Singh,  
 1069 C. P., Singh, V., Sivertz, M., Soldatov, A., Soltz, R. A., Sondheim, W. E., Sorensen, S. P.,  
 1070 Sourikova, I. V., Staley, F., Stankus, P. W., Stenlund, E., Stepanov, M., Ster, A., Stoll,  
 1071 S. P., Sugitate, T., Sullivan, J. P., Takagui, E. M., Taketani, A., Tamai, M., Tanaka, K. H.,  
 1072 Tanaka, Y., Tanida, K., Tannenbaum, M. J., Tarján, P., Tepe, J. D., Thomas, T. L., Tojo,  
 1073 J., Torii, H., Towell, R. S., Tserruya, I., Tsuruoka, H., Tuli, S. K., Tydesjö, H., Tyurin,  
 1074 N., Hecke, H. W. v., Velkovska, J., Velkovsky, M., Villatte, L., Vinogradov, A. A., Volkov,



- 1075 M. A., Vznuzdaev, E., Wang, X. R., Watanabe, Y., White, S. N., Wohn, F. K., Woody,  
1076 C. L., Xie, W., Yang, Y., Yanovich, A., Yokkaichi, S., Young, G. R., Yushmanov, I. E.,  
1077 Zajc, W. A., Zhang, C., Zhou, S., Zhou, S. J., and Zolin, L. (2005). Systematic studies of  
1078 the centrality and  $\sqrt{s_{NN}}$  dependence of the  $de_T/d\eta$  and  $dn_{ch}/d\eta$  in heavy ion collisions at  
1079 midrapidity. *Phys. Rev. C*, 71:034908. 22
- 1080 [7] Aitchison, I. and Hey, A. (2003). *Gauge Theories in Particle Physics, Volume II: QCD*  
1081 *and the Electroweak Theory, Third Edition*. Graduate Student Series in Physics. CRC  
1082 Press. 3
- 1083 [8] Anderson, M. et al. (2003). The Star time projection chamber: A Unique tool for studying  
1084 high multiplicity events at RHIC. *Nucl. Instrum. Meth.*, A499:659–678. 26
- 1085 [9] Ayala, A. (2016). Hadronic matter at the edge: A survey of some theoretical approaches  
1086 to the physics of the qcd phase diagram. *Journal of Physics: Conference Series*,  
1087 761(1):012066. vi, 5, 6
- 1088 [10] Bethe, H. A. and Ashkin, J. (1953). Passage of radiations through matter experimental  
1089 nuclear physics vol 1 ed e segre. 24
- 1090 [11] Bjorken, J. D. (1983). Highly relativistic nucleus-nucleus collisions: The central rapidity  
1091 region. *Phys. Rev. D*, 27:140–151. 15
- 1092 [12] Chatrchyan, S., Khachatryan, V., Sirunyan, A. M., Tumasyan, A., Adam, W., Bergauer,  
1093 T., Dragicevic, M., Erö, J., Fabjan, C., Friedl, M., Frühwirth, R., Ghete, V. M., Hammer,  
1094 J., Hörmann, N., Hrubec, J., Jeitler, M., Kiesenhofer, W., Knünz, V., Krammer, M., Liko,  
1095 D., Mikulec, I., Pernicka, M., Rahbaran, B., Rohringer, C., Rohringer, H., Schöfbeck, R.,  
1096 Strauss, J., Taurok, A., Wagner, P., Waltenberger, W., Walzel, G., Widl, E., Wulz, C.-E.,  
1097 Mossolov, V., Shumeiko, N., Suarez Gonzalez, J., Bansal, S., Cornelis, T., De Wolf, E. A.,  
1098 Janssen, X., Luyckx, S., Maes, T., Mucibello, L., Ochsanu, S., Roland, B., Rougny,  
1099 R., Selvaggi, M., Staykova, Z., Van Haevermaet, H., Van Mechelen, P., Van Remortel,  
1100 N., Van Spilbeeck, A., Blekman, F., Blyweert, S., D’Hondt, J., Gonzalez Suarez, R.,  
1101 Kalogeropoulos, A., Maes, M., Olbrechts, A., Van Doninck, W., Van Mulders, P.,

1102 Van Onsem, G. P., Villella, I., Clerbaux, B., De Lentdecker, G., Dero, V., Gay, A. P. R.,  
 1103 Hreus, T., Léonard, A., Marage, P. E., Reis, T., Thomas, L., Vander Velde, C., Vanlaer, P.,  
 1104 Wang, J., Adler, V., Beernaert, K., Cimmino, A., Costantini, S., Garcia, G., Grunewald,  
 1105 M., Klein, B., Lellouch, J., Marinov, A., McCartin, J., Ocampo Rios, A. A., Ryckbosch, D.,  
 1106 Strobbe, N., Thyssen, F., Tytgat, M., Verwilligen, P., Walsh, S., Yazgan, E., Zaganidis,  
 1107 N., Basegmez, S., Bruno, G., Castello, R., Ceard, L., Delaere, C., du Pree, T., Favart, D.,  
 1108 Forthomme, L., Giammanco, A., Hollar, J., Lemaitre, V., Liao, J., Militaru, O., Nuttens,  
 1109 C., Pagano, D., Pin, A., Piotrkowski, K., Schul, N., Vizan Garcia, J. M., Beliy, N.,  
 1110 Caebegs, T., Daubie, E., Hammad, G. H., Alves, G. A., Correa Martins Junior, M.,  
 1111 De Jesus Damiao, D., Martins, T., Pol, M. E., Souza, M. H. G., Aldá Júnior, W. L.,  
 1112 Carvalho, W., Custódio, A., Da Costa, E. M., De Oliveira Martins, C., Fonseca De Souza,  
 1113 S., Matos Figueiredo, D., Mundim, L., Nogima, H., Oguri, V., Prado Da Silva, W. L.,  
 1114 Santoro, A., Soares Jorge, L., Sznajder, A., Bernardes, C. A., Dias, F. A., Fernandez  
 1115 Perez Tomei, T. R., Gregores, E. M., Lagana, C., Marinho, F., Mercadante, P. G., Novaes,  
 1116 S. F., Padula, S. S., Genchev, V., Iaydjiev, P., Piperov, S., Rodozov, M., Stoykova, S.,  
 1117 Sultanov, G., Tcholakov, V., Trayanov, R., Vutova, M., Dimitrov, A., Hadjiiska, R.,  
 1118 Kozhuharov, V., Litov, L., Pavlov, B., Petkov, P., Bian, J. G., Chen, G. M., Chen, H. S.,  
 1119 Jiang, C. H., Liang, D., Liang, S., Meng, X., Tao, J., Wang, J., Wang, X., Wang, Z.,  
 1120 Xiao, H., Xu, M., Zang, J., Zhang, Z., Asawatangtrakuldee, C., Ban, Y., Guo, S., Guo,  
 1121 Y., Li, W., Liu, S., Mao, Y., Qian, S. J., Teng, H., Wang, S., Zhu, B., Zou, W., Avila,  
 1122 C., Gomez, J. P., Gomez Moreno, B., Osorio Oliveros, A. F., Sanabria, J. C., Godinovic,  
 1123 N., Lelas, D., Plestina, R., Polic, D., Puljak, I., Antunovic, Z., Kovac, M., Brigljevic, V.,  
 1124 Duric, S., Kadija, K., Luetic, J., Morovic, S., Attikis, A., Galanti, M., Mavromanolakis,  
 1125 G., Mousa, J., Nicolaou, C., Ptochos, F., Razis, P. A., Finger, M., Finger, M., Assran,  
 1126 Y., Elgammal, S., Ellithi Kamel, A., Khalil, S., Mahmoud, M. A., Radi, A., Kadastik,  
 1127 M., Müntel, M., Raidal, M., Rebane, L., Tiko, A., Azzolini, V., Eerola, P., Fedi, G.,  
 1128 Voutilainen, M., Härkönen, J., Heikkinen, A., Karimäki, V., Kinnunen, R., Kortelainen,  
 1129 M. J., Lampén, T., Lassila-Perini, K., Lehti, S., Lindén, T., Luukka, P., Mäenpää, T.,  
 1130 Peltola, T., Tuominen, E., Tuominiemi, J., Tuovinen, E., Ungaro, D., Wendland, L.,  
 1131 Banzuzi, K., Karjalainen, A., Korpela, A., Tuuva, T., Besancon, M., Choudhury, S.,

1132 Dejardin, M., Denegri, D., Fabbro, B., Faure, J. L., Ferri, F., Ganjour, S., Givernaud,  
 1133 A., Gras, P., Hamel de Monchenault, G., Jarry, P., Locci, E., Malcles, J., Millischer, L.,  
 1134 Nayak, A., Rander, J., Rosowsky, A., Shreyber, I., Titov, M., Baffioni, S., Beaudette,  
 1135 F., Benhabib, L., Bianchini, L., Bluj, M., Broutin, C., Busson, P., Charlot, C., Daci,  
 1136 N., Dahms, T., Dobrzynski, L., Granier de Cassagnac, R., Haguenaue, M., Miné, P.,  
 1137 Mironov, C., Nguyen, M., Ochando, C., Paganini, P., Sabes, D., Salerno, R., Sirois, Y.,  
 1138 Veelken, C., Zabi, A., Agram, J.-L., Andrea, J., Bloch, D., Bodin, D., Brom, J.-M.,  
 1139 Cardaci, M., Chabert, E. C., Collard, C., Conte, E., Drouhin, F., Ferro, C., Fontaine, J.-  
 1140 C., Gelé, D., Goerlach, U., Juillot, P., Le Bihan, A.-C., Van Hove, P., Fassi, F., Mercier,  
 1141 D., Beauceron, S., Beaupere, N., Bondu, O., Boudoul, G., Chasserat, J., Chierici, R.,  
 1142 Contardo, D., Depasse, P., El Mamouni, H., Fay, J., Gascon, S., Gouzevitch, M., Ille,  
 1143 B., Kurca, T., Lethuillier, M., Mirabito, L., Perries, S., Sordini, V., Tosi, S., Tschudi,  
 1144 Y., Verdier, P., Viret, S., Tsamalaidze, Z., Anagnostou, G., Beranek, S., Edelhoff, M.,  
 1145 Feld, L., Heracleous, N., Hindrichs, O., Jussen, R., Klein, K., Merz, J., Ostapchuk, A.,  
 1146 Perieanu, A., Raupach, F., Sammet, J., Schael, S., Sprenger, D., Weber, H., Wittmer,  
 1147 B., Zhukov, V., Ata, M., Caudron, J., Dietz-Laursonn, E., Erdmann, M., Güth, A.,  
 1148 Hebbeker, T., Heidemann, C., Hoepfner, K., Klingebiel, D., Kreuzer, P., Lingemann,  
 1149 J., Magass, C., Merschmeyer, M., Meyer, A., Olschewski, M., Papacz, P., Pieta, H.,  
 1150 Reithler, H., Schmitz, S. A., Sonnenschein, L., Steggemann, J., Teyssier, D., Weber, M.,  
 1151 Bontenackels, M., Cherepanov, V., Flügge, G., Geenen, H., Geisler, M., Haj Ahmad, W.,  
 1152 Hoehle, F., Kargoll, B., Kress, T., Kuessel, Y., Nowack, A., Perchalla, L., Pooth, O.,  
 1153 Rennefeld, J., Sauerland, P., Stahl, A., Aldaya Martin, M., Behr, J., Behrenhoff, W.,  
 1154 Behrens, U., Bergholz, M., Bethani, A., Borrás, K., Burgmeier, A., Cakir, A., Calligaris,  
 1155 L., Campbell, A., Castro, E., Costanza, F., Dammann, D., Diez Pardos, C., Eckerlin, G.,  
 1156 Eckstein, D., Flucke, G., Geiser, A., Glushkov, I., Gunnellini, P., Habib, S., Hauk, J.,  
 1157 Jung, H., Kasemann, M., Katsas, P., Kleinwort, C., Kluge, H., Knutsson, A., Krämer, M.,  
 1158 Krücker, D., Kuznetsova, E., Lange, W., Lohmann, W., Lutz, B., Mankel, R., Marfin, I.,  
 1159 Marienfeld, M., Melzer-Pellmann, I.-A., Meyer, A. B., Mnich, J., Mussgiller, A., Naumann-  
 1160 Emme, S., Olzem, J., Perrey, H., Petrukhin, A., Pitzl, D., Raspereza, A., Ribeiro Cipriano,  
 1161 P. M., Riedl, C., Ron, E., Rosin, M., Salfeld-Nebgen, J., Schmidt, R., Schoerner-Sadenius,

1162 T., Sen, N., Spiridonov, A., Stein, M., Walsh, R., Wissing, C., Autermann, C., Blobel,  
 1163 V., Draeger, J., Enderle, H., Erfle, J., Gebbert, U., Görner, M., Hermanns, T., Höing,  
 1164 R. S., Kaschube, K., Kaussen, G., Kirschenmann, H., Klanner, R., Lange, J., Mura, B.,  
 1165 Nowak, F., Peiffer, T., Pietsch, N., Sander, C., Schettler, H., Schleper, P., Schlieckau, E.,  
 1166 Schmidt, A., Schröder, M., Schum, T., Sola, V., Stadie, H., Steinbrück, G., Thomsen,  
 1167 J., Vanelderen, L., Barth, C., Berger, J., Chwalek, T., De Boer, W., Dierlamm, A.,  
 1168 Feindt, M., Guthoff, M., Hackstein, C., Hartmann, F., Heinrich, M., Held, H., Hoffmann,  
 1169 K. H., Honc, S., Katkov, I., Komaragiri, J. R., Lobelle Pardo, P., Martschei, D., Mueller,  
 1170 S., Müller, T., Niegel, M., Nürnberg, A., Oberst, O., Oehler, A., Ott, J., Quast, G.,  
 1171 Rabbertz, K., Ratnikov, F., Ratnikova, N., Röcker, S., Scheurer, A., Schilling, F.-P.,  
 1172 Schott, G., Simonis, H. J., Stober, F. M., Troendle, D., Ulrich, R., Wagner-Kuhr, J.,  
 1173 Weiler, T., Zeise, M., Daskalakis, G., Geralis, T., Kesisoglou, S., Kyriakis, A., Loukas,  
 1174 D., Manolakos, I., Markou, A., Markou, C., Mavrommatis, C., Ntomari, E., Gouskos, L.,  
 1175 Mertzimekis, T. J., Panagiotou, A., Saoulidou, N., Evangelou, I., Foudas, C., Kokkas, P.,  
 1176 Manthos, N., Papadopoulos, I., Patras, V., Bencze, G., Hajdu, C., Hidas, P., Horvath, D.,  
 1177 Sikler, F., Veszpremi, V., Vesztergombi, G., Beni, N., Czellar, S., Molnar, J., Palinkas, J.,  
 1178 Szillasi, Z., Karancsi, J., Raics, P., Trocsanyi, Z. L., Ujvari, B., Beri, S. B., Bhatnagar,  
 1179 V., Dhingra, N., Gupta, R., Jindal, M., Kaur, M., Mehta, M. Z., Nishu, N., Saini, L. K.,  
 1180 Sharma, A., Singh, J., Ahuja, S., Bhardwaj, A., Choudhary, B. C., Kumar, A., Kumar,  
 1181 A., Malhotra, S., Naimuddin, M., Ranjan, K., Sharma, V., Shivpuri, R. K., Banerjee,  
 1182 S., Bhattacharya, S., Dutta, S., Gomber, B., Jain, S., Jain, S., Khurana, R., Sarkar,  
 1183 S., Sharan, M., Abdulsalam, A., Choudhury, R. K., Dutta, D., Kailas, S., Kumar, V.,  
 1184 Mehta, P., Mohanty, A. K., Pant, L. M., Shukla, P., Aziz, T., Ganguly, S., Guchait, M.,  
 1185 Maity, M., Majumder, G., Mazumdar, K., Mohanty, G. B., Parida, B., Sudhakar, K.,  
 1186 Wickramage, N., Banerjee, S., Dugad, S., Arfaei, H., Bakhshiansohi, H., Etesami, S. M.,  
 1187 Fahim, A., Hashemi, M., Hesari, H., Jafari, A., Khakzad, M., Mohammadi Najafabadi,  
 1188 M., Paktinat Mehdiabadi, S., Safarzadeh, B., Zeinali, M., Abbrescia, M., Barbone, L.,  
 1189 Calabria, C., Chhibra, S. S., Colaleo, A., Creanza, D., De Filippis, N., De Palma, M.,  
 1190 Fiore, L., Iaselli, G., Lusito, L., Maggi, G., Maggi, M., Marangelli, B., My, S., Nuzzo,  
 1191 S., Pacifico, N., Pompili, A., Pugliese, G., Selvaggi, G., Silvestris, L., Singh, G., Zito,

1192 G., Abbiendi, G., Benvenuti, A. C., Bonacorsi, D., Braibant-Giacomelli, S., Brigliadori,  
 1193 L., Capiluppi, P., Castro, A., Cavallo, F. R., Cuffiani, M., Dallavalle, G. M., Fabbri, F.,  
 1194 Fanfani, A., Fasanella, D., Giacomelli, P., Grandi, C., Guiducci, L., Marcellini, S., Masetti,  
 1195 G., Meneghelli, M., Montanari, A., Navarria, F. L., Odorici, F., Perrotta, A., Primavera,  
 1196 F., Rossi, A. M., Rovelli, T., Siroli, G., Travaglini, R., Albergo, S., Cappello, G., Chiorboli,  
 1197 M., Costa, S., Potenza, R., Tricomi, A., Tuve, C., Barbagli, G., Ciulli, V., Civinini, C.,  
 1198 D'Alessandro, R., Focardi, E., Frosali, S., Gallo, E., Gonzi, S., Meschini, M., Paoletti,  
 1199 S., Sguazzoni, G., Tropiano, A., Benussi, L., Bianco, S., Colafranceschi, S., Fabbri, F.,  
 1200 Piccolo, D., Fabbriatore, P., Musenich, R., Benaglia, A., De Guio, F., Di Matteo, L.,  
 1201 Fiorendi, S., Gennai, S., Ghezzi, A., Malvezzi, S., Manzoni, R. A., Martelli, A., Massironi,  
 1202 A., Menasce, D., Moroni, L., Paganoni, M., Pedrini, D., Ragazzi, S., Redaelli, N., Sala,  
 1203 S., Tabarelli de Fatis, T., Buontempo, S., Carrillo Montoya, C. A., Cavallo, N., De Cosa,  
 1204 A., Dogangun, O., Fabozzi, F., Iorio, A. O. M., Lista, L., Meola, S., Merola, M., Paolucci,  
 1205 P., Azzi, P., Bacchetta, N., Bellan, P., Bisello, D., Branca, A., Carlin, R., Checchia, P.,  
 1206 Dorigo, T., Dosselli, U., Gasparini, F., Gasparini, U., Gozzelino, A., Kanishchev, K.,  
 1207 Lacaprara, S., Lazzizzera, I., Margoni, M., Meneguzzo, A. T., Nespolo, M., Ronchese,  
 1208 P., Simonetto, F., Torassa, E., Vanini, S., Zotto, P., Zumerle, G., Gabusi, M., Ratti,  
 1209 S. P., Riccardi, C., Torre, P., Vitulo, P., Biasini, M., Bilei, G. M., Fanò, L., Lariccia, P.,  
 1210 Lucaroni, A., Mantovani, G., Menichelli, M., Nappi, A., Romeo, F., Saha, A., Santocchia,  
 1211 A., Taroni, S., Azzurri, P., Bagliesi, G., Boccali, T., Broccolo, G., Castaldi, R., D'Agnolo,  
 1212 R. T., Dell'Orso, R., Fiori, F., Foà, L., Giassi, A., Kraan, A., Ligabue, F., Lomtadze, T.,  
 1213 Martini, L., Messineo, A., Palla, F., Rizzi, A., Serban, A. T., Spagnolo, P., Squillacioti, P.,  
 1214 Tenchini, R., Tonelli, G., Venturi, A., Verdini, P. G., Barone, L., Cavallari, F., Del Re, D.,  
 1215 Diemoz, M., Grassi, M., Longo, E., Meridiani, P., Micheli, F., Nourbakhsh, S., Organtini,  
 1216 G., Paramatti, R., Rahatlou, S., Sigamani, M., Soffi, L., Amapane, N., Arcidiacono, R.,  
 1217 Argiro, S., Arneodo, M., Biino, C., Cartiglia, N., Costa, M., Demaria, N., Graziano,  
 1218 A., Mariotti, C., Maselli, S., Migliore, E., Monaco, V., Musich, M., Obertino, M. M.,  
 1219 Pastrone, N., Pelliccioni, M., Potenza, A., Romero, A., Ruspa, M., Sacchi, R., Solano, A.,  
 1220 Staiano, A., Vilela Pereira, A., Belforte, S., Candelise, V., Cossutti, F., Della Ricca, G.,  
 1221 Gobbo, B., Marone, M., Montanino, D., Penzo, A., Schizzi, A., Heo, S. G., Kim, T. Y.,

1222 Nam, S. K., Chang, S., Kim, D. H., Kim, G. N., Kong, D. J., Park, H., Ro, S. R., Son,  
 1223 D. C., Son, T., Kim, J. Y., Kim, Z. J., Song, S., Choi, S., Gyun, D., Hong, B., Jo, M.,  
 1224 Kim, H., Kim, T. J., Lee, K. S., Moon, D. H., Park, S. K., Choi, M., Kim, J. H., Park,  
 1225 C., Park, I. C., Park, S., Ryu, G., Cho, Y., Choi, Y., Choi, Y. K., Goh, J., Kim, M. S.,  
 1226 Kwon, E., Lee, B., Lee, J., Lee, S., Seo, H., Yu, I., Bilinskas, M. J., Grigelionis, I., Janulis,  
 1227 M., Juodagalvis, A., Castilla-Valdez, H., De La Cruz-Burelo, E., Heredia-de La Cruz, I.,  
 1228 Lopez-Fernandez, R., Magaña Villalba, R., Martínez-Ortega, J., Sánchez-Hernández, A.,  
 1229 Villasenor-Cendejas, L. M., Carrillo Moreno, S., Vazquez Valencia, F., Salazar Ibarguen,  
 1230 H. A., Casimiro Linares, E., Morelos Pineda, A., Reyes-Santos, M. A., Krofcheck, D.,  
 1231 Bell, A. J., Butler, P. H., Doesburg, R., Reucroft, S., Silverwood, H., Ahmad, M.,  
 1232 Asghar, M. I., Hoorani, H. R., Khalid, S., Khan, W. A., Khurshid, T., Qazi, S., Shah,  
 1233 M. A., Shoaib, M., Bialkowska, H., Boimska, B., Frueboes, T., Gokieli, R., Górski,  
 1234 M., Kazana, M., Nawrocki, K., Romanowska-Rybinska, K., Szleper, M., Wrochna, G.,  
 1235 Zalewski, P., Brona, G., Bunkowski, K., Cwiok, M., Dominik, W., Doroba, K., Kalinowski,  
 1236 A., Konecki, M., Krolkowski, J., Almeida, N., Bargassa, P., David, A., Faccioli, P.,  
 1237 Ferreira Parracho, P. G., Gallinaro, M., Seixas, J., Varela, J., Vischia, P., Belotelov,  
 1238 I., Bunin, P., Gavrilenko, M., Golutvin, I., Gorbunov, I., Kamenev, A., Karjavin, V.,  
 1239 Kozlov, G., Lanev, A., Malakhov, A., Moisenz, P., Palichik, V., Perelygin, V., Shmatov,  
 1240 S., Smirnov, V., Volodko, A., Zarubin, A., Evstyukhin, S., Golovtsov, V., Ivanov, Y.,  
 1241 Kim, V., Levchenko, P., Murzin, V., Oreshkin, V., Smirnov, I., Sulimov, V., Uvarov,  
 1242 L., Vavilov, S., Vorobyev, A., Vorobyev, A., Andreev, Y., Dermenev, A., Gninenko,  
 1243 S., Golubev, N., Kirsanov, M., Krasnikov, N., Matveev, V., Pashenkov, A., Tlisov, D.,  
 1244 Toropin, A., Epshteyn, V., Erofeeva, M., Gavrilov, V., Kossov, M., Lychkovskaya, N.,  
 1245 Popov, V., Safronov, G., Semenov, S., Stolin, V., Vlasov, E., Zhokin, A., Belyaev, A.,  
 1246 Boos, E., Ershov, A., Gribushin, A., Klyukhin, V., Kodolova, O., Korotkikh, V., Lokhtin,  
 1247 I., Markina, A., Obraztsov, S., Perfilov, M., Petrushanko, S., Popov, A., Sarycheva, L.,  
 1248 Savrin, V., Snigirev, A., Vardanyan, I., Andreev, V., Azarkin, M., Dremine, I., Kirakosyan,  
 1249 M., Leonidov, A., Mesyats, G., Rusakov, S. V., Vinogradov, A., Azhgirey, I., Bayshev, I.,  
 1250 Bitioukov, S., Grishin, V., Kachanov, V., Konstantinov, D., Korablev, A., Krychkin,  
 1251 V., Petrov, V., Ryutin, R., Sobol, A., Tourtchanovitch, L., Troshin, S., Tyurin, N.,

1252 Uzunian, A., Volkov, A., Adzic, P., Djordjevic, M., Ekmedzic, M., Krpic, D., Milosevic, J.,  
 1253 Aguilar-Benitez, M., Alcaraz Maestre, J., Arce, P., Battilana, C., Calvo, E., Cerrada, M.,  
 1254 Chamizo Llatas, M., Colino, N., De La Cruz, B., Delgado Peris, A., Domínguez Vázquez,  
 1255 D., Fernandez Bedoya, C., Fernández Ramos, J. P., Ferrando, A., Flix, J., Fouz, M. C.,  
 1256 Garcia-Abia, P., Gonzalez Lopez, O., Goy Lopez, S., Hernandez, J. M., Josa, M. I., Merino,  
 1257 G., Puerta Pelayo, J., Quintario Olmeda, A., Redondo, I., Romero, L., Santaolalla, J.,  
 1258 Soares, M. S., Willmott, C., Albajar, C., Codispoti, G., de Trocóniz, J. F., Brun, H.,  
 1259 Cuevas, J., Fernandez Menendez, J., Folgueras, S., Gonzalez Caballero, I., Lloret Iglesias,  
 1260 L., Piedra Gomez, J., Brochero Cifuentes, J. A., Cabrillo, I. J., Calderon, A., Chuang,  
 1261 S. H., Duarte Campderros, J., Felcini, M., Fernandez, M., Gomez, G., Gonzalez Sanchez,  
 1262 J., Jorda, C., Lopez Virto, A., Marco, J., Marco, R., Martinez Rivero, C., Matorras,  
 1263 F., Munoz Sanchez, F. J., Rodrigo, T., Rodríguez-Marrero, A. Y., Ruiz-Jimeno, A.,  
 1264 Scodellaro, L., Sobron Sanudo, M., Vila, I., Vilar Cortabitarte, R., Abbaneo, D., Auffray,  
 1265 E., Auzinger, G., Baillon, P., Ball, A. H., Barney, D., Benitez, J. F., Bernet, C., Bianchi,  
 1266 G., Bloch, P., Bocci, A., Bonato, A., Botta, C., Breuker, H., Camporesi, T., Cerminara,  
 1267 G., Christiansen, T., Coarasa Perez, J. A., D'Enterria, D., Dabrowski, A., De Roeck,  
 1268 A., Di Guida, S., Dobson, M., Dupont-Sagorin, N., Elliott-Peisert, A., Frisch, B., Funk,  
 1269 W., Georgiou, G., Giffels, M., Gigi, D., Gill, K., Giordano, D., Giunta, M., Glege, F.,  
 1270 Gomez-Reino Garrido, R., Govoni, P., Gowdy, S., Guida, R., Hansen, M., Harris, P.,  
 1271 Hartl, C., Harvey, J., Hegner, B., Hinzmann, A., Innocente, V., Janot, P., Kaadze, K.,  
 1272 Karavakis, E., Kousouris, K., Lecoq, P., Lee, Y.-J., Lenzi, P., Lourenço, C., Mäki, T.,  
 1273 Malberti, M., Malgeri, L., Mannelli, M., Masetti, L., Meijers, F., Mersi, S., Meschi, E.,  
 1274 Moser, R., Mozer, M. U., Mulders, M., Musella, P., Nesvold, E., Orimoto, T., Orsini, L.,  
 1275 Palencia Cortezon, E., Perez, E., Perrozzi, L., Petrilli, A., Pfeiffer, A., Pierini, M., Pimiä,  
 1276 M., Piparo, D., Polese, G., Quertenmont, L., Racz, A., Reece, W., Rodrigues Antunes, J.,  
 1277 Rolandi, G., Rommerskirchen, T., Rovelli, C., Rovere, M., Sakulin, H., Santanastasio, F.,  
 1278 Schäfer, C., Schwick, C., Segoni, I., Sekmen, S., Sharma, A., Siegrist, P., Silva, P., Simon,  
 1279 M., Sphicas, P., Spiga, D., Spiropulu, M., Tsiros, A., Veres, G. I., Vlimant, J. R., Wöhri,  
 1280 H. K., Worm, S. D., Zeuner, W. D., Bertl, W., Deiters, K., Erdmann, W., Gabathuler,  
 1281 K., Horisberger, R., Ingram, Q., Kaestli, H. C., König, S., Kotlinski, D., Langenegger, U.,

1282 Meier, F., Renker, D., Rohe, T., Sibille, J., Bani, L., Bortignon, P., Buchmann, M. A.,  
 1283 Casal, B., Chanon, N., Deisher, A., Dissertori, G., Dittmar, M., Dünser, M., Eugster, J.,  
 1284 Freudenreich, K., Grab, C., Hits, D., Lecomte, P., Lustermann, W., Martinez Ruiz del  
 1285 Arbol, P., Mohr, N., Moortgat, F., Nägeli, C., Nef, P., Nessi-Tedaldi, F., Pandolfi, F.,  
 1286 Pape, L., Pauss, F., Peruzzi, M., Ronga, F. J., Rossini, M., Sala, L., Sanchez, A. K.,  
 1287 Starodumov, A., Stieger, B., Takahashi, M., Tauscher, L., Thea, A., Theofilatos, K.,  
 1288 Treille, D., Urscheler, C., Wallny, R., Weber, H. A., Wehrli, L., Aguilo, E., Amsler, C.,  
 1289 Chiochia, V., De Visscher, S., Favaro, C., Ivova Rikova, M., Millan Mejias, B., Otiougova,  
 1290 P., Robmann, P., Snoek, H., Tupputi, S., Verzetti, M., Chang, Y. H., Chen, K. H., Kuo,  
 1291 C. M., Li, S. W., Lin, W., Liu, Z. K., Lu, Y. J., Mekterovic, D., Singh, A. P., Volpe, R., Yu,  
 1292 S. S., Bartalini, P., Chang, P., Chang, Y. H., Chang, Y. W., Chao, Y., Chen, K. F., Dietz,  
 1293 C., Grundler, U., Hou, W.-S., Hsiung, Y., Kao, K. Y., Lei, Y. J., Lu, R.-S., Majumder, D.,  
 1294 Petrakou, E., Shi, X., Shiu, J. G., Tzeng, Y. M., Wan, X., Wang, M., Adiguzel, A., Bakirci,  
 1295 M. N., Cerci, S., Dozen, C., Dumanoglu, I., Eskut, E., Girgis, S., Gokbulut, G., Gurpinar,  
 1296 E., Hos, I., Kangal, E. E., Karapinar, G., Kayis Topaksu, A., Onengut, G., Ozdemir, K.,  
 1297 Ozturk, S., Polatoz, A., Sogut, K., Sunar Cerci, D., Tali, B., Topakli, H., Vergili, L. N.,  
 1298 Vergili, M., Akin, I. V., Aliev, T., Bilin, B., Bilmis, S., Deniz, M., Gamsizkan, H., Guler,  
 1299 A. M., Ocalan, K., Ozpineci, A., Serin, M., Sever, R., Surat, U. E., Yalvac, M., Yildirim,  
 1300 E., Zeyrek, M., Gülmez, E., Isildak, B., Kaya, M., Kaya, O., Ozkorucuklu, S., Sonmez, N.,  
 1301 Cankocak, K., Levchuk, L., Bostock, F., Brooke, J. J., Clement, E., Cussans, D., Flacher,  
 1302 H., Frazier, R., Goldstein, J., Grimes, M., Heath, G. P., Heath, H. F., Kreczko, L.,  
 1303 Metson, S., Newbold, D. M., Nirunpong, K., Poll, A., Senkin, S., Smith, V. J., Williams,  
 1304 T., Basso, L., Bell, K. W., Belyaev, A., Brew, C., Brown, R. M., Cockerill, D. J. A.,  
 1305 Coughlan, J. A., Harder, K., Harper, S., Jackson, J., Kennedy, B. W., Olaiya, E., Petyt,  
 1306 D., Radburn-Smith, B. C., Shepherd-Themistocleous, C. H., Tomalin, I. R., Womersley,  
 1307 W. J., Bainbridge, R., Ball, G., Beuselinck, R., Buchmuller, O., Colling, D., Cripps, N.,  
 1308 Cutajar, M., Dauncey, P., Davies, G., Della Negra, M., Ferguson, W., Fulcher, J., Futyan,  
 1309 D., Gilbert, A., Guneratne Bryer, A., Hall, G., Hatherell, Z., Hays, J., Iles, G., Jarvis,  
 1310 M., Karapostoli, G., Lyons, L., Magnan, A.-M., Marrouche, J., Mathias, B., Nandi, R.,  
 1311 Nash, J., Nikitenko, A., Papageorgiou, A., Pela, J., Pesaresi, M., Petridis, K., Pioppi,



M., Raymond, D. M., Rogerson, S., Rose, A., Ryan, M. J., Seez, C., Sharp, P., Sparrow, A., Stoye, M., Tapper, A., Vazquez Acosta, M., Virdee, T., Wakefield, S., Wardle, N., Whyntie, T., Chadwick, M., Cole, J. E., Hobson, P. R., Khan, A., Kyberd, P., Leslie, D., Martin, W., Reid, I. D., Symonds, P., Teodorescu, L., Turner, M., Hatakeyama, K., Liu, H., Scarborough, T., Charaf, O., Henderson, C., Rumerio, P., Avetisyan, A., Bose, T., Fantasia, C., Heiste (2012). Measurement of the pseudorapidity and centrality dependence of the transverse energy density in pb-pb collisions at  $\sqrt{s_{NN}} = 2.76$  TeV. *Phys. Rev. Lett.*, 109:152303. 6, 21

[13] Collaboration, T. A., Aamodt, K., Quintana, A. A., Achenbach, R., Acounis, S., Adamov, D., Adler, C., Aggarwal, M., Agnese, F., Rinella, G. A., Ahammed, Z., Ahmad, A., Ahmad, N., Ahmad, S., Akindinov, A., Akishin, P., Aleksandrov, D., Alessandro, B., Alfaro, R., Alfarone, G., Alici, A., Alme, J., Alt, T., Altinpinar, S., Amend, W., Andrei, C., Andres, Y., Andronic, A., Anelli, G., Anfreville, M., Angelov, V., Anzo, A., Anson, C., Antici, T., Antonenko, V., Antonczyk, D., Antinori, F., Antinori, S., Antonioli, P., Aphecetche, L., Appelshuser, H., Aprodu, V., Arba, M., Arcelli, S., Argentieri, A., Armesto, N., Arnaldi, R., Arefiev, A., Arsene, I., Asryan, A., Augustinus, A., Awes, T. C., ysto, J., Azmi, M. D., Bablock, S., Badal, A., Badyal, S. K., Baechler, J., Bagnasco, S., Bailhache, R., Bala, R., Baldisseri, A., Baldit, A., Bn, J., Barbera, R., Barberis, P.-L., Barbet, J. M., Barnfoldi, G., Barret, V., Bartke, J., Bartos, D., Basile, M., Basmanov, V., Bastid, N., Batigne, G., Batyunya, B., Baudot, J., Baumann, C., Bearden, I., Becker, B., Belikov, J., Bellwied, R., Belmont-Moreno, E., Belogianni, A., Belyaev, S., Benato, A., Beney, J. L., Benhabib, L., Benotto, F., Beol, S., Berceanu, I., Bercuci, A., Berdermann, E., Berdnikov, Y., Bernard, C., Berny, R., Berst, J. D., Bertelsen, H., Betev, L., Bhasin, A., Baskar, P., Bhati, A., Bianchi, N., Bielik, J., Bielikov, J., Bimbot, L., Blanchard, G., Blanco, F., Blanco, F., Blau, D., Blume, C., Blyth, S., Boccioni, M., Bogdanov, A., Bggild, H., Bogolyubsky, M., Boldizsr, L., Bombara, M., Bombonati, C., Bondila, M., Bonnet, D., Bonvicini, V., Borel, H., Borotto, F., Borshchov, V., Bortoli, Y., Borysov, O., Bose, S., Bosisio, L., Botje, M., Bttger, S., Bourdaud, G., Bourrion, O., Bouvier, S., Braem, A., Braun, M., Braun-Munzinger, P., Bravina, L., Bregant, M., Bruckner, G., Brun, R.,

1341 Bruna, E., Brunasso, O., Bruno, G. E., Bucher, D., Budilov, V., Budnikov, D., Buesching,  
 1342 H., Buncic, P., Burns, M., Burachas, S., Busch, O., Bushop, J., Cai, X., Caines, H.,  
 1343 Calaon, F., Caldogno, M., Cali, I., Camerini, P., Campagnolo, R., Campbell, M., Cao,  
 1344 X., Capitani, G. P., Romeo, G. C., Cardenas-Montes, M., Carduner, H., Carena, F.,  
 1345 Carena, W., Cariola, P., Carminati, F., Casado, J., Diaz, A. C., Caselle, M., Castellanos,  
 1346 J. C., Castor, J., Catanescu, V., Cattaruzza, E., Cavazza, D., Cerello, P., Ceresa, S.,  
 1347 ern, V., Chambert, V., Chapeland, S., Charpy, A., Charrier, D., Chartoire, M., Charvet,  
 1348 J. L., Chattopadhyay, S., Chattopadhyay, S., Chepurnov, V., Chernenko, S., Cherney,  
 1349 M., Cheshkov, C., Cheynis, B., Chochula, P., Chiavassa, E., Barroso, V. C., Choi, J.,  
 1350 Christakoglou, P., Christiansen, P., Christensen, C., Chykalov, O. A., Cicalo, C., Cifarelli-  
 1351 Strolin, L., Ciobanu, M., Cindolo, F., Cirstoiu, C., Clausse, O., Cleymans, J., Cobanoglu,  
 1352 O., Coffin, J.-P., Coli, S., Colla, A., Colledani, C., Combaret, C., Combet, M., Comets,  
 1353 M., Balbastre, G. C., del Valle, Z. C., Contin, G., Contreras, J., Cormier, T., Corsi, F.,  
 1354 Cortese, P., Costa, F., Crescio, E., Crochet, P., Cuautle, E., Cussonneau, J., Dahlinger,  
 1355 M., Dainese, A., Dalsgaard, H. H., Daniel, L., Das, I., Das, T., Dash, A., Silva, R. D.,  
 1356 Davenport, M., Daues, H., Caro, A. D., de Cataldo, G., Cuveland, J. D., Falco, A. D.,  
 1357 de Gaspari, M., de Girolamo, P., de Groot, J., Gruttola, D. D., Haas, A. D., Marco, N. D.,  
 1358 Pasquale, S. D., Remigis, P. D., de Vaux, D., Decock, G., Delagrange, H., Franco, M. D.,  
 1359 Dellacasa, G., Dell'Olio, C., Dell'Olio, D., Deloff, A., Demanov, V., Dnes, E., D'Erasmus,  
 1360 G., Derkach, D., Devaux, A., Bari, D. D., Bartolomeo, A. D., Giglio, C. D., Liberto,  
 1361 S. D., Mauro, A. D., Nezza, P. D., Dialinas, M., Diaz, L., Valdes, R. D., Dietel, T., Dima,  
 1362 R., Ding, H., Dinca, C., Divi, R., Dobretsov, V., Dobrin, A., Doenigus, B., Dobrowolski,  
 1363 T., Domnguez, I., Dorn, M., Drouet, S., Dubey, A. E., Ducroux, L., Dumitrache, F.,  
 1364 Dumonteil, E., Dupieux, P., Duta, V., Majumdar, A. D., Majumdar, M. D., Dyhre,  
 1365 T., Efimov, L., Efremov, A., Elia, D., Emschermann, D., Engster, C., Enokizono, A.,  
 1366 Espagnon, B., Estienne, M., Evangelista, A., Evans, D., Evrard, S., Fabjan, C. W.,  
 1367 Fabris, D., Faivre, J., Falchieri, D., Fantoni, A., Farano, R., Fearick, R., Fedorov, O.,  
 1368 Fekete, V., Felea, D., Feofilov, G., Tllez, A. F., Ferretti, A., Fichera, F., Filchagin, S.,  
 1369 Filoni, E., Finck, C., Fini, R., Fiore, E. M., Flierl, D., Floris, M., Fodor, Z., Foka, Y.,  
 1370 Fokin, S., Force, P., Formenti, F., Fragiaco, E., Fragiadakis, M., Fraissard, D., Franco,

1371 A., Franco, M., Frankenfeld, U., Fratino, U., Fresneau, S., Frolov, A., Fuchs, U., Fujita, J.,  
 1372 Furget, C., Furini, M., Girard, M. F., Gaardhje, J.-J., Gabrielli, A., Gadrat, S., Gagliardi,  
 1373 M., Gago, A., Gaido, L., Torreira, A. G., Gallio, M., Gandolfi, E., Ganoti, P., Ganti, M.,  
 1374 Garabatos, J., Lopez, A. G., Garizzo, L., Gaudichet, L., Gemme, R., Germain, M., Gheata,  
 1375 A., Gheata, M., Ghidini, B., Ghosh, P., Giolu, G., Giraudo, G., Giubellino, P., Glasow,  
 1376 R., Glssel, P., Ferreira, E. G., Gutierrez, C. G., Gonzales-Trueba, L. H., Gorbunov, S.,  
 1377 Gorbunov, Y., Gos, H., Gosset, J., Gotovac, S., Gottschlag, H., Gottschalk, D., Grabski,  
 1378 V., Grassi, T., Gray, H., Grebenyuk, O., Grebieszko, K., Gregory, C., Grigoras, C.,  
 1379 Grion, N., Grigoriev, V., Grigoryan, A., Grigoryan, C., Grigoryan, S., Grishuk, Y., Gros,  
 1380 P., Grosse-Oetringhaus, J., Grossiord, J.-Y., Grosso, R., Grynyov, B., Guarnaccia, C.,  
 1381 Guber, F., Guerin, F., Guernane, R., Guerzoni, M., Guichard, A., Guida, M., Guilloux,  
 1382 G., Gulkanyan, H., Gulbrandsen, K., Gunji, T., Gupta, A., Gupta, V., Gustafsson, H.-  
 1383 A., Gutbrod, H., Hadjidakis, C., Haiduc, M., Hamar, G., Hamagaki, H., Hamblen, J.,  
 1384 Hansen, J. C., Hardy, P., Hatzifotiadou, D., Harris, J. W., Hartig, M., Harutyunyan, A.,  
 1385 Hayrapetyan, A., Hasch, D., Hasegan, D., Hehner, J., Heine, N., Heinz, M., Helstrup, H.,  
 1386 Herghelegiu, A., Herlant, S., Corral, G. H., Herrmann, N., Hetland, K., Hille, P., Hinke,  
 1387 H., Hippolyte, B., Hoch, M., Hoebbel, H., Hoedlmoser, H., Horaguchi, T., Horner, M.,  
 1388 Hristov, P., Hivnov, I., Hu, S., Guo, C. H., Humanic, T., Hurtado, A., Hwang, D. S.,  
 1389 Ianigro, J. C., Idzik, M., Igolkin, S., Ilkaev, R., Ilkiv, I., Imhoff, M., Innocenti, P. G.,  
 1390 Ionescu, E., Ippolitov, M., Irfan, M., Insa, C., Inuzuka, M., Ivan, C., Ivanov, A., Ivanov,  
 1391 M., Ivanov, V., Jacobs, P., Jacholkowski, A., Janurov, L., Janik, R., Jasper, M., Jena, C.,  
 1392 Jirden, L., Johnson, D. P., Jones, G. T., Jorgensen, C., Jouve, F., Jovanovi, P., Junique,  
 1393 A., Jusko, A., Jung, H., Jung, W., Kadija, K., Kamal, A., Kamermans, R., Kapusta, S.,  
 1394 Kaidalov, A., Kakoyan, V., Kalcher, S., Kang, E., Kapitan, J., Kaplin, V., Karadzhev, K.,  
 1395 Karavichev, O., Karavicheva, T., Karpechev, E., Karpio, K., Kazantsev, A., Kebschull,  
 1396 U., Keidel, R., Khan, M. M., Khanzadeev, A., Kharlov, Y., Kikola, D., Kileng, B., Kim,  
 1397 D., Kim, D. S., Kim, D. W., Kim, H. N., Kim, J. S., Kim, S., Kinson, J. B., Kiprich, S. K.,  
 1398 Kisel, I., Kiselev, S., Kisiel, A., Kiss, T., Kiworra, V., Klay, J., Bsing, C. K., Kliemant, M.,  
 1399 Klimov, A., Klovning, A., Kluge, A., Kluit, R., Kniege, S., Kolevatov, R., Kollegger, T.,  
 1400 Kolojvari, A., Kondratiev, V., Kornas, E., Koshurnikov, E., Kotov, I., Kour, R., Kowalski,

1401 M., Kox, S., Kozlov, K., Krlik, I., Kramer, F., Kraus, I., Kravkov, A., Krawutschke, T.,  
 1402 Krivda, M., Kryshen, E., Kucheriaev, Y., Kugler, A., Kuhn, C., Kuijer, P., Kumar, L.,  
 1403 Kumar, N., Kumpumaeki, P., Kurepin, A., Kurepin, A. N., Kushpil, S., Kushpil, V.,  
 1404 Kutovsky, M., Kvaerno, H., Kweon, M., Labb, J.-C., Lackner, F., de Guevara, P. L.,  
 1405 Lafage, V., Rocca, P. L., Lamont, M., Lara, C., Larsen, D. T., Laurenti, G., Lazzeroni,  
 1406 C., Bornec, Y. L., Bris, N. L., Gailliard, C. L., Lebedev, V., Lecoq, J., Lee, K. S., Lee, S. C.,  
 1407 Lefvre, F., Legrand, I., Lehmann, T., Leistam, L., Lenoir, P., Lenti, V., Leon, H., Monzon,  
 1408 I. L., Lvai, P., Li, Q., Li, X., Librizzi, F., Lietava, R., Lindegaard, N., Lindenstruth, V.,  
 1409 Lippmann, C., Lisa, M., Listratenko, O. M., Littel, F., Liu, Y., Lo, J., Lobanov, V.,  
 1410 Loginov, V., Noriega, M. L., Lpez-Ramrez, R., Torres, E. L., Lorenzo, P. M., Lvhidden,  
 1411 G., Lu, S., Ludolphs, W., Lunardon, M., Luquin, L., Lusso, S., Lutz, J.-R., Luvisetto,  
 1412 M., Lyapin, V., Maevskaya, A., Magureanu, C., Mahajan, A., Majahan, S., Mahmoud,  
 1413 T., Mairani, A., Mahapatra, D., Makarov, A., Makhlyueva, I., Malek, M., Malkiewicz,  
 1414 T., Mal'Kevich, D., Malzacher, P., Mamonov, A., Manea, C., Mangotra, L. K., Maniero,  
 1415 D., Manko, V., Manso, F., Manzari, V., Mao, Y., Marcel, A., Marchini, S., Mare, J.,  
 1416 Margagliotti, G. V., Margotti, A., Marin, A., Marin, J.-C., Marras, D., Martinengo, P.,  
 1417 Martnez, M. I., Martinez-Davalos, A., Garcia, G. M., Martini, S., Chiesa, A. M., Marzocca,  
 1418 C., Masciocchi, S., Masera, M., Masetti, M., Maslov, N. I., Masoni, A., Massera, F., Mast,  
 1419 M., Mastroserio, A., Matthews, Z. L., Mayer, B., Mazza, G., Mazzaro, M. D., Mazzoni,  
 1420 A., Meddi, F., Meleshko, E., Menchaca-Rocha, A., Meneghini, S., Meoni, M., Perez, J. M.,  
 1421 Mereu, P., Meunier, O., Miake, Y., Michalon, A., Michinelli, R., Miftakhov, N., Mignone,  
 1422 M., Mikhailov, K., Milosevic, J., Minaev, Y., Minafra, F., Mischke, A., Mikowiec, D.,  
 1423 Mitsyn, V., Mitu, C., Mohanty, B., Moisa, D., Molnar, L., Mondal, M., Mondal, N.,  
 1424 Zetina, L. M., Monteno, M., Morando, M., Morel, M., Moretto, S., Morhardt, T., Morsch,  
 1425 A., Moukhanova, T., Mucchi, M., Muccifora, V., Mudnic, E., Miller, H., Miller, W., Munoz,  
 1426 J., Mura, D., Musa, L., Muraz, J. F., Musso, A., Nania, R., Nandi, B., Nappi, E., Navach,  
 1427 F., Navin, S., Nayak, T., Nazarenko, S., Nazarov, G., Nellen, L., Nendaz, F., Nianine,  
 1428 A., Nicassio, M., Nielsen, B. S., Nikolaev, S., Nikolic, V., Nikulin, S., Nikulin, V., Nilsen,  
 1429 B., Nitti, M., Noferini, F., Nomokonov, P., Nooren, G., Noto, F., Nouais, D., Nyiri,  
 1430 A., Nystrand, J., Odyniec, G., Oeschler, H., Oinonen, M., Oldenburg, M., Oleks, I.,

1431 Olsen, E. K., Onuchin, V., Oppedisano, C., Orsini, F., Ortiz-Velzquez, A., Oskamp, C.,  
 1432 Oskarsson, A., Osmic, F., sberman, L., Otterlund, I., Ovrebekk, G., Oyama, K., Pachr,  
 1433 M., Pagano, P., Pai, G., Pajares, C., Pal, S., Pal, S., Plla, G., Palmeri, A., Pancaldi,  
 1434 G., Panse, R., Pantaleo, A., Pappalardo, G. S., Pastirk, B., Pastore, C., Patarakin, O.,  
 1435 Paticchio, V., Patimo, G., Pavlinov, A., Pawlak, T., Peitzmann, T., Pnichot, Y., Pepato,  
 1436 A., Pereira, H., Peresunko, D., Perez, C., Griffo, J. P., Perini, D., Perrino, D., Peryt, W.,  
 1437 Pesci, A., Peskov, V., Pestov, Y., Peters, A. J., Petrek, V., Petridis, A., Petris, M., Petrov,  
 1438 V., Petrov, V., Petrovici, M., Peyr, J., Piano, S., Piccotti, A., Pichot, P., Piemonte, C.,  
 1439 Pikna, M., Pilastrini, R., Pillot, P., Pinazza, O., Pini, B., Pinsky, L., Morais, V. P.,  
 1440 Pismennaya, V., Piuz, F., Platt, R., Ploskon, M., Plumeri, S., Pluta, J., Pocheptsov,  
 1441 T., Podesta, P., Poggio, F., Poghosyan, M., Poghosyan, T., Polk, K., Polichtchouk, B.,  
 1442 Polozov, P., Polyakov, V., Pommeresch, B., Pompei, F., Pop, A., Popescu, S., Posa, F.,  
 1443 Pospil, V., Potukuchi, B., Pouthas, J., Prasad, S., Preghenella, R., Prino, F., Prodan, L.,  
 1444 Prono, G., Protsenko, M. A., Pruneau, C. A., Przybyla, A., Pshenichnov, I., Puddu, G.,  
 1445 Pujahari, P., Pulvirenti, A., Punin, A., Punin, V., Putschke, J., Quartieri, J., Quercigh,  
 1446 E., Rachevskaya, I., Rachevski, A., Rademakers, A., Radomski, S., Radu, A., Rak, J.,  
 1447 Ramello, L., Raniwala, R., Raniwala, S., Rasmussen, O. B., Rasson, J., Razin, V., Read,  
 1448 K., Real, J., Redlich, K., Reichling, C., Renard, C., Renault, G., Renfordt, R., Reolon,  
 1449 A. R., Reshetin, A., Revol, J.-P., Reygers, K., Ricaud, H., Riccati, L., Ricci, R. A., Richter,  
 1450 M., Riedler, P., Rigalleau, L. M., Riggi, F., Riegler, W., Rindel, E., Riso, J., Rivetti, A.,  
 1451 Rizzi, M., Rizzi, V., Cahuantzi, M. R., Red, K., Rhrich, D., Romn-Lpez, S., Romanato, M.,  
 1452 Romita, R., Ronchetti, F., Rosinsky, P., Rosnet, P., Rossegger, S., Rossi, A., Rostchin,  
 1453 V., Rotondo, F., Roukoutakis, F., Rousseau, S., Roy, C., Roy, D., Roy, P., Royer, L.,  
 1454 Rubin, G., Rubio, A., Rui, R., Rusanov, I., Russo, G., Ruuskanen, V., Ryabinkin, E.,  
 1455 Rybicki, A., Sadovsky, S., afak, K., Sahoo, R., Saini, J., Saiz, P., Salur, S., Sambyal,  
 1456 S., Samsonov, V., ndor, L., Sandoval, A., Sann, H., Santiard, J.-C., Santo, R., Santoro,  
 1457 R., Sargsyan, G., Saturnini, P., Scapparone, E., Scarlassara, F., Schackert, B., Schiaua,  
 1458 C., Schicker, R., Schioler, T., Schippers, J. D., Schmidt, C., Schmidt, H., Schneider, R.,  
 1459 Schossmailer, K., Schukraft, J., Schutz, Y., Schwarz, K., Schweda, K., Schyns, E., Scioli,  
 1460 G., Scomparin, E., Snow, H., Sedykh, S., Segato, G., Sellitto, S., Semeria, F., Senyukov,

1461 S., Seppnen, H., Serici, S., Serkin, L., Serra, S., Sesselmann, T., Sevcenco, A., Sgura, I.,  
 1462 Shabratova, G., Shahoyan, R., Sharkov, E., Sharma, S., Shigaki, K., Shileev, K., Shukla,  
 1463 P., Shurygin, A., Shurygina, M., Sibiriak, Y., Siddi, E., Siemiarczuk, T., Sigward, M. H.,  
 1464 Silenzi, A., Silvermyr, D., Silvestri, R., Simili, E., Simion, V., Simon, R., Simonetti, L.,  
 1465 Singaraju, R., Singhal, V., Sinha, B., Sinha, T., Siska, M., Sitr, B., Sitta, M., Skaali,  
 1466 B., Skowronski, P., Slodkowski, M., Smirnov, N., Smykov, L., Snellings, R., Snoeys, W.,  
 1467 Soegaard, C., Soerensen, J., Sokolov, O., Soldatov, A., Soloviev, A., Soltveit, H., Soltz,  
 1468 R., Sommer, W., Soos, C., Soramel, F., Sorensen, S., Soyk, D., Spyropoulou-Stassinaki,  
 1469 M., Stachel, J., Staley, F., Stan, I., Stavinskiy, A., Steckert, J., Stefanini, G., Stefanek,  
 1470 G., Steinbeck, T., Stelzer, H., Stenlund, E., Stocco, D., Stockmeier, M., Stoicea, G.,  
 1471 Stolpovsky, P., Strme, P., Stutzmann, J. S., Su, G., Sugitate, T., umbera, M., Suire, C.,  
 1472 Susa, T., Kumar, K. S., Swoboda, D., Symons, J., Szarka, I., Szostak, A., Szuba, M.,  
 1473 Szymanski, P., Tadel, M., Tagridis, C., Tan, L., Takaki, D. T., Taureg, H., Tauro, A.,  
 1474 Tavlet, M., Munoz, G. T., Thder, J., Tieulent, R., Timmer, P., Tolyhy, T., Topilskaya,  
 1475 N., de Matos, C. T., Torii, H., Toscano, L., Tosello, F., Tournaire, A., Traczyk, T., Trger,  
 1476 G., Tromeur, W., Truesdale, D., Trzaska, W., Tsiledakis, G., Tsilis, E., Tsvetkov, A.,  
 1477 Turcato, M., Turrisi, R., Tuveri, M., Tveter, T., Tydesjo, H., Tykarski, L., Tywoniuk, K.,  
 1478 Ugolini, E., Ullaland, K., Urbn, J., Urciuoli, G. M., Usai, G. L., Usseglio, M., Vacchi, A.,  
 1479 Vala, M., Valiev, F., Vyvre, P. V., Brink, A. V. D., Eijndhoven, N. V., Kolk, N. V. D.,  
 1480 van Leeuwen, M., Vannucci, L., Vanzetto, S., Vanuxem, J.-P., Vargas, M. A., Varma,  
 1481 R., Vascotto, A., Vasiliev, A., Vassiliou, M., Vasta, P., Vechernin, V., Venaruzzo, M.,  
 1482 Vercellin, E., Vergara, S., Verhoeven, W., Veronese, F., Vetlitskiy, I., Vernet, R., Victorov,  
 1483 V., Vidak, L., Viesti, G., Vikhlyantsev, O., Vilakazi, Z., Baillie, O. V., Vinogradov, A.,  
 1484 Vinogradov, L., Vinogradov, Y., Virgili, T., Viyogi, Y., Vodopianov, A., Volpe, G., Vranic,  
 1485 D., Vrlkov, J., Vulpescu, B., Wabnitz, C., Wagner, V., Wallet, L., Wan, R., Wang, Y.,  
 1486 Wang, Y., Wheadon, R., Weis, R., Wen, Q., Wessels, J., Westergaard, J., Wiechula, J.,  
 1487 Wiesenaecker, A., Wikne, J., Wilk, A., Wilk, G., Williams, C., Willis, N., Windelband, B.,  
 1488 Witt, R., Woehri, H., Wyllie, K., Xu, C., Yang, C., Yang, H., Yermia, F., Yin, Z., Yin, Z.,  
 1489 Ky, B. Y., Yushmanov, I., Yuting, B., Zabrodin, E., Zagato, S., Zagreev, B., Zaharia, P.,  
 1490 Zalite, A., Zampa, G., Zampolli, C., Zanevskiy, Y., Zarochentsev, A., Zaudtke, O., Zvada,

1491 P., Zbroszczyk, H., Zepeda, A., Zeter, V., Zgura, I., Zhalov, M., Zhou, D., Zhou, S., Zhu,  
1492 G., Zichichi, A., Zinchenko, A., Zinovjev, G., Zoccarato, Y., Zubarev, A., Zucchini, A.,  
1493 and Zuffa, M. (2008). The alice experiment at the cern lhc. *Journal of Instrumentation*,  
1494 3(08):S08002. 24

1495 [14] Connors, M., Nattrass, C., Reed, R., and Salur, S. (2017). Review of Jet Measurements  
1496 in Heavy Ion Collisions. vi, 11, 13, 14

1497 [15] Elia, D. and the ALICE Collaboration (2013). Strangeness production in alice. *Journal*  
1498 *of Physics: Conference Series*, 455(1):012005. 18

1499 [16] Evans, L. and Bryant, P. (2008). Lhc machine. *Journal of Instrumentation*,  
1500 3(08):S08001. 9

1501 [17] Foka, P. and Janik, M. A. (2016). An overview of experimental results from ultra-  
1502 relativistic heavy-ion collisions at the cern lhc: Bulk properties and dynamical evolution.  
1503 *Reviews in Physics*, 1:154 – 171. 10

1504 [18] Gyulassy, M. (2004). The QGP discovered at RHIC. In *Structure and dynamics*  
1505 *of elementary matter. Proceedings, NATO Advanced Study Institute, Camyuva-Kemer,*  
1506 *Turkey, September 22-October 2, 2003*, pages 159–182. 7

1507 [19] Hilke, H. J. (2010). Time projection chambers. *Reports on Progress in Physics*,  
1508 73(11):116201. vii, 26

1509 [20] Huovinen, P., Kolb, P. F., Heinz, U., Ruuskanen, P. V., and Voloshin, S. A. (2001).  
1510 Radial and elliptic flow at RHIC: further predictions. *Physics Letters B*, 503:58–64. 16

1511 [21] Jacobs, P. and Wang, X.-N. (2005). Matter in extremis: ultrarelativistic nuclear  
1512 collisions at RHIC. *Progress in Particle and Nuclear Physics*, 54:443–534. 15

1513 [22] Kapusta, J. I. (1979). Quantum chromodynamics at high temperature. *Nuclear Physics*  
1514 *B*, 148(3):461 – 498. 3

[23] Luo, X. (2016). Exploring the qcd phase structure with beam energy scan in heavy-ion collisions. *Nuclear Physics A*, 956:75 – 82. The XXV International Conference on Ultrarelativistic Nucleus-Nucleus Collisions: Quark Matter 2015. 20

[24] Nattrass, C. (2009). System, energy, and flavor dependence of jets through di-hadron correlations in heavy ion collisions. v, 10, 25

[25] Odyniec, G. (2013). The rhic beam energy scan program in star and what’s next ... *Journal of Physics: Conference Series*, 455(1):012037. 20

[26] Ozaki, S. and Roser, T. (2015). Relativistic heavy ion collider, its construction and upgrade. *Progress of Theoretical and Experimental Physics*, 2015(3):03A102. vi, 8

[27] Preghenella, R. (2011). Transverse momentum spectra of identified charged hadrons with the ALICE detector in Pb-Pb collisions at  $\sqrt{s_{NN}} = 2.76$  TeV. *PoS, EPS-HEP2011:118*. 23

[28] Qin, G.-Y. and Wang, X.-N. (2015). Jet quenching in high-energy heavy-ion collisions. *International Journal of Modern Physics E*, 24:1530014–438. 19

[29] Satz, H. (2006). Colour deconfinement and quarkonium binding. *Journal of Physics G: Nuclear and Particle Physics*, 32(3):R25. 4, 6

[30] Schenke, B. (2017). Origins of collectivity in small systems. *Nuclear Physics A*, 967:105 – 112. The 26th International Conference on Ultra-relativistic Nucleus-Nucleus Collisions: Quark Matter 2017. 15

[31] Shao, M., Barannikova, O. Yu., Dong, X., Fisyak, Y., Ruan, L., Sorensen, P., and Xu, Z. (2006). Extensive particle identification with TPC and TOF at the STAR experiment. *Nucl. Instrum. Meth.*, A558:419–429. 26

[32] Shuryak, E. V. (1988). The qcd vacuum and quark-gluon plasma. *Zeitschrift für Physik C Particles and Fields*, 38(1):141–145. 3

[33] Snellings, R. (2011). Elliptic flow: a brief review. *New Journal of Physics*, 13(5):055008. 16



- 1541 [34] Stock, R. (2004). Ultra-relativistic nucleus-nucleus collisions. Proceedings, 17th  
1542 International Conference, Quark Matter 2004, Oakland, USA, January 11-17, 2004. *J.*  
1543 *Phys.*, G30:S633–S648. 7
- 1544 [35] Strickland, M. (2014). Anisotropic hydrodynamics: Motivation and methodology.  
1545 *Nuclear Physics A*, 926:92–101. 15
- 1546 [36] Stcker, H. (2005). Collective flow signals the quarkgluon plasma. *Nuclear Physics A*,  
1547 750(1):121 – 147. Quark-Gluon Plasma. New Discoveries at RHIC: Case for the Strongly  
1548 Interacting Quark-Gluon Plasma. Contributions from the RBRC Workshop held May 14-  
1549 15, 2004. vii, 19
- 1550 [37] Vovchenko, V., Anchishkin, D., and Csernai, L. P. (2014). Time dependence of  
1551 partition into spectators and participants in relativistic heavy-ion collisions. *Phys. Rev.*  
1552 *C*, 90:044907. vi, 12
- 1553 [38] Wilde, M. (2013). Measurement of Direct Photons in pp and Pb-Pb Collisions with  
1554 ALICE. *Nucl. Phys.*, A904-905:573c–576c. 17
- 1555 [39] Wong, C.-Y. (1994). *Introduction to high-energy heavy-ion collisions*. World scientific.  
1556 vi, 12, 17, 18

# Appendices